Meniscus Tissue Engineering

Eric de Mulder

Nijmegen, 2013

The studies presented in this thesis were performed at the Orthopedic Research Laboratory, Department of Orthopedics, Radboud University Nijmegen Medical Centre, Nijmegen, the Netherlands.

ISBN
978-90-8891-621-2

Printed by
Proefschriftmaken.nl || Uitgeverij BOXPress

Cover by:
Eric de Mulder, SEM image of the polyurethane scaffold used in chapter 2 and 3

The printing of this thesis was financially supported by:

NBTE

Polyganics

UMC St. Radboud

Meniscus Tissue Engineering

Proefschrift

ter verkrijging van de graad van doctor
aan de Radboud Universiteit Nijmegen
op gezag van de rector magnificus prof. mr. S.C.J.J. Kortmann,
volgens besluit van het college van decanen
in het openbaar te verdedigen op maandag 10 juni 2013
om 13.30 uur precies

door
Eric Leonardus Winfriedus de Mulder
Geboren op 31 mei 1984
te Rheden

Promotoren:	Prof. dr. P. Buma
	Prof. dr. ing. N. Verdonschot
Copromotor:	Dr. G. Hannink

Manuscriptcommissie:	Prof. dr. W.F. Feitz
	Prof. dr. D.W. Grijpma (UT)
	Dr. W.F. Daamen

TABLE OF CONTENTS

7 Chapter 1: General introduction

25 Chapter 2: Proliferation of meniscal fibrochondrocytes cultured on a new polyurethane scaffold is stimulated by TGF-beta

41 Chapter 3: Characterization of polyurethane scaffold surface functionalization with diamines and heparin

51 Chapter 4: Platelet rich plasma can replace foetal bovine serum in human meniscus cell cultures

67 Chapter 5: Anisotropic porous biodegradable scaffolds for musculoskeletal tissue engineering

89 Chapter 6: Effect of polyurethane scaffold architecture on ingrowth speed and collagen orientation in a subcutaneous rat pocket model

103 Chapter 7: Isotropic and anisotropic collagen scaffolds induce similar hyalinelike cartilage repair in subchondral defects in rabbits

119 Chapter 8: Summary of the thesis

127 Chapter 9: Discussion and future perspectives

135 Chapter 10: Nederlandse samenvatting van het proefschrift

142 Dankwoord

146 Curriculum Vitae

147 Publications

Chapter 1

General introduction

Part of this chapter has been published in: Degradable Polymers for Skeletal Implants, Chapter 17; ISBN 978-1- 60692-426-6; Editors: P.I.J.M. Wuisman and T. M. Smit, pp; © 2008 Nova Science Publishers, Inc.

Eric de Mulder
Gerjon Hannink
Tony van Tienen
Pieter Buma

ANATOMY OF THE MENISCUS

The knee menisci fill the gap which is the result of a mismatch in form between the femoral condyles and the tibial plateau. The main function of the meniscus is to distribute stresses in a homogeneous way over the articular cartilage of the joint surfaces of tibia and femur, and in a lesser degree it has also a function in the stabilization of the knee joint. To enable these functions, the meniscus is a highly specialized fibrous structure which is optimized to resist compressive, tensile shear and is able to transfer axial loading into circumferentially directed forces[1,2].

The meniscus is composed of fibrocartilaginous tissue. The prominent fibrous nature is reflected by the high type I collagen content. The cartilage nature is reflected by the presence of lower levels of type II collagen and glycosaminoglycans (GAGs). Besides these major matrix constituents a number of minor collagens (types IV, V, VI, IX and XI) and some elastin are present in meniscus tissue[3].

The numerous type I collagen bundles, which are strong in tensile stress, but week in compression, are mainly oriented in a circumferential direction and are considered to be very important in preventing radial extrusion of the meniscus and maintaining the structural integrity during load bearing (Figure 1)[4,5]. The GAGs play an important role in the maintenance of optimal visco-elastic behavior, compressive stiffness and tissue hydration. Furthermore, GAGs and surface zones proteins are facilitating a smooth frictionless movement of the menisci over the articular surfaces of the tibia and femur[5-7].

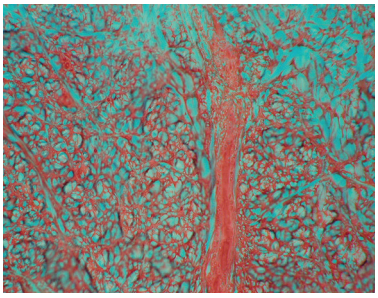

Figure 1. Safranin O stained cross-section of native meniscus tissue showing the collagen bundles. The red stained areas are GAGs (x100).

DAMAGE TO THE MENISCUS

Injuries to a healthy meniscus are often induced by a compressive force in combination with tibio-femoral rotation in the transverse plane during a movement from flexion to extension or during rapid cutting or pivoting[8]. A number of clearly different types of lesions have been described. Besides the flap tear, one of the most prominent and frequently occurring types is the bucket-handle lesion, which is a tear in the avascular white inner zone of the meniscus in a circular direction[9]. The circumferential arrangement of collagen bundles in the central portion of the meniscus provides a functional explanation for the same orientation of the bucket-handle tears [10]. However, more complex degenerative tears also occur in lower frequencies[11]. The etiology of these degenerative tears is still unknown. It has been suggested that the disease process associated with the development of osteoarthritis (OA) of the joint cartilage, may also be active in the meniscus and that a degenerative tear in a meniscus might be regarded as one of the first signs of OA[12].

CONSEQUENCES OF MENISCUS RESECTION

A tear in the meniscus will classically result in locking phenomena, abnormal (tibio-femoral) stresses and pain. These complaints will immediately disappear after resection of the tear. In the 60's and 70's a total meniscectomy was a very common surgical intervention. It was quick and easy to perform. However, in time it became clear that the removal of the meniscus generates mechanical overloading of articular cartilage which leads to the development of osteoarthritic changes in tibia and femur [13-15]. Therefore, only partial resection of the meniscus was recommended and together with introduction of arthroscopic surgery, partial meniscectomy became the state of the art. However, it also appeared that even a partial meniscectomy still induces osteoarthritic changes, whereby the damage to the articular cartilage appeared to be directly related to the amount of tissue removed[12,13]. When more than 30% of the meniscus is removed during partial meniscectomy, preservation of the peripheral rim of the meniscus is essential[16,17]. The importance of the peripheral rim for the load transmission trough the joint was first emphasized by Ahmed *et al*.[18]. The remaining rim will prevent peripheral extrusion of the meniscus by which transfer of the axial joint load into hoop stresses is still possible and the remaining part of the meniscus will also protect the uncovered articular cartilage from peak stresses. The presence or absence of an intact peripheral rim has also consequences for the type of repair technique that can be used after meniscus trauma[19,20].

REPAIR

In view of the progressive osteoarthritic changes, a great deal of effort has been put into devices to fix meniscus tears to preserve the meniscus, especially in younger patients. Suturing is a safe traditional procedure but can be time-consuming. Also the rehabilitation after meniscectomy is usually quicker than after suturing, making the choice for a particular treatment often an ethical one, especially in the competitive athlete, who wants to be back in training as soon as possible. However, when a meniscal tear occurs in combination with a rupture of the anterior cruciate ligament (ACL), the results of meniscal suturing are relatively good, also because the long rehabilitation period after ACL reconstruction offers an optimal time frame for an optimal healing period of the meniscus in the athlete[19]. Biomechanical tests under cyclic loading have shown that vertical sutures are superior to both horizontal sutures and knot-end techniques[21]. The last decade anchors, screws, staples and a variety of other devices have been advocated for the rapid fixation of loose segments[21,22]. However, some of them might damage the articular cartilage when not completely sunk beneath the surface of the meniscus[23]. If tears do not heal, the mechanical forces might in time lead to failure of the fixation. Failure rates of up to 28%-30% of meniscus repair have been reported in literature[24,25]. However, in a review from Boyd and Myers on surgical intervention techniques of the meniscus only a preliminary failure rate of 5.9% was reported[19]. Apparently the results of repair of tears may be compromised

by the lack of vascularity in the white zone of the meniscus. Vessel ingrowth is commonly associated with the ingrowth of non-differentiated progenitor cells, which might be needed in the repair process. A key growth factor in revascularization is vascular endothelial growth factor (VEGF). VEGF is down-regulated in the adult meniscus [26]. The idea rose that coating sutures with VEGF could possibly stimulate vessel ingrowth and subsequent healing of tears. Although more endothelial cells were found in the VEGF/PDLLA sutured intervention group, the tears did not heal. In addition, immunohisto-chemistry showed a strong immunostaining against matrix metalloproteinase 13 (MMP-13). MMPs are involved in the degradation of collagens in the articular cartilage[27-29]. Their effect on meniscus tissue is not known, however the up-regulation of MMPs by VEGF may have unwanted weakening effects on the still healthy matrix of the meniscus and articular cartilage. Devices that stimulate vessel ingrowth by growth factors should therefore be used with great care.

SCAFFOLD MATERIALS FOR MENISCUS REPAIR

The ideal scaffold material should be biocompatible and biodegradable in the long term. Moreover, it should permit unrestricted cellular ingrowth, allow free diffusion of nutrients, may be used as a carrier for stimulatory and inhibitory growth factors, and it should be strong enough to withstand the load in the joint and maintain its structural integrity under these loaded conditions. Furthermore, it should have a degradation profile that allows ingrowth of new tissue and thereafter allows remodeling of these tissues under the influence of load[30].

STIMULATION OF REPAIR BY ACCESS CHANNELS

In the light of the lacking vascularization in the inner white zone, the concept of creating access channels to allow vessel ingrowth was developed. In this approach an extra, preferable small, defect is created in the peripheral rim of the meniscus. The created defect connects the vascularized synovial area and red peripheral zone of the meniscus with the white zone. Various materials can be used to fill the channels and by that stimulate ingrowth of vessels and new tissue. If the channel is left empty, repair is not stimulated [31]. Besides biological tissues[31], also porous polymers, with or without reinforcement with carbon fibers[32-34], were extensively investigated for channel filling. Polymers appeared to be more reliable compared to biological materials [35]. In the polymer implant that is inserted in the access channel, generally, a fibrous tissue is formed that remodels into fibrocartilage-like tissue in time (between 3-6 months)[32,33,36-38]. The tissue that is formed in the tear itself is mainly fibrous[32,33]. The mechanical properties of the newly formed tissues in the inserted scaffold and in the tear are unknown. However, the most important goal of meniscus repair is protection of the articular cartilage. In only a few studies, the effect of polymer filled access channel on the prevention of osteoarthritic degradation was investigated. Van Tienen *et al*. investigated the effect of lesion healing with an access channel filled

with L-lactide/ε-caprolactone in Beagle dogs[39]. Although a positive effect was found on the number of lesions which did heal, the procedure and/or polymer initiated articular cartilage damage[39].

PARTIAL REPLACEMENT AFTER PARTIAL MENISCECTOMY

When a partial meniscectomy is performed and the peripheral meniscal rim is still intact, replacement of the resected tissue only by an implant might be the option of choice. So far, mainly two types of scaffold were advocated for this application in patients. At this moment collagen based scaffolds and synthetic scaffolds based on polymers are being used in clinical trials. The Menaflex™ collagen meniscus implant (CMI) was developed in the 90's. The CMI acts as a temporary template for tissue infiltration, and seems to have the ability to fill the defect with functional repair tissue in time[40-44]. Based on these reports it can be stated that the CMI is biocompatible, resorbable, and may be easily remodeled by new infiltrating tissue. Tissue ingrowth into the CMI may be stimulated by punching the rim with an awl to allow blood infiltration but other mechanisms may also be involved[35]. The main function of the CMI is to conduct tissue to differentiate into neo-meniscal tissue and by that to protect the articular cartilage. Indeed, tissue infiltration occurs in the CMI implant and preclinical and clinical biopsies showed a differentiation into fibrocartilage-like tissue[44]. After 5 years follow-up, partial meniscus replacement with Menaflex™ improved clinical scores in patients and articular cartilage degradation did not progress[45]. However, due to a lack in controls, improvements compared to meniscectomy alone cannot be made.

The second type of scaffold, still in the first clinical test phase (Actifit®, Orteq BV), is based on polycaprolacton-polyurethane (PCLPU), and has been developed and tested for total meniscal replacement in animals (see below in this chapter)[37-39]. This implant is now assessed as a scaffold for partial meniscal replacement as an alternative for the CMI. Based on the preclinical tests, the PCLPU is supposed to be a stiffer material and more resistant to tear which makes this material easier to handle and to suture to the peripheral rim. In addition, mechanical data of contact stresses in sheep cadavers after partial meniscus replacement showed lower contact pressures compared partial meniscectomy only[46]. Recently, results of a case series showed that patients with partial meniscus replacement had an improved clinical outcome and stabilization of improved cartilage condition after 2 years follow-up[47].

COMPLETE REPLACEMENT OF A MENISCUS

If the peripheral rim of the meniscus is damaged, partial replacement is no option and the entire meniscus should be replaced. Several techniques have been evaluated in mainly experimental animal studies, i.e. autologous tissues, like tendon or synovial tissue[48-50], allograft menisci [51-59], various synthetic polymer materials[60-63], and a combination of synthetic materials with autologous tissues[44,51,64].

Allograft meniscus transplantation is the only clinically available technique for total meniscus transplantation. From a biomechanical perspective an allograft may contribute to the restoration of the normal biomechanics of the knee joint[65]. The role in the protection of the articular cartilage remains a point of discussion. Some studies mention the prevention of further osteoarthritic changes[66], however, some animal studies prove the opposite[67]. In rabbits, the observation that a delayed meniscal transplantation induced even more osteoarthritic changes than a meniscectomy without transplantation is worrying[68]. Clinically, disappointing results are often associated with too severe osteoarthritis[69], improper leg alignment[58,70,71], and irradiated donor menisci[72]. By avoiding all these negative determinants, success rates were reported to be in between 60% and 94%[58,69-71,73-75]. Also a study by Wills and Laprade showed excellent results two years after allograft transplantation[76]. However, mainly the poor availability, the sizing of the implant, logistics and costs of the transplant are responsible for the small amount of procedures performed worldwide. An alternative might be a decellularized porcine meniscus[77]. This scaffold was used as xenograft for tissue regeneration after implantation in human. The remaining tissue after processing seemed to be of good biomechanical quality and not cytotoxic in cell culture experiments. This may be an alternative for the allografts in the future. Nevertheless, the search for an artificial replacement material is still ongoing.

The first animal studies on artificial meniscus replacement go back to the early 80's. Already in 1983, the use of a histocompatible Teflon net for ingrowth of regenerating meniscal tissue was described[78]. Although the authors commented on the regenerative effect of the material and the function of the knee joint as being hopeful, later studies on this material were never reported. Messner *et al.* started to use polyurethane coated Teflon or Dacron for meniscus replacement in rabbits[79-81]. The coating seemed favorable for infiltration of tissue, however, all the joints showed signs of degeneration and osteoarthritis. Also coverage of the implant with periosteal tissue did not lead to favorable results[62]. Others studied polyvinyl-alcohol hydrogel scaffold in rabbits. This material seemed to be promising in terms of chondroprotection[82]. However, the material properties needed to be improved to provide higher tear strength for suturing it to the synovium. Other material features like stiffness, and wear- or degradation characteristics were not provided.

In the 80's, our group started a collaboration with the department of polymer chemistry of the State University of Groningen for the development of a biodegradable porous polymer as a scaffold for meniscal tissue regeneration. Already in 1944, Smillie reported some meniscus regenerative capacity in humans[83]. Experimental studies from Moon *et al*. showed also a regenerative capacity in rabbits[84]. Based on this regenerative capacity, we hypothesized that a biodegradable porous polymer implant might be promising. Such an implant would enable the regeneration of a new meniscus in time by tissue ingrowth, and differentiation of the ingrown fibro-vascular tissue simultaneously with a slow degradation of the polymer into non-toxic products. A great advantage of polymers is that the porosity, the degradation rate and the mechanical properties can be adapted to the desired specifications.

The first scaffolds used in this approach consisted of polyurethanes reinforced with carbon fibers and were used for partial replacement of the meniscus[34]. However, the carbon particles induced a synovial inflammation causing extra damage to the joint. Nevertheless, tissue infiltration proved to be possible with porous materials. Newer materials based on polyurethanes have been proven to be superior. These materials were used for meniscus replacement in dogs, and after 6 to 12 weeks the scaffolds were filled with tissue and even had some cartilage protective effect on macroscopic evaluation[85]. In this study, the porous PCLPU polymer, which consists of well-defined hard segments in combination with slowly degrading polyester soft segments, was used[85,86]. The hard segments in combination with the length of the soft segment determine the stiffness of the polymer. Both the initial mechanical properties and the pore size and geometry are important parameters for the final result. Klompmaker *et al.* investigated the ingrowth of new tissue into four polyurethanes with different pore sizes (50-90, 90-150, 150-250 and 250-500 μm) in wedge-shaped defects in the meniscus of rabbits[87]. The macroporosity was 48% to 55%, and total pore volume was between 84% and 86%. In the scaffolds with the large pores, ingrowth into all pores was found. It was concluded that for complete ingrowth and incorporation of partial or total meniscus prostheses, macro-pore sizes must be in the range of 150-500 μm. By varying the initial compressive modulus, the rate of ingrowth and nature of ingrown tissue could be modified. Alternatively the mechanical properties can be controlled by the degree of porosity[86,88]. Even though polymers with a compression modulus of 40 kPa showed fast fibrous tissue ingrowth, no differentiation into fibrocartilage occurred in these scaffolds. The polymers with a compression modulus of 100 kPa however did show abundant fibrocartilage formation[87]. Others found that the scaffolds should have an initial compression modulus of at least 150 kPa to stimulate fibrocartilage formation[5].

A couple of years ago, the results of two short-term studies (3 and 6 months follow-up periods) were published, which used a dog model in which tissue ingrowth, remodeling in the scaffold and changes in mechanical properties were analyzed[37,38]. These data were compared with results of total meniscectomy. After 6 months, the ingrown tissue was fibrous-like in the peripheral zones of the meniscus prosthesis, but in the central areas cartilage-like tissue had developed (Figure 2). The collagen bundles in the pores of the scaffold were mainly directed toward the interconnections between pores, and thus the organization of the matrix was clearly different from the highly organized extracellular matrix of the native meniscus (Figure 3). The stiffness of the implant (compression modulus) after 6 months was intermediate between the compression modulus of the native meniscus and the porous polymer foam. Both the implant and the meniscectomy group showed a similar pattern of cartilage degeneration[37,39]. The results of a two-year study with the same polymer, using an implant with a smoother surface in the same model, did not show additional chondroprotection[46]. This study also showed that the scaffold was initially filled with vital fibrocartilage-like tissue but later on the core of the scaffolds became acellular with the extra-cellular matrix still in place (Figure 4). An explanation for this necrosis

might be the decrease in vascularity that was already observed in the 6 months follow up experiments. Together with the non-resorbed foam and suboptimal loading in the joint, this might have led to an insufficient oxygen supply. The implants did not cause any severe synovitis and microscopically there were no distinct signs of foreign body reaction on the degradation products. Considering the results at this stage, replacement of the whole meniscus with this polymer in a clinical setting seems not justifiable. As we have addressed earlier in this chapter, partial replacement of resected meniscus with this new material might be a valuable alternative at this stage (see paragraph "*Partial replacement after partial meniscectomy*").

From these experiments it is clear that the developed scaffolds did not have the properties needed for optimal chondroprotection. In fact, the scaffolds induced more cartilage abrasion then a meniscectomy at two years follow up. A number of factors may have been contributed to this negative result.

- The *initial mechanical tensile strength* was too low. However, after tissue ingrowth and differentiation the mechanical properties improved [38,89].

- The *tear strength* was too low. Although the initial tear strength might have been sufficient, after the follow up periods of 6 and 24 months most implants were severely damaged by the popliteus tendon. By this the implants might have been pushed peripherally by which they might have lost their chondroprotective properties.

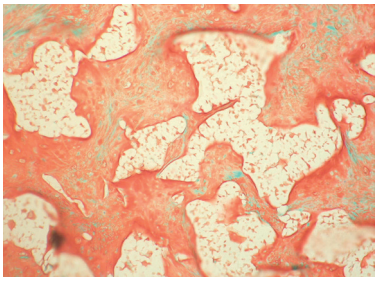

Figure 2. Safranin O stained section of cartilage-like tissue in the highly loaded inner part of the PCLPU implant at 6 months follow up (x200).

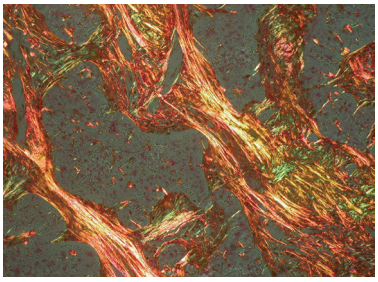

Figure 3. Picro Sirius red stained section showing the direction of the collagen fibers at 6 months follow-up (x200).

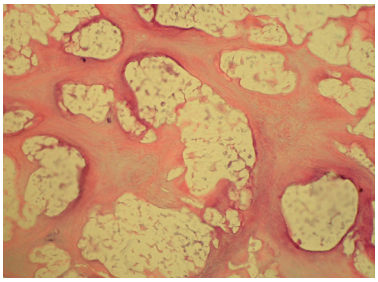

Figure 4. Area in the central region of the anterior part of the PCLPU implant at 24 months after implantation. Notice the absence of living cells (x200).

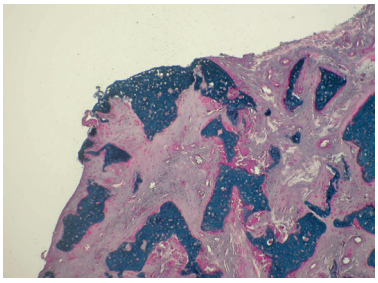

Figure 5. Sudan black stained section of implant at 24 months follow up. Notice the exposure of the PCLPU to the joint cavity (x200).

- The *degradation* of the scaffold was not complete. Even after 24 months, polymer was exposed to the articular surfaces of tibia and femur (Figure 5). The exact effect of this polymer exposure is not known but the more severe degradation of cartilage present in the 24 months implant group indicated that exposure of the implant to the cartilage surface is a negative factor.

- The *animal model* might have been suboptimal. The beagle dog is a relatively small animal for open meniscus surgery.

NEW APPROACHES

An important property of implants is their initial mechanical properties. When mechanical properties of the scaffolds are insufficient, osteoarthritic changes can occur before the infiltrated tissue has differentiated into the typical fibrocartilage that increases the mechanical properties of the implanted scaffold. Because of the relatively poor initial mechanical properties of many scaffolds (e.g. PGA and PGLA scaffolds), pre-seeding the scaffold and subsequently implanting it subcutaneously for a few days in the animal that has to be treated for a period of time (depending on the animal model) to allow tissue ingrowth, may be an option. Then the construct could have improved its mechanical properties, where after it can be used to replace the meniscus[90]. The alternative is to make implants that perfectly match both the geometry of the implant site and have the same initial mechanical properties as the native meniscus.

Furthermore, seeded cells might enhance meniscus regeneration in polymers after transplantation. A promising approach to decrease the initial friction is to pre-seed the scaffolds with cells that can produce matrix before they are implanted[90]. Poly-glycolic acid (PGA) fiber meshes which were mechanically reinforced by bonding PGA fibers at cross points with 75:25 poly(lactic-co-glycolic) acid, were seeded with allogenic meniscal cells. After one week of culture they were implanted into rabbits knees and a regenerated meniscus was formed. Although the authors state that the effect on osteoarthritic changes was improved by the cell-seeding technique, no quantitative data were added to substantiate this statement[91]. More recently, a research group from Bologna, Italy, investigated the use of a novel hyaluronic acid/ polycaprolactone material for meniscal tissue engineering[92]. This novel material was implanted in sheep with and without augmentation with chondrocytes. In addition, two different surgical procedures were tested. Adding chondrocytes did not have any macroscopically detectable effect. A transosseous horn fixation performed better compared to a fixation of the implant to the meniscal ligament. In cell seeded implants more cartilage tissue was found and this implant seemed to reduce cartilage degradation if compared to cell free implants.

Using a self-assembly (SA), scaffoldless method, Aufderheide and Athanasiou showed that a co-culture of meniscal fibrochondrocytes (MFCs) with chondrocytes in an agarose mould resulted in the generation of anisotropic collagen fibrils after 8 weeks[93]. The mechanical properties were even better compared to cells cultured

in PGA scaffolds[93]. It was suggested that the geometric constraint imposed by the ring-shaped, nonadhesive mold guides collagen fibril directionality and, thus, alters mechanical properties. Co-culturing articular chondrocytes (ACs) and MFCs in this manner appears to be a promising new method for tissue engineering fibrocartilaginous tissues exhibiting a spectrum of mechanical and biomechanical properties. A Japanese study showed an increased regenerative and reparative effect on meniscal cells when these cells were added to a platelet rich plasma gel[94].

Murphy and Barry showed that stem cell therapy could be promising for cartilage and meniscus regeneration[95]. They injected mesenchymal stem cells in osteoarthritic knees as a result of earlier ACL transsection and lateral meniscectomy. They showed that this treatment induces a meniscus-like regenerative tissue containing collagen type II and signs of hyaline matrix formation[95].

With the currently available salt leaching techniques our and other groups were able to create open structures in polymers with acceptable biomechanical properties[96,97]. Recently, techniques are developed as Rapid Prototyping to fabricate 3-dimensional scaffolds for tissue-engineering purposes. The mechanical properties of many different soft and hard tissues, including bovine cartilage, could be mimicked by copolymers by using a 3-dimensional fiber deposition technique, simply by varying the scaffold porosity, the scaffold architecture, and/or the copolymer composition[88]. It may be possible to make scaffolds with an optimized pore structure for meniscus regeneration. Ideally, such scaffolds could guide the infiltrating tissue into the preferable direction, for example peripheral collagen fibers into peripheral circumferential tunnels to better withstand hoop stresses during loading of the joint (Figure 6). Furthermore, these techniques may improve the biomechanical properties of the scaffolds and as such their initial performance in the knee joint before the actual tissue infiltration has completed.

An approach to avoid initial damage by high friction of the implant could be to coat the implant materials with substances to promote a smooth frictionless movement in the joint. Particularly hyaluronic acid (HA) and the other constituents

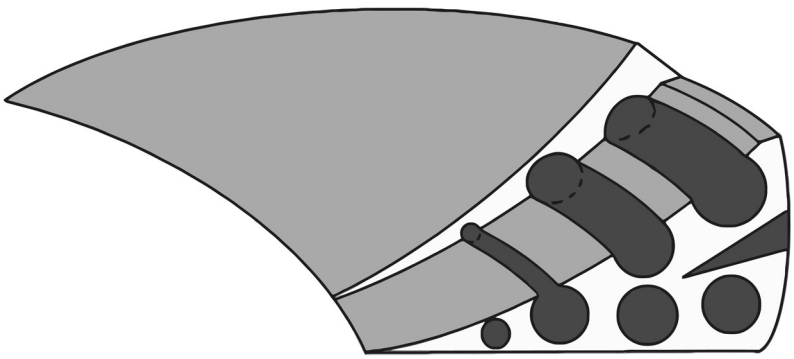

Figure 6. Schematic representation of scaffold design to enable the differentiation of tissue into the desired configuration.

of GAGs, such as the highly hydrated chondroitin sulphate, keratan-sulphate and/or dermatan-sulphate could be used for this purpose. Particularly hyaluronic acid, a non-sulphated glycosaminoglycan, is present in high quantities in the synovial fluid and has a function in the lubrication of the joint. Currently, this substance is used as an injectable material to relieve complaints associated with severe osteoarthritis in patients. It also seems to have a protective effect on cartilage degeneration when used in animal models to prevent damage to the cartilage by surgical interventions[98,99]. HA can also be used as a building block for drug delivery, tissue engineering, wound repair and visco-supplementation[100].

OUTLINE OF THIS THESIS

This thesis shows the results of new potentials for meniscus tissue engineering. The first chapters are mainly focused on engineering a cell based meniscus construct. As stated in the paragraph "*Scaffold materials for meniscus repair"* the ideal scaffold material for meniscus tissue engineering should be biocompatible and biodegradable. The aim for **CHAPTER 2** was to study a new scaffold material for meniscus tissue engineering. Besides biocompatibility and biodegradability, the scaffold should permit cell ingrowth, allow free diffusion of nutrients and should be strong enough to withstand the load in the knee-joint. The scaffold studied is a polyurethane (PU) based on poly D/L lactic acid and polycaprolactone with urethane linkers. Via solvent leaching a porous scaffold was obtained and subsequently tested for above mentioned properties for *in vitro* meniscus tissue engineering.

To increase the potential of the PU scaffold further, incorporation of bioactive macromolecules or growth factors are wanted (paragraph "*Scaffold materials for meniscus repair"*). These macromolecules should increase regeneration speed and quality of repair tissue. The macromolecule of interest is heparin, known for its growth factor adhering capacity and ability to re-differentiate meniscus cells. In **CHAPTER 3** a new surface treatment to coat this PU scaffold was studied.

In paragraph "*New approaches",* current studies of meniscus tissue engineering have been discussed. An interesting option would be pre-culturing cells inside the scaffold. These cells would synthesize matrix and thereby increase mechanical stiffness and reduce incorporation time of the tissue engineered constructs. However, a big limitation of cell cultured constructs lies in the supplements added to the culture medium. Fetal bovine serum is a widely used and potent supplement of culture medium. It is known to induce proliferation and matrix synthesis of a wide variety of cells, including meniscus cells. But due to its bovine origin, application of cell cultured constructs with fetal bovine serum supplemented to the medium is limited due to potential bovine pathogens. Replacement for this fetal bovine serum is highly wanted for safety reasons and could facilitate future clinical applications of cell cultured tissue engineered constructs. In **CHAPTER 4** we analyzed if platelet rich plasma could replace bovine serum in meniscus tissue engineering.

Scaffolds for musculoskeletal tissue engineering, e.g. meniscus and articular cartilage, should follow a number of requirements. A number of these requirements have been tested in chapter 2 and chapter 3. One property of scaffolds not mentioned before is the effect of scaffold architecture in tissue engineering. As proposed in paragraph "*New approaches"*, anisotropic scaffolds with a high porosity and aligned channels can guide extracellular matrix into similar organization as the native meniscus. In **CHAPTER 5** we provided an overview of all current methods to produce different types of anisotropic scaffolds used for musculoskeletal tissue engineering. Subsequently, in **CHAPTER 6** one of the described methods, *modified Thermal Induced Phase Separation*, was used to obtain anisotropic scaffolds from the studied PU scaffold material (chapter 2). Subsequently, these anisotropic scaffolds are tested for the ability to guide extra cellular matrix into similar organization as the native meniscus in a subcutaneous rat pocket model.

In addition to guidance for extracellular matrix, anisotropic scaffolds can also be used to guide cell migration. In articular cartilage repair, micro-fracturing/Pridy-drilling is used to create a channel between the cartilage and the subchondral bone. This enables mesenchymal stem cells from the underlying bone marrow to migrate into defect and regenerate the articular cartilage surface. However, in large defects regeneration is of an inferior fibrous cartilage type. In these large defects, scaffolds can be inserted into the defect to guide and stimulate cell migration, thereby increasing regeneration speed and quality. In **CHAPTER 7** isotropic and anisotropic collagen scaffolds were inserted into articular cartilage defects of a rabbit model, and the effects of scaffold architecture on stem cell migration and articular cartilage regeneration were tested.

In CHAPTER 8 the results of the studies performed in this thesis were summarized and the implementation of this research into future perspectives of meniscus tissue engineering are discussed in **CHAPTER 9**.

REFERENCE LIST

1. Fithian DC, Kelly MA, Mow VC. Material properties and structure-function relationships in the menisci. Clin Orthop Relat Res 1990(252):19-31.
2. Walker PS, Erkman MJ. The role of the menisci in force transmission across the knee. Clin Orthop Relat Res 1975(109):184-92.
3. McDevitt CA, Webber RJ. The ultrastructure and biochemistry of meniscal cartilage. Clin Orthop Relat Res 1990(252):8-18.
4. Macnicol MF, Thomas NP. The knee after meniscectomy. J Bone Joint Surg Br 2000;82(2):157-9.
5. Setton LA, Guilak F, Hsu EW, Vail TP. Biomechanical factors in tissue engineered meniscal repair. Clin Orthop Relat Res 1999(367 Suppl):S254-72.
6. Ghosh P, Taylor TK. The knee joint meniscus. A fibrocartilage of some distinction. Clin Orthop Relat Res 1987(224):52-63.
7. Sun Y, Berger EJ, Zhao C, An KN, Amadio PC, Jay G. Mapping lubricin in canine musculoskeletal tissues. Connect Tissue Res 2006;47(4):215-21.
8. Brindle T, Nyland J, Johnson DL. The meniscus: review of basic principles with application to surgery and rehabilitation. J Athl Train 2001;36(2):160-9.
9. Ververidis AN, Verettas DA, Kazakos KJ, Tilkeridis CE, Chatzipapas CN. Meniscal bucket handle tears: a retrospective study of arthroscopy and the relation to MRI. Knee Surg Sports Traumatol Arthrosc 2006;14(4):343-9.
10. Petersen W, Tillmann B. Collagenous fibril texture of the human knee joint menisci. Anat Embryol (Berl) 1998;197(4):317-24.
11. Christoforakis J, Pradhan R, Sanchez-Ballester J, Hunt N, Strachan RK. Is there an association between articular cartilage changes and degenerative meniscus tears? Arthroscopy 2005;21(11):1366-9.
12. Englund M, Lohmander LS. Risk factors for symptomatic knee osteoarthritis fifteen to twenty-two years after meniscectomy. Arthritis Rheum 2004;50(9):2811-9.
13. Cox JS, Nye CE, Schaefer WW, Woodstein IJ. The degenerative effects of partial and total resection of the medial meniscus in dogs' knees. Clin Orthop Relat Res 1975(109):178-83.
14. Jaureguito JW, Elliot JS, Lietner T, Dixon LB, Reider B. The effects of arthroscopic partial lateral meniscectomy in an otherwise normal knee: a retrospective review of functional, clinical, and radiographic results. Arthroscopy 1995;11(1):29-36.
15. Maletius W, Messner K. The effect of partial meniscectomy on the long-term prognosis of knees with localized, severe chondral damage. A twelve- to fifteen-year followup. Am J Sports Med 1996;24(3):258-62.
16. Hede A, Larsen E, Sandberg H. Partial versus total meniscectomy. A prospective, randomised study with long-term follow-up. J Bone Joint Surg Br 1992;74(1):118-21.
17. Hede A, Larsen E, Sandberg H. The long term outcome of open total and partial meniscectomy related to the quantity and site of the meniscus removed. Int Orthop 1992;16(2):122-5.
18. Ahmed AM. The load-bearing role of the knee meniscus. In: Mow VC, Arnoczky SP, Jackson DW, editors. Knee Meniscus: Basic and Clinical Foundations. New York: Raven Press, Ltd.; 1992. p 59-73.
19. Boyd KT, Myers PT. Meniscus preservation; rationale, repair techniques and results. Knee 2003;10(1):1-11.
20. Linke RD, Ulmer M, Imhoff AB. [Replacement of the meniscus with a collagen implant (CMI)]. Oper Orthop Traumatol 2006;18(5-6):453-62.
21. Farng E, Sherman O. Meniscal repair devices: a clinical and biomechanical literature review. Arthroscopy 2004;20(3):273-86.
22. Miller MD, Kline AJ, Jepsen KG. "All-inside" meniscal repair devices: an experimental study in the goat model. Am J Sports Med 2004;32(4):858-62.
23. Laprell H, Stein V, Petersen W. Arthroscopic all-inside meniscus repair using a new refixation device: a prospective study. Arthroscopy 2002;18(4):387-93.
24. Kurzweil PR, Friedman MJ. Meniscus: Resection, repair, and replacement. Arthroscopy 2002;18(2 Suppl 1):33-9.
25. Lee GP, Diduch DR. Deteriorating outcomes after meniscal repair using the Meniscus Arrow in knees undergoing concurrent anterior cruciate ligament reconstruction: increased failure rate with long-term follow-up. Am J Sports Med 2005;33(8):1138-41.
26. Petersen W, Pufe T, Starke C, Fuchs T, Kopf S, Raschke M, Becker R, Tillmann B. Locally applied angiogenic factors--a new therapeutic tool for meniscal repair. Ann Anat 2005;187(5-6):509-19.
27. Kurz B, Lemke AK, Fay J, Pufe T, Grodzinsky AJ, Schunke M. Pathomechanisms of cartilage destruction by mechanical injury. Ann Anat 2005;187(5-6):473-85.
28. Stoop R, Buma P, van der Kraan PM, Hollander AP, Clark Billinghurst R, Robin Poole A, van den Berg WB.

Differences in type II collagen degradation between peripheral and central cartilage of rat stifle joints after cranial cruciate ligament transection. Arthritis Rheum 2000;43(9):2121-31.
29. Stoop R, van der Kraan PM, Buma P, Hollander AP, Poole AR, van den Berg WB. Denaturation of type II collagen in articular cartilage in experimental murine arthritis. Evidence for collagen degradation in both reversible and irreversible cartilage damage. J Pathol 1999;188(3):329-37.
30. Arnoczky SP. Building a meniscus. Biologic considerations. Clin Orthop Relat Res 1999(367 Suppl):S244-53.
31. Gao JZ. [Experimental study on healing of old tear in the avascular portion of menisci in dogs]. Zhonghua Wai Ke Za Zhi 1990;28(12):726-9, 782.
32. Behling CA, Spector M. Quantitative characterization of cells at the interface of long-term implants of selected polymers. J Biomed Mater Res 1986;20(5):653-66.
33. Veth RP, den Heeten GJ, Jansen HW, Nielsen HK. Repair of the meniscus. An experimental investigation in rabbits. Clin Orthop Relat Res 1983(175):258-62.
34. Veth RP, Jansen HW, Leenslag JW, Pennings AJ, Hartel RM, Nielsen HK. Experimental meniscal lesions reconstructed with a carbon fiber-polyurethane-poly(L-lactide) graft. Clin Orthop Relat Res 1986(202):286-93.
35. Buma P, van Tienen T, Veth R. The collagen meniscus implant. Expert Rev Med Devices 2007;4(4):507-16.
36. Klompmaker J, Jansen HW, Veth RP, Nielsen HK, de Groot JH, Pennings AJ, Kuijer R. Meniscal repair by fibrocartilage? An experimental study in the dog. J Orthop Res 1992;10(3):359-70.
37. van Tienen TG, Heijkants RG, de Groot JH, Pennings AJ, Schouten AJ, Veth RP, Buma P. Replacement of the knee meniscus by a porous polymer implant: a study in dogs. Am J Sports Med 2006;34(1):64-71.
38. van Tienen TG, Heijkants RG, de Groot JH, Schouten AJ, Pennings AJ, Veth RP, Buma P. Meniscal replacement in dogs. Tissue regeneration in two different materials with similar properties. J Biomed Mater Res B Appl Biomater 2006;76(2):389-96.
39. van Tienen TG, Heijkants RG, Buma P, De Groot JH, Pennings AJ, Veth RP. A porous polymer scaffold for meniscal lesion repair--a study in dogs. Biomaterials 2003;24(14):2541-8.
40. Choi G, Vigorita VJ, DiCarlo EF. Second-look biopsy study of human collagen meniscal implants: A histological analysis of 81 cases.; 2008. p 128.
41. Reguzzoni M, Manelli A, Ronga M, Raspanti M, Grassi FA. Histology and ultrastructure of a tissue-engineered collagen meniscus before and after implantation. J Biomed Mater Res B Appl Biomater 2005;74(2):808-16.
42. Rodkey WG, Steadman JR, Li ST. A clinical study of collagen meniscus implants to restore the injured meniscus. Clin Orthop Relat Res 1999(367 Suppl):S281-92.
43. Steadman JR, Rodkey WG. Tissue-engineered collagen meniscus implants: 5- to 6-year feasibility study results. Arthroscopy 2005;21(5):515-25.
44. Stone KR, Steadman JR, Rodkey WG, Li ST. Regeneration of meniscal cartilage with use of a collagen scaffold. Analysis of preliminary data. J Bone Joint Surg Am 1997;79(12):1770-7.
45. Bulgheroni P, Murena L, Ratti C, Bulgheroni E, Ronga M, Cherubino P. Follow-up of collagen meniscus implant patients: clinical, radiological, and magnetic resonance imaging results at 5 years. Knee 2010;17(3):224-9.
46. Brophy RH, Cottrell J, Rodeo SA, Wright TM, Warren RF, Maher SA. Implantation of a synthetic meniscal scaffold improves joint contact mechanics in a partial meniscectomy cadaver model. J Biomed Mater Res A 2010;92(3):1154-61.
47. Verdonk P, Beaufils P, Bellemans J, Djian P, Heinrichs EL, Huysse W, Laprell H, Siebold R, Verdonk R, Actifit Study G. Successful treatment of painful irreparable partial meniscal defects with a polyurethane scaffold: two-year safety and clinical outcomes. Am J Sports Med 2012;40(4):844-53.
48. Bruns J, Kahrs J, Kampen J, Behrens P, Plitz W. Autologous perichondral tissue for meniscal replacement. J Bone Joint Surg Br 1998;80(5):918-23.
49. Kohn D, Wirth CJ, Reiss G, Plitz W, Maschek H, Erhardt W, Wulker N. Medial meniscus replacement by a tendon autograft. Experiments in sheep. J Bone Joint Surg Br 1992;74(6):910-7.
50. Veth RP, den Heeten GJ, Jansen HW, Nielsen HK. An experimental study of reconstructive procedures in lesions of the meniscus. Use of synovial flaps and carbon fiber implants for artificially made lesions in the meniscus of the rabbit. Clin Orthop Relat Res 1983(181):250-4.
51. Cummins JF, Mansour JN, Howe Z, Allan DG. Meniscal transplantation and degenerative articular change: an experimental study in the rabbit. Arthroscopy 1997;13(4):485-91.
52. Kohn D, Verdonk R, Aagaard H, Seil R, Dienst M. Meniscal substitutes--animal experience. Scand J Med Sci Sports 1999;9(3):141-5.
53. Messner K, Kohn D, Verdonk R. Future research in meniscal replacement. Scand J Med Sci Sports 1999;9(3):181-3.
54. Rijk PC. Meniscal allograft transplantation--part II: alternative treatments, effects on articular cartilage, and future directions. Arthroscopy 2004;20(8):851-9.
55. Rijk PC. Meniscal allograft transplantation--part I: background, results, graft selection and preservation, and

surgical considerations. Arthroscopy 2004;20(7):728-43.
56. Rijk PC, Tigchelaar-Gutter W, Bernoski FP, Van Noorden CJ. Functional changes in articular cartilage after meniscal allograft transplantation: a quantitative histochemical evaluation in rabbits. Arthroscopy 2006;22(2):152-8.
57. Stone KR. Meniscus replacement. Clin Sports Med 1996;15(3):557-71.
58. van Arkel ER, de Boer HH. Survival analysis of human meniscal transplantations. J Bone Joint Surg Br 2002;84(2):227-31.
59. Verdonk R, Kohn D. Harvest and conservation of meniscal allografts. Scand J Med Sci Sports 1999;9(3):158-9.
60. King D. The healing of semilunar cartilages. 1936. Clin Orthop Relat Res 1990(252):4-7.
61. Kobayashi M, Toguchida J, Oka M. Preliminary study of polyvinyl alcohol-hydrogel (PVA-H) artificial meniscus. Biomaterials 2003;24(4):639-47.
62. Messner K, Lohmander LS, Gillquist J. Cartilage mechanics and morphology, synovitis and proteoglycan fragments in rabbit joint fluid after prosthetic meniscal substitution. Biomaterials 1993;14(3):163-8.
63. Wood DJ, Minns RJ, Strover A. Replacement of the rabbit medial meniscus with a polyester-carbon fibre bioprosthesis. Biomaterials 1990;11(1):13-6.
64. Stone KR, Rodkey WG, Webber R, McKinney L, Steadman JR. Meniscal regeneration with copolymeric collagen scaffolds. In vitro and in vivo studies evaluated clinically, histologically, and biochemically. Am J Sports Med 1992;20(2):104-11.
65. Alhalki MM, Hull ML, Howell SM. Contact mechanics of the medial tibial plateau after implantation of a medial meniscal allograft. A human cadaveric study. Am J Sports Med 2000;28(3):370-6.
66. Aagaard H, Jorgensen U, Bojsen-Moller F. Reduced degenerative articular cartilage changes after meniscal allograft transplantation in sheep. Knee Surg Sports Traumatol Arthrosc 1999;7(3):184-91.
67. Rijk PC, de Rooy TP, Coerkamp EG, Bernoski FP, van Noorden CJ. Radiographic evaluation of the knee joint after meniscal allograft transplantation. An experimental study in rabbits. Knee Surg Sports Traumatol Arthrosc 2002;10(4):241-6.
68. Rijk PC, Van Eck-Smit BL, Van Noorden CJ. Scintigraphic assessment of rabbit knee joints after meniscal allograft transplantation. Arthroscopy 2003;19(5):506-10.
69. Noyes FR, Barber-Westin SD. Irradiated meniscus allografts in the human knee. A two to five year follow-up study. Orthop Trans 1995;19:417.
70. van Arkel ER, de Boer HH. Human meniscal transplantation. Preliminary results at 2 to 5-year follow-up. J Bone Joint Surg Br 1995;77(4):589-95.
71. van Arkel ER, Goei R, de Ploeg I, de Boer HH. Meniscal allografts: evaluation with magnetic resonance imaging and correlation with arthroscopy. Arthroscopy 2000;16(5):517-21.
72. Yahia LH, Drouin G, Zukor D. The irradiation effect on the initial mechanical properties of meniscal grafts. Biomed Mater Eng 1993;3(4):211-21.
73. Garret JC. Free meniscal transplantation: a prospective study of 44 cases. Arthroscopy 1993;9:368-369.
74. Milachowski KA, Weismeier K, Wirth CJ. Homologous meniscus transplantation. Experimental and clinical results. Int Orthop 1989;13(1):1-11.
75. Rath E, Richmond JC. The menisci: basic science and advances in treatment. Br J Sports Med 2000;34(4):252-7.
76. Wills NJ, LaPrade RF. Clinical outcomes of meniscal allografts.; 2008. p 127.
77. Stapleton TW, Ingram J, Katta J, Knight R, Korossis S, Fisher J, Ingham E. Development and characterization of an acellular porcine medial meniscus for use in tissue engineering. Tissue Eng Part A 2008;14(4):505-18.
78. Toyonaga T, Uezaki N, Chikama H. Substitute meniscus of Teflon-net for the knee joint of dogs. Clin Orthop Relat Res 1983(179):291-7.
79. Messner K, Fahlgren A, Persliden J, Andersson BM. Radiographic joint space narrowing and histologic changes in a rabbit meniscectomy model of early knee osteoarthrosis. Am J Sports Med 2001;29(2):151-60.
80. Messner K, Gillquist J. Prosthetic replacement of the rabbit medial meniscus. J Biomed Mater Res 1993;27(9):1165-73.
81. Sommerlath K, Gillquist J. The effect of a meniscal prosthesis on knee biomechanics and cartilage. An experimental study in rabbits. Am J Sports Med 1992;20(1):73-81.
82. Kobayashi M, Chang YS, Oka M. A two year in vivo study of polyvinyl alcohol-hydrogel (PVA-H) artificial meniscus. Biomaterials 2005;26(16):3243-8.
83. Smillie IS. Observations on the regeneration of the semilunar cartilages in man. Br J Surg 1944;31:398-401.
84. Moon MS, Kim JM, Ok IY. The normal and regenerated meniscus in rabbits. Morphologic and histologic studies. Clin Orthop Relat Res 1984(182):264-9.
85. Klompmaker J, Veth RP, Jansen HW, Nielsen HK, de Groot JH, Pennings AJ. Meniscal replacement using a porous polymer prosthesis: a preliminary study in the dog. Biomaterials 1996;17(12):1169-75.

86. Heijkants RG, van Calck RV, van Tienen TG, de Groot JH, Buma P, Pennings AJ, Veth RP, Schouten AJ. Uncatalyzed synthesis, thermal and mechanical properties of polyurethanes based on poly(epsilon-caprolactone) and 1,4-butane diisocyanate with uniform hard segment. Biomaterials 2005;26(20):4219-28.
87. Klompmaker J, Jansen HW, Veth RP, Nielsen HK, de Groot JH, Pennings AJ. Porous implants for knee joint meniscus reconstruction: a preliminary study on the role of pore sizes in ingrowth and differentiation of fibrocartilage. Clin Mater 1993;14(1):1-11.
88. Moroni L, Poort G, Van Keulen F, de Wijn JR, van Blitterswijk CA. Dynamic mechanical properties of 3D fiber-deposited PEOT/PBT scaffolds: an experimental and numerical analysis. J Biomed Mater Res A 2006;78(3):605-14.
89. van Tienen TG, Heijkants RG, Buma P, de Groot JH, Pennings AJ, Veth RP. Tissue ingrowth and degradation of two biodegradable porous polymers with different porosities and pore sizes. Biomaterials 2002;23(8):1731-8.
90. Ibarra C, Ellisseff J, Vacanti JP, Cao Y, Kim TH, Upton J, Langer R, Vacanti CA. Meniscal tissue engineered by subcutaneous implantation of fibrochondrocytes on polymer develops biomechanical compressive properties similar to normal meniscus. . 1997. p 549.
91. Kang SW, Son SM, Lee JS, Lee ES, Lee KY, Park SG, Park JH, Kim BS. Regeneration of whole meniscus using meniscal cells and polymer scaffolds in a rabbit total meniscectomy model. J Biomed Mater Res A 2006;78(3):659-71.
92. Kon E, Chiari C, Marcacci M, Delcogliano M, Salter DM, Martin I, Ambrosio L, Fini M, Tschon M, Tognana E and others. Tissue engineering for total meniscal substitution: animal study in sheep model. Tissue Eng Part A 2008;14(6):1067-80.
93. Aufderheide AC, Athanasiou KA. Assessment of a bovine co-culture, scaffold-free method for growing meniscus-shaped constructs. Tissue Eng 2007;13(9):2195-205.
94. Ishida K, Kuroda R, Miwa M, Tabata Y, Hokugo A, Kawamoto T, Sasaki K, Doita M, Kurosaka M. The regenerative effects of platelet-rich plasma on meniscal cells in vitro and its in vivo application with biodegradable gelatin hydrogel. Tissue Eng 2007;13(5):1103-12.
95. Murphy JM, Fink DJ, Hunziker EB, Barry FP. Stem cell therapy in a caprine model of osteoarthritis. Arthritis Rheum 2003;48(12):3464-74.
96. Chiari C, Koller U, Dorotka R, Eder C, Plasenzotti R, Lang S, Ambrosio L, Tognana E, Kon E, Salter D and others. A tissue engineering approach to meniscus regeneration in a sheep model. Osteoarthritis Cartilage 2006;14(10):1056-65.
97. de Groot JH, Zijlstra FM, Kuipers HW, Pennings AJ, Klompmaker J, Veth RP, Jansen HW. Meniscal tissue regeneration in porous 50/50 copoly(L-lactide/epsilon-caprolactone) implants. Biomaterials 1997;18(8):613-22.
98. Han F, Ishiguro N, Ito T, Sakai T, Iwata H. Effects of sodium hyaluronate on experimental osteoarthritis in rabbit knee joints. Nagoya J Med Sci 1999;62(3-4):115-26.
99. Kobayashi K, Amiel M, Harwood FL, Healey RM, Sonoda M, Moriya H, Amiel D. The long-term effects of hyaluronan during development of osteoarthritis following partial meniscectomy in a rabbit model. Osteoarthritis Cartilage 2000;8(5):359-65.
100. Luo Y, Prestwich GD. Hyaluronic acid-N-hydroxysuccinimide: a useful intermediate for bioconjugation. Bioconjug Chem 2001;12(6):1085-8.

Chapter 2

Proliferation of meniscal fibrochondrocytes cultured on a new polyurethane scaffold is stimulated by TGF-beta

J. Biomaterials Applications, 2013

Eric de Mulder
Gerjon Hannink
Maud Giele
Nico Verdonschot
Pieter Buma

ABSTRACT

The aim of this study was to investigate if newly developed polyurethane (PU) scaffolds are suitable as scaffold for cell seeded meniscus tissue engineered constructs. Scaffolds were seeded with goat meniscal fibrochondrocytes and cultured to assess changes in biological and mechanical properties. Furthermore, the effect of TGF-β on these properties were investigated. For this PU scaffolds were made from poly D/L lactide and caprolactone as soft segments and 1,4-butanediisocyanate for the urethane hard segments. The porosity of the scaffolds was 95%. Isolated goat meniscal fibrochondrocytes were seeded on the scaffolds and cultured with or without the addition of 10 ng/ml TGF-β in standard culture medium. After 2, 4 and 6 weeks of culture, scaffolds were analyzed for cell proliferation, matrix synthesis and mechanical properties.

Results of scanning electron microscopy and histology showed that the scaffolds had an interconnected isotropic pore structure. Without addition of TGF-β cells did not proliferate during the culture period and isolated meniscus fibrochondrocytes were more frequently located in the peripheral parts of the scaffold. Fibrochondrocytes supplemented with TGF-β were distributed throughout the construct. Clustered cells were surrounded by matrix which stained slightly positive for GAGs. Also collagen production was increased significantly after 4 and 6 weeks of culture compared to cultures without TGF-β and also more GAG staining was found after 4 and 6 weeks in the sections of the TGF-β stimulated cultures. Despite the increase in matrix production, the compressive stiffness of the constructs was not increased during the culture period.

In conclusion, meniscal fibrochondrocytes were able to adhere to the polyurethane scaffold. However, the scaffold itself does not stimulate proliferation and matrix production. The addition of TGF-β resulted in a strong induction of both proliferation and extracellular matrix production.

INTRODUCTION

Menisci are semilunar shaped structures located in pairs in each knee joint. They fill the gap between the round femoral condyle and the rather flat (medial) or even concave (lateral) tibia plateau. Although the meniscus has quite a number of functions in the knee joint, the main function of the meniscus is to distribute stresses in a homogenous way over the articular surfaces of the tibia and femur. To withstand the high forces in the knee, the fibro-cartilage of the meniscus has a highly circumferentially oriented type I collagen fiber organization. Moreover, it contains also type II collagen and some glycosaminoglycans (GAG's), particularly in the inner highly loaded part of the meniscus[1]. The composition of the tissue enables the meniscus to withstand compressive and tensile shear forces and to maintain its position under load. Thereby it transfers axial loads into circumferential directed forces[2,3].

Meniscus injury will generate pain and cause mechanical locking of the knee joint. The most frequent occurring meniscus trauma's are tears. The peripheral part of the meniscus is the so-called red zone which is vascularized. Since vascularization is a key player in regeneration after trauma[4,5], tears in this location normally can heal[4-6]. When tears occur in the inner 2/3 of the meniscus, also called the white zone of the meniscus, no or very limited regeneration is possible due to a lack of vascularization.

The flap tear and bucket handle tear are the most common meniscus injuries. In the past, the resulting loose fragments were arthroscopically removed. Although this treatment is an enormous improvement compared to a total meniscectomy, even a partial meniscectomy will result in osteoarthritic changes in the articular cartilage[7]. Also the amount of meniscal tissue removed has a direct relationship with the induction of late osteoarthritis[8,9]. Upon removal of meniscal tissue more load is directly transferred from the condyles to the tibial plateau resulting in large peak stresses which causes an early onset of osteoarthritis[3,7]. Therefore, in order to preserve the contact area of the meniscus, the general practice these days is fixation of the loose fragment to the main body of the meniscus by suturing, anchors or screws[10]. Unfortunately the used fixation devices are still inferior to cope with the forces applied on the meniscus, resulting in high rates of ruptures or even osteochondral defects[11]. When fixation is not possible or insufficient, a partial meniscectomy is inevitable.

Regeneration of the lost part of the meniscus would be the most optimal treatment. A scaffold that replaces the meniscus tissue could guide new tissue ingrowth into the lost meniscus and by that meniscus regeneration could be established. Two implants based on scaffolds are already in clinical use, namely a scaffold based on collagen (Menaflex™) and one based on a synthetic polymer(Actifit®)[12,13]. The Menaflex™ implant has already been implanted for a number of years and supports ingrowth of new meniscus like tissue. However, the scaffold shrinks in size after 5 years[13-15]. The Actifit® implant, based on a synthetic caprolactone-urethane polymer,

is only recently available in Europe. Preclinical animal experiments showed that implantation of this scaffold in a partial defect will enable equal contact pressures as a normal meniscus, whereas without implantation contact pressures increase[16]. After implantation the scaffold had rapid ingrowth of tissue and no cartilage defects were present after one year[17]. These experiments were conducted in partial meniscus defects, but when implanted as a total meniscus replacement, the scaffold was not strong enough and failed to protect the cartilage from damage[18,19]. Recently, the first patient study with Actifit® as a partial replacement has been published. After one year follow up, implant was integrated with native meniscus tissue, and biopsies showed fully vital tissue[20].

In contrast to partial meniscal replacement, the only clinical used treatment for total meniscus replacement is allograft transplantation[21]. Even though clinical results are satisfactory, there exists a minor risk of disease transfer, the availability is limited due size matching and the allograft meniscus can re-tear, shrink and dislocate[22].

Tissue engineering could be a promising alternative approach to replace the lost tissue after (partial) menisectomy. Pre-cultured cell seeded scaffolds showed better integration with the surrounding meniscus tissue in an *ex vivo* setup[23]. Also in *in vivo* experiments cell seeded constructs showed better integration with adjacent tissue after implantation in defects[24,25]. Pre-seeding cells on a scaffold also strongly improved the mechanical properties compared to the initial scaffold[26]. Three cell types are most often used so far, namely mesenchymal stem cells (MSC)[23], chondrocytes[27], meniscal fibrochondrocytes (MFCs)[28], or a combination of these cell types[27]. Which cell type is best suited for these cell seeded constructs remains unknown. To stimulate these cell based meniscal constructs, a number of growth factors (GF) have been tested. Most commonly used are TGF-β, IGF, bFGF and PDGF[28-32]. These GFs stimulate cell proliferation, matrix production and migration, thereby reducing the time needed to engineer new meniscus tissue.

Which type of scaffold is best suited for meniscus TE is still pending. Scaffolds of many different composites, e.g., based on hydrogels, biologic polymer (collagen / silk) or synthetic polymer (PLA / PGA / PCL), have been described in literature[18,33,34]. A synthetic polymer scaffold with very promising characteristics has already been described in detail by Spaans *et al*. and van Minnen *et al*.[35,36]. They synthesized a polyurethane (PU) co-polymer porous scaffold with poly D/L lactic acid and poly-ε-caprolactone as soft block segments and 1,4-butanediisocyanate as hard block urethane segments[36]. These highly porous scaffolds were tested both *in vitro* and *in vivo* for cytotoxicity and degradation. The *in vitro* experiments showed that after 12 weeks only 3.4% mass was degraded, thereby categorized as a slow degrading scaffold. Cytotoxicity tests showed that scaffolds did not change the proliferation speed and metabolic activity of fibroblast after direct contact[37]. The long term test showed some cytotoxicity, however, this was ascribed to the accumulation of degradation products in their *in vitro* test system[37]. The *in vivo* experiments of short till long term subcutaneous implantation showed no toxicity. The scaffolds followed

a gradual resorption pattern over 3 years. First encapsulation and infiltration with connective tissue was observed. Subsequently, degradation and resorption by macrophages and giant cells was found. Scaffolds were not completely resorbed after 3 years but they expected it to be totally resorbed after 3.5 – 4 years[38].

The PU described above has a number of novel aspects compared to other synthetic polymer scaffolds previously used for meniscus tissue engineering purposes or in clinical practice. The scaffold described in this study has a 95% porosity compared to approximately 80% porosity of most other scaffolds[19,39]. This high porosity is required to increase surface area for cell attachment, tissue ingrowth and moreover, facilitating adequate transport of nutrients and cellular waste products[40]. With decreasing porosity, nutrient and waste exchange of cells in the deeper regions is limited, leading to necrotic sites in the center of the scaffold[19]. Another advantage of a high porosity is that it, in general, will lead to a faster speed of resorption as less polymer material has to be degraded. Reducing the time foreign materials remain present in the body has been shown to lower the risk on immunological responses. In addition, with smaller amounts of polymer material to be degraded, lower acidic levels will be reached. Higher acidity levels are known to reduce tissue regeneration speed[37]. The high porosity of the material used in our study also aims to ensure a faster resorption rate, low immunological risk, and high tissue regeneration speed. Furthermore, the use of a co-polymer from caprolactone and both isomers of lactic acid exclude crystalline regions in this material. It has been described that increasing crystallinity results in highly stable remnants and increase inflammatory risk in a late degradation stage[41].

The aim of this study was to improve the properties of the PU scaffolds as described by van Minnen *et al*.[36] by a tissue engineering approach for total meniscus replacement. Pre-seeding cells on scaffolds could have beneficial effects on biological and mechanical properties. In this study biological properties (i.e. proliferation, distribution and matrix production) were tested after culture MFCs on this PU scaffold. Furthermore, we tested the effect of TGF-β on these biological properties. Finally the mechanical properties of this tissue engineered construct was determined to assess whether it is comparable to native meniscus.

MATERIAL AND METHODS

Scaffold preparation.

Scaffolds were composed of 50% DL(50/50)-lactide (PDLLA, Purac) and 50% ε-caprolactone (PCL, Acros Organics) by ring opening polymerization with 1,4-butanediol (BDO) as initiator. The final macrodiol prepolymer had a molecular weight (M_N) of 2000 g/mole. Subsequently this was end-capped with 1,4-butanediisocyanate (BDI). Chain extension was performed with a BDO-BDI-BDO urethane block which resulted in a hard block urethane segment with a uniform length of five urethane moieties. Final PU consisted of 22.5 w/w % hard urethane

segments and 77.5 w/w % amorphous polyester soft segments. Polymers were solvent casted, frozen and lyophilized. The obtained scaffolds had a 95% porosity[36]. Finally, scaffolds were frozen in liquid N_2, punched with a 6 mm internal diameter dermal punch and cut into 3 mm high cylinders. After cutting the scaffolds, SEM images were made to evaluate the internal pore structure of the scaffolds (JEOL JSM 6310, JEOL Ltd, Herts, UK).

Cell isolation

Both lateral and medial menisci from four skeletal mature female Dutch milk goats (Capra Hircus Sana) were isolated immediately after sacrifice under aseptic conditions. Tissue collection was approved by the Animal Ethics Committee of the Radboud University, Nijmegen. Isolation of meniscal fibrochondrocytes was performed according to earlier reported protocols[28]. In short, menisci were washed 3 times with PBS/1x PSF (Penicillin/streptomycin/fungizone, Gibco, Carlsbad, CA USA). Subsequently, the outer rim was removed and inner part was cut into small pieces. These pieces were digested in DMEM/F12 + 1x PSF with 3 mg/ml collagenase II (Worthington, Lakewood, NJ USA) for 48 hour in a 5% CO_2, 37^{O}C controlled culture incubator. Digest was filtered over 70 µm tissue filter bags and filtrate was centrifuged for 10 min at 1100 rpm to pellet the cells. Cells were washed 2 times with PBS and plated in culture flasks. Cells were cultured in standard medium (DMEM/F12 + 10% FBS + 1x PSF) in a culture incubator. At 70% confluence cells were passed once by trypsinization using standard procedures. Passage 1 cells were harvested, frozen in cryo-vials and preserved in liquid nitrogen until use.

Cell culture

Before start of the experiment cells were defrosted and expanded twice. Finally, cells were isolated, counted and used for cell culture experiments. MFCs isolated had a >95% cell viability determined by trypaan blue exclusion. Scaffolds were ethanol desinfected in series till 96% EtOH, washed three times with sterile PBS and incubated o/n in standard culture medium. Scaffolds were squeezed to remove excess medium and passage 4 MFCs, a total of $5x10^5$ in 50 µl, were placed on top of each scaffold and incubated for 60 minutes in an incubator. After incubation standard medium was added with or without 10 ng/ml TGF-β (R&D Systems, Minneapolis, MN USA). Total medium was refreshed three times a week.

Pilot tests were performed with different concentrations of TGF-β (1 ng, 10 ng and 100 ng/ml). If 10 ng/ml or 100 ng/ml was added, proliferation was shown to increase. However, no differences were observed between 10 ng and 100 ng. Therefore 10 ng/ml was used in the current experiments. Scaffolds were cultured for 2, 4 and 6 weeks without or with the addition of 10 ng/ml TGF-β in standard medium and performed in triplo.

Picogreen analyses

After 2, 4 and 6 weeks of culture samples were washed with PBS and frozen in Milli Q. After repeated freeze/thaw cycles samples were measured using PicoGreen dsDNA assay kit as per manufacturer's protocol (Invitrogen, Carlsbad, CA USA).

Collagen analyses

After 2, 4 and 6 weeks of culture samples were washed and frozen in PBS. Samples were analyzed to quantify the amount of collagen using a colorimetric hydroxyproline assay[42]. In short, samples were hydrolyzed in 6N HCl by autoclaving for 20 hours at 110^{O}C. The hydrolyzate was washed twice with Milli Q. Chloramin-T was added and incubated for 20 minutes at room temperature. Subsequently, Ehrlich's reagent was added and chromophore was developed during 20 minutes at 60^{O}C. Finally, absorbance was read at 570 nm using a spectrophotometer.

Routine histology

Scaffolds were paraffin embedded and sections of 7 μm in thickness were cut. Sections were deparaffinized, and rehydrated. Oil Red O with hematoxylin (ORO/H) for cell staining, and alcian blue for GAG staining, were used for routine histology. For ORO/H staining, sections were shortly incubated in oil red O. Hereafter cell nuclei were counterstained with hematoxylin and mounted with aquamount. For alcian blue, sections were washed in 3% acetic acid, incubated for 45 min in alcian blue. After washing cell nuclei were counterstained with nucleus red and mounted with DPX. All samples were analyzed under light microscopy and pictures were recorded with an Olympus digital camera and a photo program software (analySIS Soft Imaging System, GmbH, Münster, Germany).

Mechanical analyses

At day 0 and after 2, 4, and 6 weeks of culture samples were tested for mechanical stiffness. Samples were placed in a Bose ElectroForce BioDynamic bioreactor mounted with a 22N load cell housed in a 37^{O}C incubator (BOSE, MN USA). The specimen chamber was filled with PBS and scaffolds were compressed at 1 mm/min till 20% compression. With the obtained stress/strain curve the Young's Modulus was calculated as the steepness of this curve.

Statistics

A two way ANOVA was used on all datasets with treatment (TGF yes/no) and time (0, 2, 4 and 6 weeks) as factors. All data were expressed as mean ± SEM. For all experiments, differences were considered statistically significant for P values <0.05. Statistical analysis was performed using SPSS 16.0 software (SPSS Inc., Chicago, IL USA).

RESULTS

SEM analyses

SEM images showed that the scaffolds had macro-pores in the range from 100-300 µm in diameter. All macro-pores were interconnected by micro-pores ranging from 10-30 µm. Furthermore, an overall isotropic pore architecture was observed (Figure 1). Histology of scaffolds not used for culture experiments confirmed the isotropy of the scaffolds.

Cell quantification

The picogreen analyses showed a significant increase in the amount of DNA of TGF-β stimulated cultures at each time point compared to the non-stimulated cultures ($p<0.001$, Figure 2). The effect of treatment was also shown over time. Untreated samples did not differ over time, in contrast to DNA content of TGF-β treated samples, that did increase over time ($p<0.001$). The difference in cell quantity was highest after 6 weeks of culture. DNA content was 3.75x higher in the TGF-β stimulated group compared to the non-stimulated group (Figure 2).

Collagen quantification

Non-stimulated cell cultures did not show any increase in collagen production per scaffold over time ($p>0.99$). TGF-β stimulated cell cultures expressed a higher amount of collagen content. After 6 weeks of culture the TGF-β stimulated group synthesized 15.6 times more collagen compared to standard culture medium group, 15.6 µg/scaffold and 1.0 µg/scaffold, respectively ($p<0.001$). This increase was also time dependant since

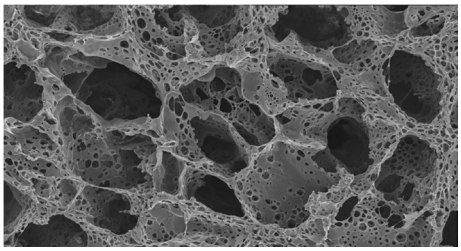

Figure 1: SEM image of the PU scaffold used for cell culture. Diameters range from 100 – 300 µm for the macro pores and 10 - 30 µm for the interconnected pores. Pores were isotropically distributed throughout the scaffold.

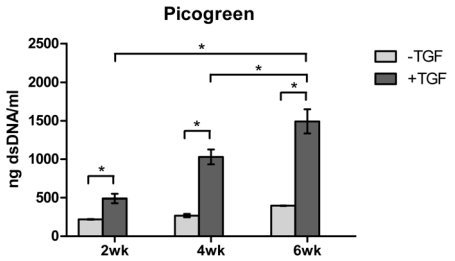

Figure 2: Picogreen assay of cell cultures on scaffolds treated with of without TGF-β. Untreated samples did not increased significant in time. Treated samples did significantly increase over time. Treated samples are also significant higher in DNA content compared to untreated samples (n=3).

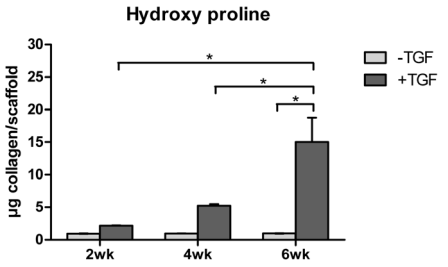

Figure 3: Collagen synthesis of constructs after 2, 4 and 6 weeks of culture determined by a colorimetric hydroxyproline assay. The 6 week TGF-β treated group is significantly higher compered to the untreated group (n=3).

this was significantly higher compared to the 2 and 4 week cultured scaffolds with TGF-β ($p<0.001$, Figure 3).

Histological analyses

Irrespective to the culture period, isolated MFCs were homogeneously distributed throughout the scaffolds which were not stimulated by TGF-β, however, in the periphery slightly more cells were present. After 6 weeks of culture more cells were present at the outer surface but they did not formed a continuous layer. No matrix was seen around the cells with alcian blue staining indicating that cells did not produce matrix (Figure 4).

In the cultures stimulated with TGF-β, more cells were present. Already after a culture period of two weeks more cell clusters were found than isolated cells, not only on the surface of the scaffolds but also in the deeper regions. After 4 and 6 weeks the difference with the non-stimulated scaffolds was even more pronounced. On the surface of the scaffold a continuous layer of MFCs surrounding the scaffold was present. Clusters of cells were found up to the centre of the scaffolds. With the alcian blue staining the difference between non stimulated and stimulated cultures was further illustrated. After 4 and 6 weeks GAG positive matrix was observed around cells in the TGF-β treated groups (Figure 4).

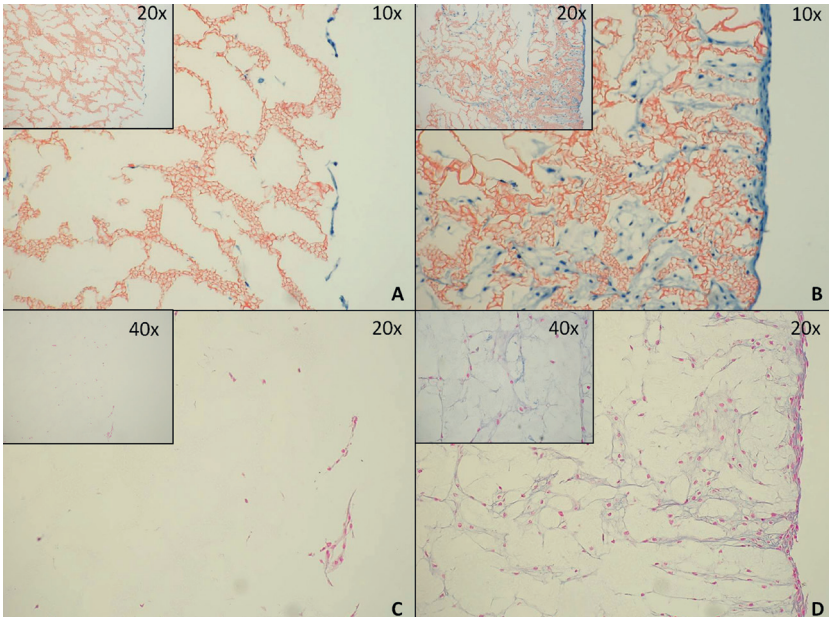

Figure 4: Oil red O / Hematoxylin (A, B) and aclian blue stainings (C,D) of the scaffolds cultered with MFCs after 6 weeks. Panel A and C are non-stimulated cultures. Panels B and D with TGF-ß. Proliferation and higher numbers of MFCs in the center are clearly visible in the TGF-ß treated group. Lower panel showes alcian blue staining to visualize GAG's. Only in the TGF-ß treated groups GAG formation is seen around cell clusters.

Mechanical analysis

No significant differences were found in Youngs moduli between scaffolds cultured with or without TGF-β. In time the control scaffolds without cells did not change in mechanical stiffness. For the cell cultured constructs no change in Young's modulus in time was measured as well (Figure 5).

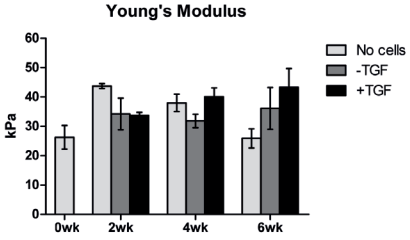

Figure 5: The compressive Young's modulus was determined by compressing the scaffolds till 20% at 1 mm/min in PBS at 37°C. No significant decrease or increase of mechanical stiffness was observed (n=3).

DISCUSSION

Until this date, scaffolds based on collagen or caprolactone urethane (PU) have been developed to regenerate partial defects in human menisci[13,20]. These scaffolds are implanted without cells. Results are promising for partial defect repair, but not applicable for all patients. Furthermore, it is not possible to treat defects involving the rim of the meniscus with these scaffolds. To repair such a defect with a scaffold, it is worthwhile to invest the possibility to enhance the biological and mechanical properties by seeding cells prior implantation. These pre-cultured scaffolds are able to integrate with the host tissue stronger and faster[23]. To supply sufficient volume for cells to grow and synthesize matrix a 95%, highly interconnective porous scaffold was used.

The first aim of this study was to investigate the biological properties of cell seeded scaffolds. Scaffolds made from 50/50 P(D/L)LA / PCL with BDI were seeded with MFCs and cultured up to 6 weeks. This study shows that MFCs can be cultured on this scaffold. However, they did not proliferate and ECM synthesis did not increase in time. Also the number of cells in the center of the scaffold was limited. This could be due to the hydrophobic nature of the scaffold, or by a lack of nutrition in the center[43]. Another explanation could be that passage 4 MFCs lose the ability to proliferate or synthesize matrix.

To enhance biological response, 10 ng/ml TGF-β was added to standard medium. TGF-β is known to induce proliferation and matrix syntheses. Addition of TGF-β increased proliferation of MFCs cultured in these scaffolds. This effect of TGF-β is in line with results described by others[30,44,45]. Moreover, collagen and GAG, which are two main components of the meniscus ECM, also increased after TGF-β stimulation. Increase in matrix was not only due to an increase in cell numbers. As indicated with the picogreen assay total cell number was 3.75 times higher compared to non-stimulated cultures. Collagen synthesis was increased more than 15 times compared

to non-stimulated cultures. This means that collagen production per cell was also strongly increased by TGF-β. In addition, this proves that passage 4 MFCs are still able to proliferate, if correct stimuli are presented to the cells. Which indicates that the aforementioned loss of proliferation is not the case. The result that MFCs will not proliferate in the scaffold, under normal culture conditions, points out that the surface characteristics of this scaffold is not bio-inductive for these cells. A study from Gunja *et al.* reported that environmental characteristic have a great effect on MFCs. They showed that with increasing passage number, up to passage 4, MFCs alter gene expressions for collagen and GAG's. Reversal effects could be initiated if re-cultured on a collagen or GAG coated surface[46]. For future applications of this scaffold it could be advantageous to coat the scaffolds surface with bioactive markers such as collagen or GAG. This would improve correct gene expression, and in the end, lead to native like meniscal tissue.

The second aim of this study was not realized. The initial Young's Modulus of the scaffold was 26 kPa and did not reduce significantly after 6 weeks of culture due to degradation. This short term degradation stability is in line with previous studies. In here it was shown that scaffolds remained physically intact up till 20 weeks[47]. The initial compressive stiffness measured is below that of human meniscal tissue. Others showed that native menisci vary in mechanical stiffness between 30 – 100 kPa depending on sample site[48,49]. Since cell proliferation and matrix deposition can increase stiffness, the cell seeded scaffolds were expected to have a higher stiffness[50]. The TGF-β stimulated group, which synthesized the most ECM, did not increase significantly in mechanical stiffness. However, the mean Youngs modulus of these cultures after 6 weeks was 43 kPa. Possibly, if culture times prolonges matrix synthesis will increase, thereby the Youngs modulus will increase further and could become similar as native meniscus tissue. On the other hand, perhaps initial cell density was too low. Many methods have been described to increase cell density. The most obvious would be to increase total number of seeding cells. Alternatively, optimizing seeding efficiency can increase initial cell density and distribution. Cell seeding techniques can be divided into static or dynamic systems. Examples of static systems are droplet and cell suspension[51]. Recently more dynamic seeding systems have been described which uses specially developed devices such as perfusion systems, spinner flasks of bioreactors[51]. These dynamic seeding techniques yield higher densities and better homogeneous cell distribution[51]. Also bioreactors can be promising to increase the biological properties. When dynamic mechanical loading is applied on cell seeded scaffolds, proliferation and matrix synthesize increase compared to static cultures[52]. Furthermore the produced matrix was unorganized while in the meniscus collagen fibers are highly oriented. Methods to increase biological properties further, could lead to more *in vivo* like mechanical properties. New methods to increase mechanical properties are *in vivo* cultures of cell seeded constructs. If pre-seeded scaffolds are cultured subcutaneously, the mechanical modulus becomes higher when compared to in vitro pre-seeded constructs[53]. On the other hand, scaffolds could be adapted to create initially stiffer scaffolds resembling native meniscus more closely.

In summary, meniscal fibrochondrocytes can be cultured in PU scaffolds made from poly D/L lactide and caprolactone and 1,4-butanediisocyanate. However, the scaffold did not permit proliferation of these cells. Addition of TGF-β will increase the biological properties significantly. The mechanical properties, however, remained similar. Further research needs to focus on changing the scaffolds properties to increase biological and mechanical behavior during culture. Methods to change these properties could be coating the scaffolds surface with biologic cues such as proteins. This can increase the cellular response during cell cultures.

REFERENCE LIST

1. Petersen W, Tillmann B. Collagenous fibril texture of the human knee joint menisci. Anat Embryol (Berl) 1998;197(4):317-324.
2. Fithian DC, Kelly MA, Mow VC. Material properties and structure-function relationships in the menisci. Clin Orthop Relat Res 1990(252):19-31.
3. Walker PS, Erkman MJ. The role of the menisci in force transmission across the knee. Clin Orthop Relat Res 1975(109):184-192.
4. Arnoczky SP, Warren RF. Microvasculature of the human meniscus. Am J Sports Med 1982;10(2):90-95.
5. Arnoczky SP, Warren RF. The microvasculature of the meniscus and its response to injury. An experimental study in the dog. Am J Sports Med 1983;11(3):131-141.
6. McDevitt CA, Webber RJ. The ultrastructure and biochemistry of meniscal cartilage. Clin Orthop Relat Res 1990(252):8-18.
7. McDermott ID, Amis AA. The consequences of meniscectomy. J Bone Joint Surg Br 2006;88(12):1549-1556.
8. Fairbank TJ. Knee joint changes after meniscectomy. J Bone Joint Surg Br 1948;30B(4):664-670.
9. Cox JS, Nye CE, Schaefer WW, Woodstein IJ. The degenerative effects of partial and total resection of the medial meniscus in dogs' knees. Clin Orthop Relat Res 1975(109):178-183.
10. Starke C, Kopf S, Petersen W, Becker R. Meniscal repair. Arthroscopy 2009;25(9):1033-1044.
11. Jarvela S, Sihvonen R, Sirkeoja H, Jarvela T. All-inside meniscal repair with bioabsorbable meniscal screws or with bioabsorbable meniscus arrows: a prospective, randomized clinical study with 2-year results. Am J Sports Med 2010;38(11):2211-2217.
12. de Groot JH. Polyurethane scaffolds for meniscal tissue regeneration. Med Device Technol 2005;16(7):18-20.
13. Steadman JR, Rodkey WG. Tissue-engineered collagen meniscus implants: 5- to 6-year feasibility study results. Arthroscopy 2005;21(5):515-525.
14. Bulgheroni P, Murena L, Ratti C, Bulgheroni E, Ronga M, Cherubino P. Follow-up of collagen meniscus implant patients: clinical, radiological, and magnetic resonance imaging results at 5 years. Knee 2010;17(3):224-229.
15. Rodkey WG, DeHaven KE, Montgomery WH, III, Baker CL, Jr., Beck CL, Jr., Hormel SE, Steadman JR, Cole BJ, Briggs KK. Comparison of the collagen meniscus implant with partial meniscectomy. A prospective randomized trial. J Bone Joint Surg Am 2008;90(7):1413-1426.
16. Brophy RH, Cottrell J, Rodeo SA, Wright TM, Warren RF, Maher SA. Implantation of a synthetic meniscal scaffold improves joint contact mechanics in a partial meniscectomy cadaver model. J Biomed Mater Res A 2010;92(3):1154-1161.
17. Maher SA, Rodeo SA, Doty SB, Brophy R, Potter H, Foo LF, Rosenblatt L, Deng XH, Turner AS, Wright TM and others. Evaluation of a porous polyurethane scaffold in a partial meniscal defect ovine model. Arthroscopy 2010;26(11):1510-1519.
18. Hannink G, van Tienen TG, Schouten AJ, Buma P. Changes in articular cartilage after meniscectomy and meniscus replacement using a biodegradable porous polymer implant. Knee Surg Sports Traumatol Arthrosc 2010.
19. Welsing RT, van Tienen TG, Ramrattan N, Heijkants R, Schouten AJ, Veth RP, Buma P. Effect on tissue differentiation and articular cartilage degradation of a polymer meniscus implant: A 2-year follow-up study in dogs. Am J Sports Med 2008;36(10):1978-1989.
20. Verdonk R, Verdonk P, Huysse W, Forsyth R, Heinrichs EL. Tissue Ingrowth After Implantation of a Novel, Biodegradable Polyurethane Scaffold for the Treatment of Partial Meniscal Lesions. Am J Sports Med 2011.
21. Elattar M, Dhollander A, Verdonk R, Almqvist KF, Verdonk P. Twenty-six years of meniscal allograft transplantation: is it still experimental? A meta-analysis of 44 trials. Knee Surg Sports Traumatol Arthrosc 2010.
22. McDermott I. Meniscal tears, repairs and replacement: their relevance to osteoarthritis of the knee. Br J Sports Med 2011.
23. Pabbruwe MB, Kafienah W, Tarlton JF, Mistry S, Fox DJ, Hollander AP. Repair of meniscal cartilage white zone tears using a stem cell/collagen-scaffold implant. Biomaterials 2010;31(9):2583-2591.
24. Kon E, Chiari C, Marcacci M, Delcogliano M, Salter DM, Martin I, Ambrosio L, Fini M, Tschon M, Tognana E and others. Tissue engineering for total meniscal substitution: animal study in sheep model. Tissue Eng Part A 2008;14(6):1067-1080.
25. Zellner J, Mueller M, Berner A, Dienstknecht T, Kujat R, Nerlich M, Hennemann B, Koller M, Prantl L, Angele M and others. Role of mesenchymal stem cells in tissue engineering of meniscus. J Biomed Mater Res A 2010;94(4):1150-1161.
26. Gunja NJ, Athanasiou KA. Effects of co-cultures of meniscus cells and articular chondrocytes on PLLA scaffolds. Biotechnol Bioeng 2009;103(4):808-816.

27. Aufderheide AC, Athanasiou KA. Assessment of a bovine co-culture, scaffold-free method for growing meniscus-shaped constructs. Tissue Eng 2007;13(9):2195-2205.
28. Pangborn CA, Athanasiou KA. Growth factors and fibrochondrocytes in scaffolds. J Orthop Res 2005;23(5):1184-1190.
29. Izal I, Ripalda P, Acosta CA, Forriol F. In Vitro Healing of Avascular Meniscal Injuries with Fresh and Frozen Plugs Treated with TGF-beta1 and IGF-1 in Sheep. Int J Clin Exp Pathol 2008;1(5):426-434.
30. Pangborn CA, Athanasiou KA. Effects of growth factors on meniscal fibrochondrocytes. Tissue Eng 2005;11(7-8):1141-1148.
31. Tumia NS, Johnstone AJ. Platelet derived growth factor-AB enhances knee meniscal cell activity in vitro. Knee 2008.
32. Zhang J, Zeng B, Zhao J. [Effects of basic fibroblast growth factor gene transfection on biochemistry of meniscal fibrochondrocytes]. Zhongguo Xiu Fu Chong Jian Wai Ke Za Zhi 2006;20(12):1253-1256.
33. Kang SW, Son SM, Lee JS, Lee ES, Lee KY, Park SG, Park JH, Kim BS. Regeneration of whole meniscus using meniscal cells and polymer scaffolds in a rabbit total meniscectomy model. J Biomed Mater Res A 2006;78(3):659-671.
34. Mandal BB, Park SH, Gil ES, Kaplan DL. Multilayered silk scaffolds for meniscus tissue engineering. Biomaterials 2010.
35. Spaans CJ, de Groot JH, Belgraver VW, Pennings AJ. A new biomedical polyurethane with a high modulus based on 1,4-butanediisocyanate and epsilon-caprolactone. J Mater Sci Mater Med 1998;9(12):675-678.
36. van Minnen B, van Leeuwen MB, Stegenga B, Zuidema J, Hissink CE, van Kooten TG, Bos RR. Short-term in vitro and in vivo biocompatibility of a biodegradable polyurethane foam based on 1,4-butanediisocyanate. J Mater Sci Mater Med 2005;16(3):221-227.
37. van Minnen B, Stegenga B, van Leeuwen MB, van Kooten TG, Bos RR. A long-term in vitro biocompatibility study of a biodegradable polyurethane and its degradation products. J Biomed Mater Res A 2006;76(2):377-385.
38. van Minnen B, van Leeuwen MB, Kors G, Zuidema J, van Kooten TG, Bos RR. In vivo resorption of a biodegradable polyurethane foam, based on 1,4-butanediisocyanate: a three-year subcutaneous implantation study. J Biomed Mater Res A 2008;85(4):972-982.
39. Moroni L, Poort G, Van KF, de W, Jr., van Blitterswijk CA. Dynamic mechanical properties of 3D fiber-deposited PEOT/PBT scaffolds: an experimental and numerical analysis. J Biomed Mater Res A 2006;78(3):605-614.
40. Karande TS, Ong JL, Agrawal CM. Diffusion in musculoskeletal tissue engineering scaffolds: design issues related to porosity, permeability, architecture, and nutrient mixing. Ann Biomed Eng 2004;32(12):1728-1743.
41. Bergsma JE, de Bruijn WC, Rozema FR, Bos RR, Boering G. Late degradation tissue response to poly(L-lactide) bone plates and screws. Biomaterials 1995;16(1):25-31.
42. Reddy GK, Enwemeka CS. A simplified method for the analysis of hydroxyproline in biological tissues. Clin Biochem 1996;29(3):225-229.
43. Ishizaki T, Saito N, Takai O. Correlation of cell adhesive behaviors on superhydrophobic, superhydrophilic, and micropatterned superhydrophobic/superhydrophilic surfaces to their surface chemistry. Langmuir 2010;26(11):8147-8154.
44. Gunja NJ, Uthamanthil RK, Athanasiou KA. Effects of TGF-beta1 and hydrostatic pressure on meniscus cell-seeded scaffolds. Biomaterials 2009;30(4):565-573.
45. Ye C, Deng Z, Li B. [Effect of three growth factors on proliferation and cell phenotype of human fetal meniscal cells]. Zhongguo Xiu Fu Chong Jian Wai Ke Za Zhi 2007;21(10):1137-1141.
46. Gunja NJ, Athanasiou KA. Passage and reversal effects on gene expression of bovine meniscal fibrochondrocytes. Arthritis Res Ther 2007;9(5):R93.
47. Zuidema J, van MB, Span MM, Hissink CE, van Kooten TG, Bos RR. In vitro degradation of a biodegradable polyurethane foam, based on 1,4-butanediisocyanate: a three-year study at physiological and elevated temperature. J Biomed Mater Res A 2009;90(3):920-930.
48. Bursac P, Arnoczky S, York A. Dynamic compressive behavior of human meniscus correlates with its extracellular matrix composition. Biorheology 2009;46(3):227-237.
49. Chia HN, Hull ML. Compressive moduli of the human medial meniscus in the axial and radial directions at equilibrium and at a physiological strain rate. J Orthop Res 2008;26(7):951-956.
50. Wan LQ, Jiang J, Miller DE, Guo XE, Mow VC, Lu HH. Matrix Deposition Modulates the Viscoelastic Shear Properties of Hydrogel-Based Cartilage Grafts. Tissue Eng Part A 2011.
51. Martin I, Wendt D, Heberer M. The role of bioreactors in tissue engineering. Trends Biotechnol 2004;22(2):80-86.
52. Ballyns JJ, Bonassar LJ. Dynamic compressive loading of image-guided tissue engineered meniscal constructs. J Biomech 2011;44(3):509-516.
53. Calve S, Lytle IF, Grosh K, Brown DL, Arruda EM. Implantation increases tensile strength and collagen

content of self-assembled tendon constructs. J Appl Physiol 2010;108(4):875-881.

Chapter 3

Characterization of polyurethane scaffold surface functionalization with diamines and heparin

J. Biomedical Materials Research, Part A, 2013

Eric de Mulder
Gerjon Hannink
Martin Koens
Dennis Löwik
Nico Verdonschot
Pieter Buma

ABSTRACT

Polyurethane scaffolds (PU's) have a good biocompatibility, but lack cell recognition sites. In this study we functionalized the surface of a PU, P(D/L)LA and PCL (50:50) containing urethane segments, with heparin. The first step in this functionalization, aminolysis, lead to free amine groups on the surface of the PU. Free amine content was determined to be 6.4 nmol/ml/mg scaffold, a significant increase of 230%. Subsequently, heparin was cross-linked. Immunohistochemistry demonstrated the presence of heparin homogeneous throughout the 3D porous scaffold. Young's modulus decreased significantly till 50% of the native stiffness after aminolysis and did not change after heparin cross-linking. Contact angle on PU films significantly decreased from 82.7 to 64.3 degrees after heparin cross-linking, indicating a more hydrophilic surface.

This functionalization beholds great potential for tissue engineering purposes. When used in a load bearing environment, caution is necessary due to reduction in mechanical stiffness.

INTRODUCTION

Recent advances in polymer chemistry have significantly improved biomaterial scaffolds for use in Tissue Engineering (TE), but a need for optimalization of the currently available scaffolds remains. A synthetic scaffold material widely used for TE purposes is polyurethane (PU). Although many PU's are biocompatible[1], their hydrophobic nature limits cell adhesion. Cell adhesion is one of the key factors affecting the eventual results of tissue engineering constructs. It is known that cells have a higher affinity for hydrophilic surfaces[2]. Several techniques to increase the hydrophilicity of polymer surfaces have been published. Recently, a surface activation technique using diamines has been described[3,4]. Highly reactive diamines are able to break ester groups of the polymer open, and subsequently covalently bind with one amine group to the scaffold leaving the second amine group unreacted. This free amine group can be used for the covalent coupling of a variety of macromolecules, such as collagen and chondroitin sulphate. Subsequently, these macromolecules might influence cell proliferation, differentiation and matrix synthesis[4-6].

A group of macromolecules of major interest are glycosaminoglycans (GAGs), and in particular heparin. GAGs can create an appropriate environment for cellular signaling, and are common constituents of cell surfaces and extracellular matrices. In addition, heparin is able to bind and modulate various proteins including growth factors, cytokines, and extracellular matrix proteins[7]. Attachment of GAGs may therefore offer the opportunity to exploit their bio-characteristics and valorize the biomaterials they are attached to. It has been shown that gene expression alters with increasing passage number of isolated meniscal fibrochondrocytes. However, re-culturing of these cells on collagen or GAG coated surfaces has been shown to partly restore gene expression[8].

The purpose of this study was to functionalize PU scaffolds with diamines and subsequently bind heparin as a carrier for future applications in tissue engineering. Functionalized scaffolds were evaluated mechanically, biochemically and histologically.

MATERIAL AND METHODS

Scaffold preparation

Scaffolds were composed of 50% DL(50/50)-lactide (PDLLA, Purac) and 50% ε-caprolactone (PCL, Acros Organics) by ring opening polymerization with 1,4-butanediol (BDO) as initiator. The final macrodiol prepolymer had a molecular weight (MN) of 2000 g/mole. Subsequently this was end-capped with 1,4-butanediisocyanate (BDI). Chain extension was performed with a BDO-BDI-BDO urethane block which resulted in a hard block urethane segment with a uniform length of five urethane moieties. Final PU consisted of 22.5 w/w % hard urethane segments and 77.5 w/w % amorphous polyester soft segments. Polymers were solvent casted, frozen and lyophilized. The obtained 3D porous scaffolds had a

95% porosity (kindly provided by Polyganics BV, the Netherlands) [9]. Scaffolds were frozen in liquid nitrogen, and cylinders of 8.0mm in diameter and 5.0mm in height were cut using a dermal punch. In addition, polymer films were made of the same polymer solution. The solution was poured into glass petridishes and dried by air, resulting in polymer films with a thickness of 0.2mm. From these films, 16.0 mm diameter samples were punched.

Surface coating with heparin

Aminolysis of the scaffolds was performed by immersing the samples in 5% 1,6-hexanedamine (Merck, NJ, USA) in isopropanol. Different incubations times were tested. However, when scaffolds were incubated over 120 minutes, samples started to fall apart (results not shown). Therefore an incubation time of 60 minutes at room temperature was chosen for all future experiments. After stringent washing with demineralized water samples were freeze dried over night. From the 3D porous scaffolds the amount of free amines was quantified via 1M ninhydrin staining and absorbance spectroscopy at 535 nm (n=5) [10]. Subsequently, scaffolds were prepared for cross-linking with heparin. Scaffolds were saturated with 50mM 2-morpholinoethane sulphonic acid buffer (MES, pH 5.0). The reaction was performed via standard carbodiimide cross-linking [11,12]. A total of 0.25% heparin sulphate (w/v) (Organon, Oss, the Netherlands) was added to 33mM 1-ethyl-3-dimethyl aminopropyl carbodiimide (EDC) and 6mm N-hydroxysuccinimide (NHS) in MES buffer. After 4h of incubation at room temperature, the scaffolds were washed in 0.1M Na_2HPO_4, 1M NaCl, 2M NaCl and demineralized water.

Immunofluorescence staining

Surface coated 3D porous scaffolds were analyzed with heparin specific immunofluorescence staining (n=5) [13]. Cryosections of 4µm were prepared and blocked for one hour with 1% BSA/PBS. Subsequently, sections were incubated with the following antibodies in 1% BSA/PBS for one hour: HS4C3 1:10 , P5D4 1:10 and finally ALEXA 488 labeled goat anti mouse IgG 1:200 (HS4C3 and P5D4 were kindly provided by Dr. T.H. van Kuppevelt, Radboud University Nijmegen, NCMLS, the Netherlands). Sections were mounted with Mowiol and analyzed with fluorescence microscopy.

Hydrophilicity test

The sessile droplet method was used to calculate the surface hydrophilicity of each of the surface treated polymer films produced [14]. A water droplet was placed on top of the film and photographed. The contact angle was determined by measuring the angle between polymer film and droplet (n=5).

Mechanical analyses

Porous 3D scaffolds with and without diamine activation and subsequent heparin cross-linking were subjected to mechanical compression (n=6) under physiological

conditions (PBS, 37^{O}C). Mechanical tests were performed with a BOSE® ElectroForce® BioDynamic™ bioreactor with an orthopaedic chamber, equipped with a 22N load-cell (BOSE, MN, USA). Scaffolds were compressed at a speed of 1mm/min and forces were recorded till 50% compression using WinTest® software (BOSE, MN, USA). The Young's modulus (YM) was calculated as the slope of the straight line portion of the stress-strain curve.

Statistical analyses

Statistical analyses were performed by one-way ANOVA with a Tukey HSD post-hoc test (SPSS v18, Chicago, IL, USA). P-values < 0.05 were considered significant. All quantitative data were expressed as mean ± SEM.

RESULTS

Aminolysis

After aminolysis for 60 min, the amount of free amines significantly increased from 2.8 ± 0.71 nmol/ml/mg scaffold to 6.4 ± 0.66 nmol/ml/mg scaffold for native and aminolyzed 3D porous scaffolds respectively as measured by ninhydrin quantification (p = 0.006) (Figure 1).

Immunofluorescence staining

Immunofluorescence analysis showed positive heparin staining after completing the two step reaction (see + + group in Figure 2). Omitting aminolysis, no heparin was detected on the scaffolds (- + Figure 2). Heparin staining was visible homogenously throughout the entire porous scaffold and over the entire film.

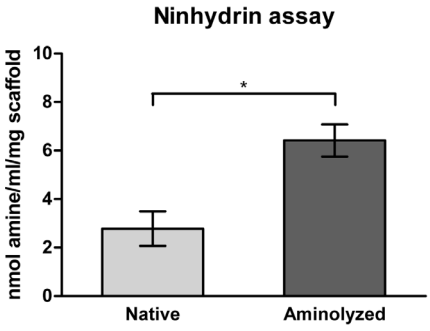

Figure 1: Ninhydrin assay. Aminolyzed scaffolds contained significant more free amines after diamin treatment (p=0.006, n=5).

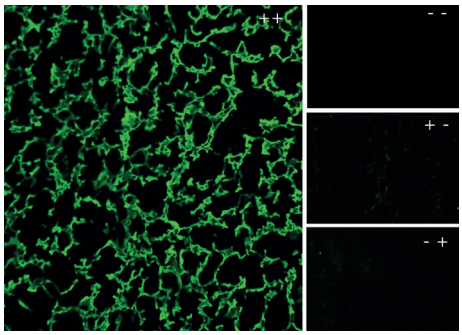

Figure 2: Heparin specific immuno-fluorescence staining on 3d porous PU scaffolds. First mark -/+ aminolysis, second mark -/+ heparin cross-linking. Notice that only activated and heparin cross-linked scaffolds (++) show positive heparin staining (n=5).

Hydrophilicity test

Droplets on native films had a contact angle of 82.7^{O} ± 0.71. After aminolysis, the contact angle significantly decreased till 65.4^{O} ± 0.98 (p = 0.006) indicating a more hydrophilic surface compared to the native scaffold. Heparin cross-linking caused no further change in contact angle 64.3^{O} ± 1.03 compared to aminolyzed scaffolds, but was significantly lower compared to the native films (p = 0.006) (Figure 3).

Mechanical stiffness

The Young's modulus of the native scaffold was 23.3 ± 2.0 kPa. The aminolyzed scaffolds had a significant lower modulus of 12.2 ± 0.9 kPa (p = 0.003). Heparin cross-linking had no further influence on the scaffolds' stiffness (13.2 ± 0.4 kPa) (Figure 4).

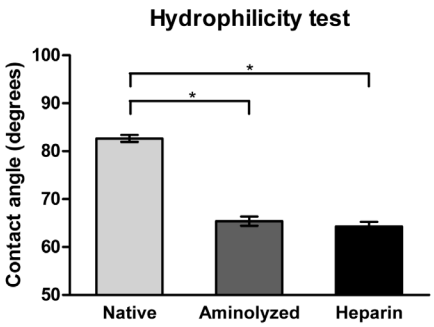

Figure 3: Aminolyzed and heparin cross-linked PU films show significant lower contact angle, meaning an increased hydrophilicity (p=0.006, n=5).

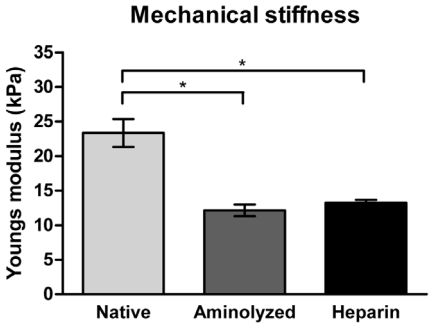

Figure 4: Young's Modulus after 50% compression. Aminolyzed and heparin cross-linked scaffolds have lower Young's moduli compared to native scaffold (p=0.003, n=6).

DISCUSSION

The aim of this study was to test the possibility to coat a PU scaffold with heparin. The PU of interest was a co-polymer of P(d/l)LA and PCL further reacted with butanediisocyanate to introduce urethane bonds. The method for surface coating this PU scaffold with heparin showed to be effective. A two step reaction was necessary to cross-link heparin. The first reaction, aminolysis, resulted in free amines that could be employed to immobilize heparin. The amines measured in untreated scaffolds were due to the reaction of isocyanate endgroups with water. During this reaction amine groups can be formed. This reaction happens most likely during the stringent washing after the aminolyse step. However, these "background" amines are not able to result in successful cross-linking of heparin as shown with the immunofluorescence analysis since without this first step no heparin could be detected.

For successful tissue engineering of *in vitro* seeded constructs it is important that cells will adhere, proliferate and synthesize extracellular matrix. With respect to the biological effects of the heparin coating, we showed that the surface hydrophilicity

increased, indicated by the lower contact angle. This increase in hydrophilicity potentially result in a faster ingrowth of cells and tissue when cultured or implanted. Furthermore, other studies showed that heparin coated on polymer scaffolds increased neo-vascularization when implanted subcutaneously[15]. This increase in neo-vascularization can boost tissue regeneration even further.

In this study aminolysis caused a reduction in mechanical stiffness of nearly 50%. Cross-linking of heparin to the free amine had no further effect on mechanical stiffness. If this coating technique would be used for a cell based tissue engineered construct, this effect on mechanical properties seems to be less important since it has been shown that cell based constructs will increase in modulus over time due to matrix production by the seeded cells[16]. To increase matrix synthesis by cells, future research should focus on growth factor binding to heparin. An interesting growth factor for cell based tissue engineered constructs is TGF-β. It is known that TGF-β has heparin binding sites and, in addition, can induce proliferation of a wide range of cell types[17,18]. Other growth factors with heparin binding sites are amongst others: VEGF, EGF, BMP and FGF[15,19]. In contrast, if this construct would be used for a cell-less application, mechanical stiffness could be increased by reducing overall porosity of the scaffold. However, decreasing porosity of the scaffold is known to compromise cell migration and tissue regeneration[20].

In conclusion, this two step reaction results in a surface coating of heparine on a PU scaffold. Special care has to be taken to find a balance between mechanical properties and surface adaptation. For each specific application in which these functionalized scaffolds will be used, the porosity of the scaffold should be considered.

REFERENCE LIST

1. Marois Y, Guidoin R. Biocompatibility of Polyurethanes. In: Vermette P, Griesser HJ, Laroche G, Guidoin R, editors. Biomedical Applications of Polyurethanes. Georgetown: Landes Bioscience; 2001. p 77-96.
2. Hsieh CH, Kuo WT, Huang YC, Huang YY. High-efficiency cell seeding method by relatively hydrophobic culture strategy. J Biomed Mater Res B Appl Biomater 2011;98(1):38-46.
3. Zhu Y, Gao C, Liu X, Shen J. Surface modification of polycaprolactone membrane via aminolysis and biomacromolecule immobilization for promoting cytocompatibility of human endothelial cells. Biomacromolecules. 2002;3(6):1312-1319.
4. Chang KY, Cheng LW, Ho GH, Huang YP, Lee YD. Fabrication and characterization of poly(gamma-glutamic acid)-graft-chondroitin sulfate/polycaprolactone porous scaffolds for cartilage tissue engineering. Acta Biomater. 2009;5(6):1937-1947.
5. Zhu Y, Chian KS, Chan-Park MB, Mhaisalkar PS, Ratner BD. Protein bonding on biodegradable poly(L-lactide-co-caprolactone) membrane for esophageal tissue engineering. Biomaterials 2006;27(1):68-78.
6. Zhu Y, Gao C, Liu X, He T, Shen J. Immobilization of biomacromolecules onto aminolyzed poly(L-lactic acid) toward acceleration of endothelium regeneration. Tissue Eng 2004;10(1-2):53-61.
7. Stringer SE, Gallagher JT. Heparan sulphate. Int J Biochem Cell Biol 1997;29(5):709-14.
8. Gunja NJ, Athanasiou KA. Passage and reversal effects on gene expression of bovine meniscal fibrochondrocytes. Arthritis Res.Ther. 2007;9(5):R93.
9. van Minnen B, van Leeuwen MB, Stegenga B, Zuidema J, Hissink CE, van Kooten TG, Bos RR. Short-term in vitro and in vivo biocompatibility of a biodegradable polyurethane foam based on 1,4-butanediisocyanate. J Mater Sci Mater Med 2005;16(3):221-7.
10. Chang KY, Hung LH, Chu IM, Ko CS, Lee YD. The application of type II collagen and chondroitin sulfate grafted PCL porous scaffold in cartilage tissue engineering. J.Biomed.Mater.Res.A 2009.
11. Pieper JS, Hafmans T, Veerkamp JH, van Kuppevelt TH. Development of tailor-made collagen-glycosaminoglycan matrices: EDC/NHS crosslinking, and ultrastructural aspects. Biomaterials 2000;21(6):581-93.
12. Nuininga JE, Koens MJ, Tiemessen DM, Oosterwijk E, Daamen WF, Geutjes PJ, van Kuppevelt TH, Feitz WF. Urethral reconstruction of critical defects in rabbits using molecularly defined tubular type I collagen biomatrices: key issues in growth factor addition. Tissue Eng Part A 2010;16(11):3319-28.
13. van Kuppevelt TH, Dennissen MA, van Venrooij WJ, Hoet RM, Veerkamp JH. Generation and application of type-specific anti-heparan sulfate antibodies using phage display technology. Further evidence for heparan sulfate heterogeneity in the kidney. J.Biol.Chem. 1998;273(21):12960-12966.
14. Das T, Sharma PK, Krom BP, van der Mei HC, Busscher HJ. Role of eDNA on the adhesion forces between Streptococcus mutans and substratum surfaces: influence of ionic strength and substratum hydrophobicity. Langmuir 2011;27(16):10113-8.
15. Singh S, Wu BM, Dunn JC. The enhancement of VEGF-mediated angiogenesis by polycaprolactone scaffolds with surface cross-linked heparin. Biomaterials 2011;32(8):2059-69.
16. Talukdar S, Nguyen QT, Chen AC, Sah RL, Kundu SC. Effect of initial cell seeding density on 3D-engineered silk fibroin scaffolds for articular cartilage tissue engineering. Biomaterials 2011;32(34):8927-37.
17. de Mulder EL, Hannink G, Giele M, Verdonschot N, Buma P. Proliferation of meniscal fibrochondrocytes cultured on a new polyurethane scaffold is stimulated by TGF-ss. J Biomater Appl 2011.
18. McCaffrey TA, Falcone DJ, Du B. Transforming growth factor-beta 1 is a heparin-binding protein: identification of putative heparin-binding regions and isolation of heparins with varying affinity for TGF-beta 1. J Cell Physiol 1992;152(2):430-40.
19. Ashikari-Hada S, Habuchi H, Kariya Y, Itoh N, Reddi AH, Kimata K. Characterization of growth factor-binding structures in heparin/heparan sulfate using an octasaccharide library. J Biol Chem 2004;279(13):12346-54.
20. van Tienen TG, Heijkants RG, Buma P, de Groot JH, Pennings AJ, Veth RP. Tissue ingrowth and degradation of two biodegradable porous polymers with different porosities and pore sizes. Biomaterials 2002;23(8):1731-8.

Chapter 4

Platelet rich plasma can replace foetal bovine serum in human meniscus cell cultures

Tissue Engineering, Part C, in press

Eric de Mulder [#]
Veronica Gonzales [#]
Trix de Boer
Gerjon Hannink
Tony van Tienen
Waander van Heerde
Pieter Buma

[#] both authors contributed equally

ABSTRACT

Concerns over foetal bovine serum (FBS) limit the clinical application of cultured tissue engineered constructs. Therefore we investigated if platelet rich plasma (PRP) can fully replace FBS for meniscus tissue engineering purposes.

Human PRP and platelet poor plasma (PPP) were isolated from three healthy adult donors. Human meniscal fibrochondrocytes (MFCs) were isolated from resected tissue after a partial meniscectomy on a young patient. Passage 4 MFC's were cultured in monolayer for 24 hours, 3 and 7 days. Six different culture media were used containing different amounts of either PRP and PPP and compared to a medium containing 10% FBS. dsDNA was quantified and gene expression levels of collagen types I and II and aggrecan were measured at different time points with qPCR in the cultured MFCs.

After 7 days the dsDNA quantity was significantly higher in MFCs cultured in 10% and 20% PRP compared to the other PRP and PPP conditions, but equal to 10% FBS. Collagen type I expression was lower in MFCs cultured with medium containing 5% PRP, 10% and 20% PPP compared to FBS. When medium with 10% PRP or 20% PRP was used, expressions were not significantly different from medium containing 10% FBS. Collagen type II expression was absent in all medium conditions. Aggrecan expression did not show differences between the different media used. However, after 7 days a higher aggrecan expression was measured in most culture conditions, except for 5% PRP, which was similar compared to FBS. Statistical significance was found between donors at various time points in DNA quantification and gene expression, but the same donors were not statistically different in all conditions. At 7 days cell cultured with 10% PRP and 20% PRP showed a higher density, with large areas of clusters, compared to other conditions.

In MFC culture medium FBS can be replaced by 10% PRP or 20% PRP without altering proliferation and gene expression of human meniscal fibrochondrocytes.

INTRODUCTION

Meniscal tears are one of the most common injuries of the knee joint. Only tears in the red vascularized outer 1/3 zone can repair spontaneously. Spontaneous repair of tears in the white avascular inner 2/3 zone, however, is limited due to lack of vascularization[1,2]. Treatment for meniscal tears depends on type, size and location of the tear. Preferably tears will be sutured to the main body of the meniscus to maintain the integrity of the meniscus. If fixation is impossible or fails, a (partial) meniscectomy can be considered to relieve pain and improve function of the knee joint. However, with increasing portion of meniscus tissue removed, the risk of early osteoarthritis increases due to overloading of the articular cartilage[3,4]. For partial meniscectomized knees two clinical available scaffolds, Menaflex™ and Actifit®, are used to replace the lost part of the meniscus. They have been shown to improve the clinical performance to some extent[5-7]. A biomechanical analysis showed that the Actifit implant restores contact mechanics[8]. For total meniscus replacements a caprolactone-urethane based scaffold appeared mechanically too weak to cope with the high forces in the joint and cartilage degradation was not prevented[9,10]. Tissue engineering would potentially resolve the problem of scaffolds that are initially too weak to be implanted.

Meniscus tissue engineering will lead to improved biological and functional mechanical properties of the pre-seeded scaffold[11]. Meniscal fibrochondrocytes (MFCs) have shown to be suitable cells for meniscus tissue engineering[12]. MFCs can be easily isolated from resected meniscus tissue of the patient itself thereby avoiding immunological responses and providing the proper phenotype[4]. Furthermore, MFCs have been shown to enable *in vitro* meniscus tissue engineering[12,13].

In research for tissue engineering applications foetal bovine serum (FBS) is widely used as a supplement to standard cell culture media to induce proliferation and matrix synthesis of a variety of cells. However, the potential risk of bovine pathogens in FBS serum limits its use in clinical applications[14,15]. An alternative for FBS is therefore urgently needed. Platelet rich plasma (PRP) could potentially be a good alternative for FBS. Platelets contain a variety of growth factors, of which TGF-beta, IGF, VEGF and PDGF are the most abundant[16-20]. PRP has been shown to stimulate the repair of a wide variety of soft and hard musculo-skeletal tissues such as bone, muscle, skin, tendon and cartilage[21,22]. In a number of tissue engineering studies the effect of various PRP volume percentages supplemented to medium on MFCs, chondrocytes and subchondral mesenchymal progenitor cells was investigated[23-26]. Ishida *et al* studied the effect of PRP (3%, 10% and 30%) on rabbit MFCs in culture and showed increased proliferation and matrix synthesis compared to their FBS control[23]. Currently there are three concentrations of FBS used for meniscus cell cultures: 1%, 10% and 20%[19]. However 10% FBS has been most widely used in meniscus fibrochondrocyte cultures[19,20,24,27-29].

The objective of this study was to determine if and which volume concentrations (5%, 10%, 20%) of PRP can be used as a functional substitute for the standard 10%

FBS in meniscus fibrochondrocyte cell culture medium.

MATERIALS AND METHODS

Cell Isolation

Meniscal tissue was obtained during a partial meniscectomy on a young physically very active male donor (age 18). MFCs where isolated from the meniscus tissue according to previously described protocols[13]. Isolated MFCs were washed twice with PBS and expanded in monolayer culture. Once cells reached 70% confluence the cells were passed once and subsequent confluent cell cultures were trypsinized and cryopreserved until use. All cell cultures were performed in a 5% CO2, 37OC controlled incubator with standard culture medium. Standard culture medium was defined as DMEM/F12 + 10% FBS + 1% PSF (penicillin/streptomycin/fungizone, Gibco, Carlsbad, CA, USA).

Platelet Rich Plasma and Platelet Poor Plasma

Blood samples were collected from healthy human donors (n=3) after informed consent was obtained. Peripheral venous blood was collected in 4.5ml hirudin containing blood collection vials (S-Monovette, Sarstedt AG & Co. Numbrecht, Germany) to avoid any influence of platelet-dependent Protease Activating Receptor (PAR) signalling by thrombin[30,31]. One half of whole blood was centrifuged at 200g for 15 min to obtain PRP, the other half at 2750g for 15 minutes to obtain PPP. After centrifugation, the upper phase containing PRP and PPP respectively, were transferred and pooled for each donor. Whole blood, PRP and PPP were measured with fluorescent flow cytometry to quantify platelet concentration (Sysmex XE-5000; Hamburg-Norderstedt, Germany). PRP and PPP were stored at -20 °C until use. PRP samples were not normalized for platelet count.

Cell culture experiment

MFCs were defrosted and expanded in monolayer till passage 3 in standard culture medium. Afterwards, cells were trypsinized medium was added to neutralize trypsin, counted (with trypan blue exclusion and DMEM/F12), seeded (50,000 MFCs per well) in 24-well plates and cultured overnight in standard culture medium containing FBS. Following overnight culture, cells were washed twice with DMEM/F12 and subsequently experimental culture medium was added to each well. Seven different experimental culture media were tested. Base medium was DMEM/F12 + 1% PSF with one of the following conditions: 10% FBS, 5%, 10%, or 20% PRP or 5%, 10% or 20% PPP (v/v). PRP and PPP vials of each donor were defrosted only once before use. MFCs were cultured for 24 hours, 3 and 7 days in triplicate for each donor. On day 3 and day 6 the experimental medium was refreshed with corresponding experimental culture medium.

Picogreen analysis

After 24 hours, 3 and 7 days of culture, cells from each experimental culture medium (n=3) were frozen in MilliQ (-20°C). After repeated freeze/thaw cycles, PicoGreen dsDNA assay kit was used according to manufacturer's protocol to quantify the amount of dsDNA (Invitrogen, Carlsbad, CA, USA).

RNA isolation and gene expression

After 24 hours, 3 and 7 days, trizol (Sigma-Aldrich, MO, USA) was added to the cells of each condition (n=3) and stored at -80°C. RNA was isolated via standard chloroform phase separation[32]. The supernatant was isolated and RNA was precipitated with isopropanol, washed twice with 75% ETOH, air dried, solubilised in RNAse free water and subjected to reverse transcriptase polymerase chain reaction (RT-PCR) to obtain cDNA. Finally, a quantitative PCR (qPCR) was performed on individual samples by an "ABI/PRISM 7000 sequence detection system" (Aplied Biosystems, Foster City, USA). qPCR was prepared as follows: 1µl forward primer (5µM), 1 µl reverse primer (5µM) and 5 µl of Sybr Green PCR Master mix (Applied Biosystems, Foster City, USA) were added to 3µl cDNA. qPCR was performed for 40 cycles. Three specific gene expression markers for meniscus tissue engineering, i.e. collagen type I and II, and aggrecan, were measured with GAPDH as household gene (see table 1 for primer sequences). The Ct value shows the point in which the amplification plot passes the threshold, due to the release of the fluorescence from mRNA transcription. GAPDH was the internal control for all genes and used to normalize delta Ct levels for any variability in cell numbers. Delta delta Ct levels were calculated by subtracting the delta Ct level of the gene of interest from the delta Ct level of the control (FBS). The fold change in the gene expression relative to the control was calculated using the equation $2^{-\Delta\Delta Ct}$. FBS is designated with a dashed line at 1 on the y-axis, as seen in Figure 2 and 3. All primers were validated in the Rheumatology department at Nijmegen Centre for Molecular Life Sciences[33].

Gene	forward primer (5' → 3')	reverse primer (5' → 3')
Collagen type I	CAAGGAGTCTGCATGTCTAAGTGCTA	ACTCTTGTAAAGAAATTGGCATGTTG
Collagen type II	CACGTACACTGCCCTGAAGGA	CGATAACAGTCTTGCCCCACTT
Aggrecan	GCCTGCGCTCCAATGACT	ATGGAACACGATGCCTTTCAC
GAPDH	ATCTTCTTTTGCGTCGCCAG	TTCCCCATGGTGTCTGAGC

Table 1: primer sequences used for real-time PCR. Primers were obtained from Biolegio bv, Nijmegen, Netherlands.

Histology

Monolayer cell cultures were fixated after 24 hours, 3 and 7 days in their wells, stained with haematoxylin and eosin and mounted using Permacol UV (Permacol, the Netherlands) (n=3). All samples were analyzed with light microscopy and photographed with an Olympus digital camera at the same magnification.

Statistics

All data were expressed as mean ± SEM. Picogreen data were log transformed and subjected to a Two-Way ANOVA with a post-hoc Fisher-LSD test. For qPCR, delta Ct levels were subjected to Two-Way ANOVA with a post-hoc Fisher-LSD test. P-values < 0.05 were considered significant. Statistical analysis was performed using SPSS v16.0 software (SPSS Inc., Chicago, IL, USA). Statistical analysis of the Picogreen and qPCR data was completed in two steps. In the first Two-Way ANOVA the effect of condition and the time points on dsDNA or gene expression was analysed with the donors pooled. The second Two-Way ANOVA analysed the effect of donor and condition on time points.

RESULTS

Platelet count

Platelet concentrations were measured in whole blood, PRP and PPP from each donor. The platelet concentration in whole blood was on average 131±26 $x10^9$/L (donor 1: 148 $x10^9$/L, donor 2: 105 $x10^9$/L, donor 3: 141 $x10^9$/L). For PRP average platelet count was 140±20 $x10^9$/L (donor 1: 165 $x10^9$/L, donor 2: 98 $x10^9$/L, donor 3: 162 $x10^9$/L). In PPP platelet concentrations were not detectable in all three donors.

DNA quantification

The average amount of dsDNA in cells cultured for 24 hours and 3 days in standard medium containing 10% FBS was 51.5 ± 1.7 ng/ml and 90.1 ± 7.9 ng/ml, respectively. During these time points no differences were measured between conditions or in time as a condition ($p>0.050$, data not shown). However, at 7 days of culture a significant increase of dsDNA was measured compared to 24 hours and 3 days cultures. In addition, significant differences between culture conditions were measured. Cells grown in medium containing FBS, 10% and 20% PRP had a significant higher amount of dsDNA compared to all other conditions at 7 days (Figure 1). Statistical significance between donors was found only at 7 days; dsDNA in cells cultured with plasma of D2<D3=D1 (respectively, 55.2, 76,4, 64,9 ng/ml). The average minimum and maximum values of donors pooled dsDNA are presented in table 2.

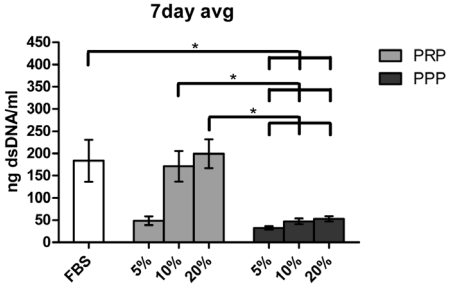

Figure 1: Average dsDNA of all donors after 7 days of monolayer cell culture (n=3). A significant increase of 10% and 20% platelet rich plasma was measured compared to all platelet poor plasma concentrations ($p<0.05$). When 5% of platelet rich plasma was used, dsDNA was significantly lower compared to the control (FBS).

Time point	Condition		Min value dsDNA (ng/ml)	Max value dsDNA (ng/ml)
24hour	PRP	5%	14.2	93.1
		10%	25.0	105.5
		20%	50.7	103.7
	PPP	5%	17.6	118.7
		10%	21.3	123.8
		20%	38.1	88.2
3 days	PRP	5%	29.9	75.4
		10%	46.0	83.1
		20%	42.8	88.0
	PPP	5%	40.9	100.7
		10%	35.3	88.7
		20%	36.7	77.1
7 days	PRP	5%	23.0	99.5
		10%	64.2	354.1
		20%	77.0	376.0
	PRP	5%	19.0	48.3
		10%	30.0	92.0
		20%	38.0	90.8

Table 2: The minimum and maximum values of dsDNA (ng/ml) in DNA quantification in all PRP and PPP conditions of pooled donors.

Gene expression

mRNA of Collagen type I in cells cultured for 24 hours was up-regulated compared to 3 and 7 days (time: $p < 0.050$, Figure 2). Furthermore, there was a significant difference between the different media and control medium containing 10% FBS at 3 and 7 days (Fig. 2B and 2C). At 3 days Collagen type I mRNA in cells cultured with medium containing 5% PRP was significantly up-regulated if compared to media containing 10% and 20% PRP (Figure 2B). At 7 days of culture no differences in collagen type I expression were found between the different culture conditions. All PRP and PPP conditions were down-regulated at 7 days in collagen type I expression (Figure 2C). No donor-specific differences were measured at 24 hours and 7 days in collagen type I expression. However, at 3 days D2<D3 ($p<0.050$) and D1=D2 and D3 ($p=0.062$ and 0.097, respectively).

Expression of collagen type II mRNA was late or not detected at all time points for all treatments (Ct>40, data not shown).

Aggrecan showed to have stable expression for all cells independent of plasma supplement and culture time (Figure 3). Although at 7 days all treatments, except 5% PRP, were up-regulated by a minimum of 6-fold increase (Figure 3C, $p=0.096$). Donor variability for Aggrecan expression was significantly different after 24h (D1 < D2 = D3, $p<0.050$) and 3 days (D3 > D1 = D2, $p<0.050$) but absent at 7 days of culture ($p=0.166$).

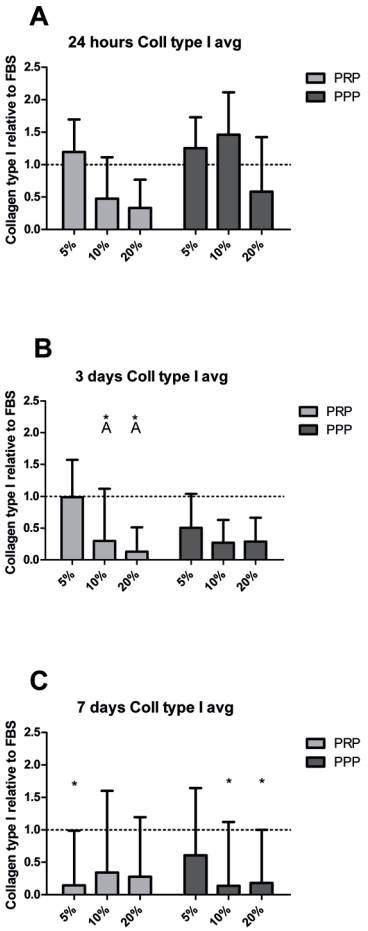

*Figure 2: MFC related gene expression of collagen type I at 24 hours, 3 and 7 days expressed in fold change (A, B and C respectively, n=9). At 3 days medium containing 10% PRP and 20% PRP showed a statistical significance compared to FBS, designated with an *. The A represents statistical significance between 5% PRP and a specific condition. At 7 days of culturing in medium containing 5% PRP, 10% PPP and 20% PPP collagen type I was significantly later expressed compared to FBS. FBS is designated with a dashed line at 1 on the y-axis, all the conditions were adjusted to FBS.*

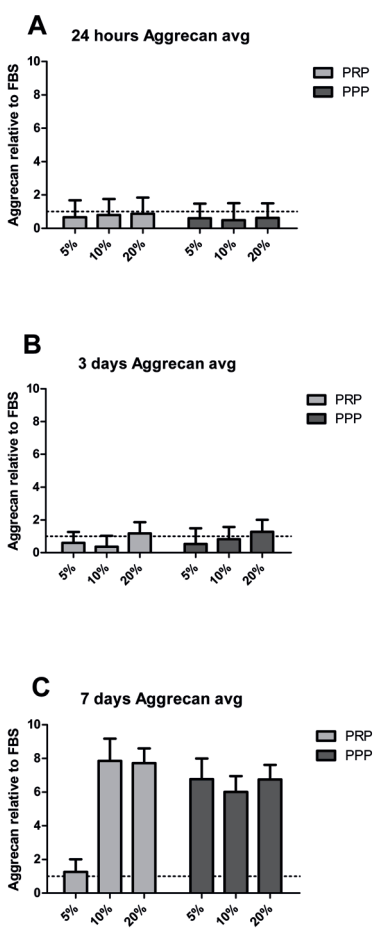

Figure 3: MCF-related gene expression of aggrecan at 24 hours, 3 and 7 days expressed in fold change (A, B and C respectively, n=9). No significant differences between treatments were measured. FBS is designated with a dashed line at 1 on the y-axis, all the conditions were adjusted to FBS.

Histological analysis

At 24 hrs MFCs were distributed homogeneously throughout the well plate (Figure 4). Locally small clusters of cells were present in each condition. At 24 hours of culture cells reached an approximate 20% confluence and their phenotype was mainly fibroblast like or spindle shaped if located individually and more rounded

/ chondrocyte-like if cells were clustered. The phenotype changed at 3 days of culture. More cells were clustered. Cells in the centre of the clusters were rounded, towards the edges of the clusters and isolated cells showed to be mainly spindle shaped / fibroblast like. Cells reached an approximate confluence of 40%. At 7 days the phenotype remained spindle shaped / fibroblast-like, however, differences in confluence were observed. Cells cultured with 10% PRP and 20% PRP showed a higher density (approximately 70% confluence) with large areas of clusters that were fused together, compared to other conditions (40%-50% confluence). No differences between donors were observed (results not shown).

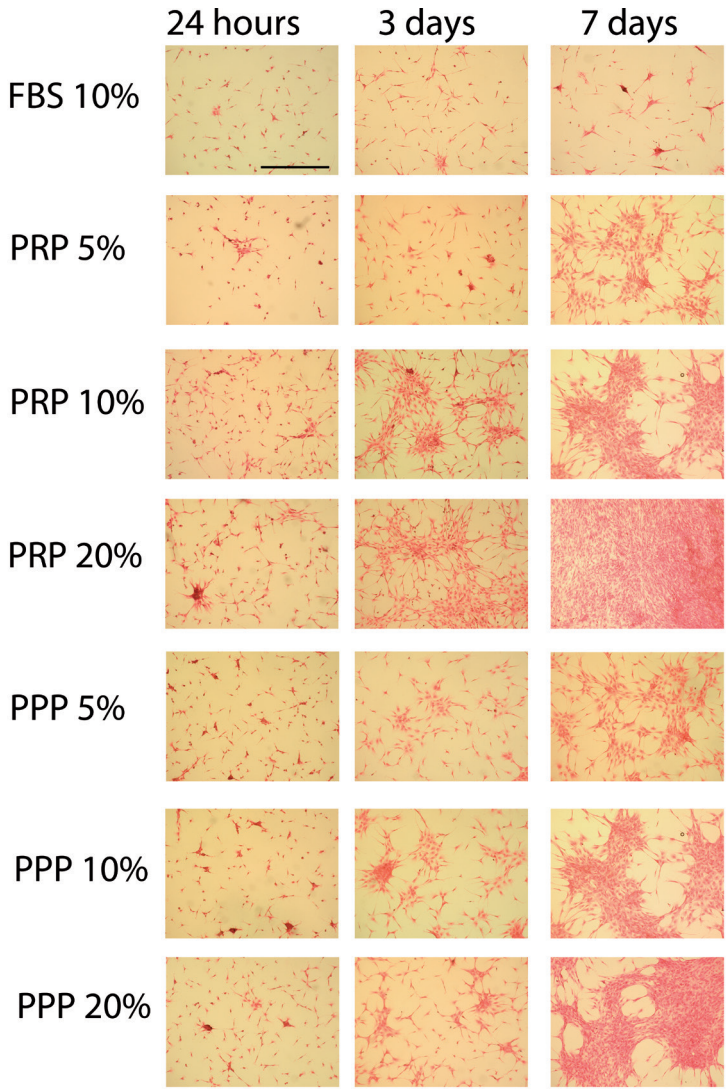

Figure 4: Haematoxylin & Eosin histological analysis of MFCs in 24 hours, 3 days and 7 days in all conditions.

DISCUSSION

Tissue engineering appears to be a promising treatment option for (partial) meniscus replacement[34]. In most meniscal tissue engineering studies FBS is used as a potent supplement in the culture medium[23,34]. However, clinical application of FBS in a cultured construct is not allowed because of the risk of disease transfer or xeno-immunization[14,15]. In the present study, we showed that concentrations of 10% and 20% of PRP as an alternative for FBS supplementation, induce similar effects for proliferation and gene expression on cultured meniscal fibrochondrocytes as compared to the standard medium containing 10% FBS.

PRP can easily be isolated from patients' own blood or donors. Surprisingly in this study, the platelet concentrations did not increase from whole blood to PRP. This could be related to the method used for PRP isolation. Differences in centrifugation speed, the vials used and centrifugation time have shown to influence final platelet concentrations in PRP[22,35-38]. Further, during centrifugation platelets might be trapped in the buffy coat located between the RBCs and plasma. Since we observed that in hirudin blood vials, as were used in this study, the buffy coat was thinner compared with citrate blood vials, we speculate that this might be one of the reasons for the relative low platelet counts. Hirudin also inhibits PAR signalling by thrombin which also might be a factor to cause a thinner buffy coat[30,31].

We showed that proliferation of MFCs remained similar until 3 days, but at 7 days differences in cell numbers were found between conditions. Supplements of 10% and 20% PRP strongly showed an increase in the number of cells compared to PPP samples. Therefore the effects can be related to the platelet content and not solely to the plasma. Furthermore this effect seems platelet concentration dependent since the effect was not observed at 5% PRP. Ishida *et al.* studied also PRP concentration dependent effects on meniscus fibroblasts. They investigated short-term effects (48 hrs) of PRP and PPP on the vitality of cultured meniscus cells[23]. After a pre-culture of 24 hrs in 10% FBS, cultures were continued for 24 hrs in 1% FBS supplemented with 3, 10, 30% PRP or similar concentrations of PPP[23]. PRP concentrations up-regulated the viability of meniscus cells in a dose dependent manner after 48 hrs. A clear comparison with our data is difficult since the study of Ishida *et al.* was shorter (48 hrs), the control was 1% FBS and the PRP sand PPP was added to this 1% FBS[23]. In our study we compared the effect of PRP and PPP to 10% FBS and studied increase in cell numbers based on DNA and not vitality of the cells. In an in vivo model they described a positive effect of PRP on defect healing in the meniscus compared or PPP, but no details were included about the concentration of PRP or platelets that accounted for this positive effect[23].

Collagen type I was initially up-regulated in 5% PRP as well as 5% and 10% PPP at 24 hours. However, in time collagen type I was down-regulated in both PRP and PPP compared to FBS at 3 and 7 days. Collagen type II was not expressed in our experiment, which might be due to MFCs were used at passage 4 according to Gunja *et al.*[39]. Collagen type II expression decreases as the passage number increases[39].

Aggrecan at 24 hours and 2 days had similar or lower expression than that of FBS in all conditions of PRP and PPP. However, at 7 days aggrecan was up-regulated in 10% & 20% PRP and all PPP concentrations compared with FBS. The 5% PRP concentration was comparable to the 10% FBS control. This shows that potentially in the PPP and RRP serum interesting factors are present that can influence the expression of fibrochondrocyte specific genes independent from the effect of the platelets. Since it is well known that meniscus fibroblast change their phenotype in cultures at increasing passages[28,39], further research in specific factors in PPP and PRP might be beneficial for future meniscus tissue engineering. Our result also differs from the reported decreased aggrecan expression in PRP conditions reported by Ishida *et al.*[23]. A possible explanation for this discrepancy in the amount of aggrecan expression might be that the metabolic half-life of aggrecan is much shorter compared to collagen[40]. We speculate that the age of the MFCs might play a crucial role, since aggrecan expression increases after puberty[41]. McAlinden *et al.* stated that aggrecan in the meniscus is important to withstand compressive forces[41]. The increased amount of aggrecan expression in our results maybe a combined effect of the age of the subject and the fact that the donor was physically very active. Karube and Shoji already showed that GAG content of menisci decreases with aging[42]. The age of the rabbits of the study of Ishida was not mentioned in their paper and further detailed studies are needed to clarify this.

There are not many studies which describe a clear effect of PRP and PPP on cell proliferation. Mazzocca *et al.* studied the effect of PRPs obtained by different separation methods on osteoblasts, monocytes and on tenocytes[22]. They compared the effects of three different PRP isolation procedures on proliferation (assessed by thimidine incorporation). They found a similar positive effect of all PRPs compared to 2, 5, 10 or 15% BSA which was used as a control (dependent on the cell type). The different PRP had all a stimulatory effect on the proliferation of the investigated cell types compare to the FBS controls, but since they mixed PRPs with 2% FBS in the final test their results did not allow the conclusion that PRPs can replace FBS completely.

Besides an effect on proliferation PRP might stimulate the migration and differentiation of cells. Kruger *et al.* showed that PRP can stimulate the migration of subchondral progenitor cells and stimulate a chondrogenic differentiation of the stem cells[26]. This might also explain the positive effect on gap healing as described by Ishida *et al.* by PRP added to an a-cellular gelatine hydrogel[23].

Collagen type II expression remained undetermined at all times points. This lack of expression can be due to improper mRNA isolation. However, based on published results in which collagen type II expression was clearly detectable in chondrocytes cells with the same set of primers, it is more likely due to a low or a lack of expression of collagen type II in these cells[33]. It has been reported that differences in stimulation or culture conditions can influence the expression of collagen type matrix proteins[28]. In an engineered meniscus construct, the final extracellular matrix should predominantly consist of collagen type I similar to that of the native meniscus tissue.

Although, other collagens such as collagen type II, III and VI have been shown to be present in the meniscus as well[43].

Some differences in responsiveness between donors were measured at the earlier time points for collagen type I and aggrecan expressions, while results between donors levelled out at 7 days of culture. Despite the fact that platelet number may be responsible for these observed variations, a large study reported a poor correlation between platelet counts and specific growth factor concentrations[18,44]. However other studies demonstrated a clear effect between the growth factor content of platelets and the biological activity which was induced[45]. Further, it is well known that besides the growth factors platelets contain a variety of other proteins or chemokines which also might influence the reaction of cells or tissues[46].

In conclusion, medium supplemented with 10% and 20% PRP can replace standard medium supplemented with 10% foetal bovine serum in meniscal fibrochondrocytes culture while maintaining proliferation and gene expression levels. This opens new perspectives with respect to the clinical utility of MFC in tissue engineering and the use of PRP as autologous supplement.

REFERENCES

1. Arnoczky SP, Warren RF. The microvasculature of the meniscus and its response to injury. An experimental study in the dog. Am J Sports Med.11:131. 1983.
2. Arnoczky SP, Warren RF. Microvasculature of the human meniscus. Am J Sports Med.10:90. 1982.
3. Rangger C, Kathrein A, Klestil T, Glotzer W. Partial meniscectomy and osteoarthritis. Implications for treatment of athletes. Sports Med.23:61. 1997.
4. Makris EA, Hadidi P, Athanasiou KA. The knee meniscus: structure-function, pathophysiology, current repair techniques, and prospects for regeneration. Biomaterials.32:7411. 2011.
5. Verdonk P, Beaufils P, Bellemans J, Djian P, Heinrichs EL, Huysse W, et al. Successful treatment of painful irreparable partial meniscal defects with a polyurethane scaffold: two-year safety and clinical outcomes. Am J Sports Med.40:844. 2012.
6. Rodkey WG, DeHaven KE, Montgomery WH, 3rd, Baker CL, Jr., Beck CL, Jr., Hormel SE, et al. Comparison of the collagen meniscus implant with partial meniscectomy. A prospective randomized trial. J Bone Joint Surg Am.90:1413. 2008.
7. Vrancken AC, Buma P, van Tienen TG. Synthetic meniscus replacement: a review. Int Orthop.37:291. 2013.
8. Maher SA, Rodeo SA, Potter HG, Bonassar LJ, Wright TM, Warren RF. A pre-clinical test platform for the functional evaluation of scaffolds for musculoskeletal defects: the meniscus. HSS J.7:157. 2011.
9. Welsing RT, van Tienen TG, Ramrattan N, Heijkants R, Schouten AJ, Veth RP, et al. Effect on tissue differentiation and articular cartilage degradation of a polymer meniscus implant: A 2-year follow-up study in dogs. Am J Sports Med.36:1978. 2008.
10. Hannink G, van Tienen TG, Schouten AJ, Buma P. Changes in articular cartilage after meniscectomy and meniscus replacement using a biodegradable porous polymer implant. Knee Surg Sports Traumatol Arthrosc.19:441. 2011.
11. Mandal BB, Park SH, Gil ES, Kaplan DL. Multilayered silk scaffolds for meniscus tissue engineering. Biomaterials.32:639. 2011.
12. Baker BM, Nathan AS, Huffman GR, Mauck RL. Tissue engineering with meniscus cells derived from surgical debris. Osteoarthritis Cartilage.17:336. 2009.
13. de Mulder EL, Hannink G, Giele M, Verdonschot N, Buma P. Proliferation of meniscal fibrochondrocytes cultured on a new polyurethane scaffold is stimulated by TGF-beta. J Biomater Appl.27:617. 2013.
14. Hodgson J. To treat or not to treat: that is the question for serum. Biotechnology (N Y).13:333. 1995.
15. Selvaggi TA, Walker RE, Fleisher TA. Development of antibodies to fetal calf serum with arthus-like reactions in human immunodeficiency virus-infected patients given syngeneic lymphocyte infusions. Blood.89:776. 1997.
16. Eppley BL, Woodell JE, Higgins J. Platelet quantification and growth factor analysis from platelet-rich plasma: implications for wound healing. Plast Reconstr Surg.114:1502. 2004.
17. Frechette JP, Martineau I, Gagnon G. Platelet-rich plasmas: growth factor content and roles in wound healing. J Dent Res.84:434. 2005.
18. Weibrich G, Kleis WK, Hafner G, Hitzler WE. Growth factor levels in platelet-rich plasma and correlations with donor age, sex, and platelet count. J Craniomaxillofac Surg.30:97. 2002.
19. Webber RJ, Harris MG, Hough AJ, Jr. Cell culture of rabbit meniscal fibrochondrocytes: proliferative and synthetic response to growth factors and ascorbate. J Orthop Res.3:36. 1985.
20. Huey DJ, Athanasiou KA. Maturational growth of self-assembled, functional menisci as a result of TGF-beta1 and enzymatic chondroitinase-ABC stimulation. Biomaterials.32:2052. 2011.
21. Cole BJ, Seroyer ST, Filardo G, Bajaj S, Fortier LA. Platelet-rich plasma: where are we now and where are we going? Sports Health.2:203. 2010.
22. Mazzocca AD, McCarthy MB, Chowaniec DM, Dugdale EM, Hansen D, Cote MP, et al. The positive effects of different platelet-rich plasma methods on human muscle, bone, and tendon cells. Am J Sports Med.40:1742. 2012.
23. Ishida K, Kuroda R, Miwa M, Tabata Y, Hokugo A, Kawamoto T, et al. The regenerative effects of platelet-rich plasma on meniscal cells in vitro and its in vivo application with biodegradable gelatin hydrogel. Tissue Eng.13:1103. 2007.
24. Akeda K, An HS, Okuma M, Attawia M, Miyamoto K, Thonar EJ, et al. Platelet-rich plasma stimulates porcine articular chondrocyte proliferation and matrix biosynthesis. Osteoarthritis Cartilage.14:1272. 2006.
25. van Buul GM, Koevoet WL, Kops N, Bos PK, Verhaar JA, Weinans H, et al. Platelet-rich plasma releasate inhibits inflammatory processes in osteoarthritic chondrocytes. Am J Sports Med.39:2362. 2011.
26. Kruger JP, Hondke S, Endres M, Pruss A, Siclari A, Kaps C. Human platelet-rich plasma stimulates migration and chondrogenic differentiation of human subchondral progenitor cells. J Orthop Res.30:845. 2012.
27. Adesida AB, Grady LM, Khan WS, Hardingham TE. The matrix-forming phenotype of cultured human meniscus

cells is enhanced after culture with fibroblast growth factor 2 and is further stimulated by hypoxia. Arthritis Res Ther.8:R61. 2006.
28. Adesida AB, Mulet-Sierra A, Laouar L, Jomha NM. Oxygen tension is a determinant of the matrix-forming phenotype of cultured human meniscal fibrochondrocytes. PLoS One.7:e39339. 2012.
29. Gunja NJ, Uthamanthil RK, Athanasiou KA. Effects of TGF-beta1 and hydrostatic pressure on meniscus cell-seeded scaffolds. Biomaterials.30:565. 2009.
30. Liu LW, Vu TK, Esmon CT, Coughlin SR. The region of the thrombin receptor resembling hirudin binds to thrombin and alters enzyme specificity. J Biol Chem.266:16977. 1991.
31. Greinacher A, Warkentin TE. The direct thrombin inhibitor hirudin. Thromb Haemost.99:819. 2008.
32. Chomczynski P, Sacchi N. Single-step method of RNA isolation by acid guanidinium thiocyanate-phenol-chloroform extraction. Anal Biochem.162:156. 1987.
33. Blaney Davidson EN, Remst DF, Vitters EL, van Beuningen HM, Blom AB, Goumans MJ, et al. Increase in ALK1/ALK5 ratio as a cause for elevated MMP-13 expression in osteoarthritis in humans and mice. J Immunol.182:7937. 2009.
34. Ionescu LC, Mauck RL. Porosity and cell preseeding influence electrospun scaffold maturation and meniscus integration in vitro. Tissue Eng Part A.19:538. 2013.
35. Mei-Dan O, Carmont MR. Novel Applications of Platelet-Rich Plasma Technology in Musculoskeletal Medicine and Surgery. Oper Tech Orthop.22:56. 2012.
36. McCarrel TM, Minas T, Fortier LA. Optimization of leukocyte concentration in platelet-rich plasma for the treatment of tendinopathy. J Bone Joint Surg Am.94:e143(1. 2012.
37. Sampson S, Gerhardt M, Mandelbaum B. Platelet rich plasma injection grafts for musculoskeletal injuries: a review. Curr Rev Musculoskelet Med.1:165. 2008.
38. Dohan Ehrenfest DM, Bielecki T, Jimbo R, Barbe G, Del Corso M, Inchingolo F, et al. Do the fibrin architecture and leukocyte content influence the growth factor release of platelet concentrates? An evidence-based answer comparing a pure platelet-rich plasma (P-PRP) gel and a leukocyte- and platelet-rich fibrin (L-PRF). Curr Pharm Biotechnol.13:1145. 2012.
39. Gunja NJ, Athanasiou KA. Passage and reversal effects on gene expression of bovine meniscal fibrochondrocytes. Arthritis Res Ther.9:R93. 2007.
40. Verdonk PC, Forsyth RG, Wang J, Almqvist KF, Verdonk R, Veys EM, et al. Characterisation of human knee meniscus cell phenotype. Osteoarthritis Cartilage.13:548. 2005.
41. McAlinden A, Dudhia J, Bolton MC, Lorenzo P, Heinegard D, Bayliss MT. Age-related changes in the synthesis and mRNA expression of decorin and aggrecan in human meniscus and articular cartilage. Osteoarthritis Cartilage.9:33. 2001.
42. Karube S, Shoji H. Compositional changes of glycosaminoglycans of the human menisci with age and degenerative joint disease. Nihon Seikeigeka Gakkai Zasshi.56:51. 1982.
43. McDevitt CA, Webber RJ. The ultrastructure and biochemistry of meniscal cartilage. Clin Orthop Relat Res.8. 1990.
44. Singh RP, Marwaha N, Malhotra P, Dash S. Quality assessment of platelet concentrates prepared by platelet rich plasma-platelet concentrate, buffy coat poor-platelet concentrate (BC-PC) and apheresis-PC methods. Asian J Transfus Sci.3:86. 2009.
45. Cho HS, Song IH, Park SY, Sung MC, Ahn MW, Song KE. Individual variation in growth factor concentrations in platelet-rich plasma and its influence on human mesenchymal stem cells. Korean J Lab Med.31:212. 2011.
46. Wiesner T, Bugl S, Mayer F, Hartmann JT, Kopp HG. Differential changes in platelet VEGF, Tsp, CXCL12, and CXCL4 in patients with metastatic cancer. Clin Exp Metastasis.27:141. 2010.

Chapter 5

Anisotropic porous biodegradable scaffolds for musculoskeletal tissue engineering

Materials, 2009

Eric de Mulder
Pieter Buma
Gerjon Hannink

ABSTRACT

It has been generally accepted that tissue engineered constructs should closely resemble the in-vivo mechanical and structural properties of the tissues they are intended to replace. However, most scaffolds produced so far were isotropic porous scaffolds with non-characterized mechanical properties, different from those of the native healthy tissue. Tissues that are formed into these scaffolds are initially formed in the isotropic porous structure and since most tissues have significant anisotropic extracellular matrix components and concomitant mechanical properties, the formed tissues have no structural and functional relationships with the native tissues. The complete regeneration of tissues requires a second differentiation step after resorption of the isotropic scaffold. It is doubtful if the required plasticity for this remains present in already final differentiated tissue. It would be much more efficacious if the newly formed tissues in the scaffold could differentiate directly into the anisotropic organization of the native tissues. Therefore, anisotropic scaffolds that enable such a direct differentiation might be extremely helpful to realize this goal. Up to now, anisotropic scaffolds have been fabricated using modified conventional techniques, solid free-form fabrication techniques, and a few alternative methods. In this review we present the current status and discuss the procedures that are currently being used for anisotropic scaffold fabrication.

INTRODUCTION

Damage to the tissues of the musculoskeletal system often result in failure to repair or the formation of regenerated tissue of inferior mechanical quality. Tissue engineering (TE) and regenerative medicine (RM) apply the principles of biology, embryology and engineering to develop functional substitutes for these damaged tissues. TE and RM typically involve implanting cells, with or without stimulating growth factors, into some form of supporting structural device, the so-called scaffold. The cells are allowed to grow, differentiate, and produce new tissue with their own specific extracellular matrix (ECM). In time, the formed tissue should also replace the space occupied by the scaffold. After resorption of the scaffold, the tissue formed should remodel into tissue with a large resemblance to the native tissue. This can be before or after implantation into the patient. In some cases the in-vitro culture period can be omitted and the scaffold can replace the deceased tissue directly, utilizing the host's own body as a 'bioreactor'. Cell harvest, scaffold seeding and implantation can then be performed in a single surgical event[1]. Taking this approach one step further, the scaffolding material can be inserted without cells. In this case, regeneration relies totally on the recruitment of native cells into the implanted scaffold and the subsequent deposition of an ECM[2]. Another option is the incorporation of cells directly into the scaffold during the scaffold fabrication process[3]. No matter which strategy is used, the scaffold itself is critical to the success of the construct, and in most cases actively directs the behavior of the cells within the scaffold.

Factors governing scaffold design are complex and include considerations of scaffold architecture, pore size and pore morphology, mechanical properties, surface properties, degradation speed, and degradation products. The scaffold architecture and surface properties should enhance initial cell attachment and allow efficacious seeding into the entire scaffold, or if this is difficult, migration into the scaffold. The scaffold should enhance the mass transfer of metabolites, provide sufficient space for remodeling of the newly formed tissue matrix and the development of vascularization. Furthermore, it must provide sufficient mechanical strength, particularly initially before the new tissue has matured into functional tissue. In other words, the scaffold degradation profile should be designed in a way it supports the construct during the remodeling process. Factors affecting the rate of remodeling include the type of tissue, and the anatomy and physiology of the host tissue.

A variety of materials have been used to produce scaffolds for the replacement and repair of damaged or traumatized musculoskeletal tissues. These materials include metals, ceramics, natural and synthetic polymers, and their combinations. In this review we will focus only on polymers. Both natural and synthetic polymers have been studied for use as scaffold materials in both TE and RM. Natural polymeric scaffolds have been produced from processed ECM constituents, such as collagen, elastin or hyaluronic acid. Natural polymeric scaffolds may also be produced from polymers derived from plants (alginate) or insects (chitosan). The most frequently used synthetic polymers are poly(lactic acid) (PLA), poly(glycolic acid) (PGA),

poly(lactic-co-glycolic acid) (PLGA), poly(caprolactone) (PCL) and copolymers of these materials[4-7]. Generally, these materials have been approved for human use by the Food and Drug Administration. In addition, their degradation rates can be tailored to match that of new tissue formation. PLA is more hydrophobic and less crystalline than PGA and degrades at a slower rate, while PCL degrades even slower. The degradation rate of the polymers can be easily controlled by altering the ratio of the different copolymers in the formulation, by changing the chain-length of the monomers or by changing the cross-linking density[4,8]. In addition to degradation rate, certain physical characteristics of the scaffold must be considered when designing a substrate to be used in TE. In order to promote tissue growth, the scaffold must have a large surface area to allow cell attachment. This is usually done by creating highly porous scaffolds. In these foam-like scaffolds, the pores should be large enough and interconnected with each other to allow cells to penetrate deeply into the scaffold and to facilitate nutrient and waste exchange by cells deep inside the scaffold. Moreover, the scaffolds should have appropriate mechanical properties to provide temporary support within a specific application. These characteristics are often dependent on both polymer and method of scaffold fabrication.

Several methods have been developed to create highly porous scaffolds, including particle leaching[9,10], gas (CO2) foaming[11], freeze-drying[12], thermal induced phase separation (TIPS)[13,14], liquid/liquid phase separation in combination with freeze extraction[15], electrospinning[16], and particle sintering[17,18]. Also combinations of these techniques have been described[19]. More sophisticated tissue engineered constructs may utilize polymer scaffolds as a delivery vehicle for cells or bioactive proteins. Recently, a new class of scaffolds has been described in which synthetic polymers have been coated or blended with natural polymers[20,21].

Although these conventionally produced scaffolds hold great promise and have been applied to engineer a variety of tissues with varying success, most are limited by some flaws, which restrict their scope of applications[22]. In addition, the processing methods offer little capability to precisely control pore size, pore geometry, pore interconnectivity, spatial distribution of pores, and construction of internal channels within the scaffold. The major limitation of the conventionally fabricated scaffolds is their isotropic nature. The tissue that is formed into the pores of an isotropic scaffold is a negative or mirror image of the scaffold itself, and since most tissue has significant anisotropic arranged extracellular matrix components and concomitant mechanical properties, the tissue formed has no structural and mechanical relationship with the native tissue[23]. For complete regeneration of the tissue a second differentiation step is needed during and after resorption of the isotropic scaffold. It is doubtful if such a plasticity can be expected from already final differentiated tissue. It would be much more efficacious if the newly formed tissues in the scaffold could differentiate directly into the anisotropic organization of native tissues. Anisotropic scaffolds with a porous, tubular or other structure, that enable direct differentiation into the native tissue configuration might be extremely helpful to realize this goal.

The introduction of solid free-form (SFF) technologies have initiated the start

of a new exiting and revolutionary era for scaffold design and production[22]. SFF techniques are computerized fabrication techniques that can produce highly complex, layer-by-layer build, three-dimensional physical objects, using data generated by computer aided design (CAD) systems or computer-based medical imaging modalities. The most promising techniques to generate scaffolds with a highly anisotropic pore structure are SFF technologies, such as 3D fiber deposition (3DF), fused deposition modeling (FDM), bioplotting, stereolithography (STL), and selective laser sintering (SLS), but also modified "conventional" techniques, such as modified thermal induced phase separation (modified TIPS) and electrospinning. In this review we will present the current status and discuss the procedures which are currently in use for anisotropic scaffold production.

SOLID FREE-FORM FABRICATION

Solid free-form technologies, also commonly known as rapid prototyping (RP), are computer aided manufacturing (CAM) techniques that can rapidly produce highly complex three dimensional physical objects using data generated by computer aided design (CAD) programs, or converted from computerbased medical imaging modalities, such as MRI and CT[24,25]. Unlike conventional computerized machining processes, which involve the removal of materials from a stock, SFF techniques use the underlying concept of layered manufacturing whereby three-dimensional objects are fabricated with layer-by-layer building via the processing of solid sheet, liquid or powder material stocks[22]. The flexibility and outstanding manufacturing capabilities of SFF have been employed for biomedical applications, such as production of scale replicas of human bones[26], body organs[27], and advanced customized drug delivery devices[28]. The direct utilization of CAD models as inputs for scaffold fabrication allows complex scaffold designs to be realized. Patient specific data and scaffold structural properties required for regenerating specific tissues can be incorporated into scaffold design via CAD. The application of CAD strategies in conjunction with SFF fabrication will allow scaffolds with highly uniform pore morphologies, unlimited range of pore sizes, porosities and complete pore interconnectivity to be realized with unprecedented accuracy and consistency for patient specific application[22]. In addition, SFF techniques employ a diverse range of processing conditions which include solvent and/or porogen free processes and processing at room temperature. Some SFF techniques allow pharmaceutical and biological agents to be incorporated into the scaffold during fabrication[28-30]. The utilization of CAD will also allow scaffolds with optimized mechanical and structural properties to be fabricated. The following sections will focus on SFF techniques that have been used for fabricating anisotropic scaffolds.

3D fiber deposition / fused deposition modeling

3D fiber deposition and FDM are similar techniques. The majority of 3DF/FDM techniques are nozzle-based systems. Polymers are thermally processed when they

pass a nozzle and are deposited as a relatively thick fiber on a collector plate. After deposition on the collector plate, the fibers cool down, solidify and the scaffold is ready for use (Figures 1A, 1B). Fiber diameter can be controlled by changing parameters, such as nozzle diameter, deposition speed, extrusion speed and viscosity of the polymer, and can range between 170-750 μm[31-33]. A wide range of polymers, including hydrogels, have been used in 3DF/FDM[34-37]. However, most of the produced scaffolds have an internal isotropic organization. Each successive layer is deposited under a different angle, creating a specific lay-down pattern[38,39]. Most used lay-down patterns are 0/90º, 0/45/90/135º and 0/60/120º. The compressive stiffness of the scaffold can range from 4 - 80 MPa, depending on the lay-down pattern, fiber thickness, and the polymers used for fabrication[38]. Using a 0/45º lay-down pattern, the compressive stiffness in the z plane is different compared to the compressive stiffness in the x/y plane, thereby resulting in mechanical anisotropy. Anatomically 3D fiber deposited trachea, menisci and vertebra have recently been fabricated from patient-derived computer-based medical imaging modalities[25,35,40]. In addition, shell/core fibers have been produced by exploiting viscous encapsulation, a rheological phenomenon in polymeric blends flowing through narrow ducts[41]. Furthermore, by printing fibers directly aligned in one layer followed by a semi-open layer, anisotropic scaffolds with aligned channels can be created (unpublished data). In this way, also nutrient supply in the deeper zones of the scaffolds could be facilitated[42].

Bioplotter

Bioplotting was first described by Wilson and Boland[43]. They modified a commercial inkjet printer into a custom-made bioplotter. After cleaning the ink cartridges, the containers were refilled with solutions containing marker proteins (y-biotine, steptavidine, streptavidine-BSA and BSA) or with endothelial or smooth muscle cells. The resolution of this technique has been shown to be approximately 25-50 μm in both the x and y directions[43,44]. Using this technique, complex structures containing viable cells after printing have been produced[45]. However, after printing a 25% cell death was observed[43]. It has been shown that cell death could be strongly reduced by avoiding dehydration of the cells after printing by increasing the water content of the gels in which the cells are encapsulated[43,46,47]. Incorporation of growth factors or other biological cues, such as calcium phosphates, specific adhesive peptides, and collagen can modulate cell function and degradation of the scaffold[34]. In this way, an instructive microenvironment for embedded or seeded cells can be created[48]. Cohen *et al*. were able to fabricate a geometrically complex structure in the shape of a meniscus using alginate as scaffold material[44]. However, so far, no anisotropic scaffolds have been fabricated using bioplotting. Using multiple cartridges, zonal distribution of multiple cell types and biological cues anisotropic scaffolds should be relatively easily achieved[34].

Stereolithography

Stereolithography is the oldest RP technique[49]. It is based on spatially controlled

photopolymerization of a liquid resin by a laser. As the resin only solidifies where illuminated, a specific pattern can be created in one single layer. By repeating this process, three-dimensional structures can be built in a layer-by-layer manner (Figures 1C, 1D)[50,51]. In conventional STL machines one laser beam is used for photopolymerization. However, recently new systems have been developed which use two lasers in the near infrared spectrum, the so-called two photon polymerization technique (2PP)[52-55].

A prerequisite for polymers to be used in STL are end-groups that can be polymerized by light[3,50,54-60]. Epoxy resins are very popular for the generation of non-resorbable STL molds. These molds are used to shape polymers into conventional made scaffolds for various tissue engineering or regenerative medicine purposes[61-63]. Two resorbable materials are particularly interesting for STL scaffold production. First, scaffolds based on poly-DL-lactic acid (PDLLA) are very popular for bone tissue engineering. A second very promising material that has been recently introduced is poly(propylene fumarate) (PPF)[64,65]. Hydrolysis of the ester bonds allows PPF to degrade into fumaric acid and propylene glycol, both of which are non-toxic products[55]. Scaffolds made from PFF have mechanical properties in the MPa range (15-40 MPa) and are also suitable for bone tissue engineering.

The accuracy of STL is dependent on a number of parameters. The most important ones are the machine, the method (one photon versus two photon polymerization)[49,53,54], the laser power[53,65], the scan speed[65], and the length of the laser beam path into the polymer[66]. In general, commercial STL machines have a resolution in the order of 200–250 μm. Some claim a resolution of 75 μm or even lower but then they might fail to create open pores[59]. Others claim even accuracies of 10–100 μm, however this has been shown to be the ultimate limit of accuracy with conventional machines[54]. The penetration depth, and by that the accuracy in the z-direction, may be increased by adding specific dyes to the polymer which reduce the penetration depth of the UV beam. With conventional STL the layer thickness can then be reduced from 29 to 7 μm[66]. The structural resolution of 2PP polymerization is in general much higher and can be even lower than 100 nm[53,54].

A matter of attention is the matching between CAD files and the produced scaffold structures. Shrinkage of resins used for STL is a general phenomenon and might be up to 25%[64,65]. However, if the shrinkage is isotropic, which is generally the case, the CAD files might be adapted to the expected percentage of shrinkage of a specific polymer with a good matching as a result[3,65]. Generally, the difference between the CAD file and the produced structure will not exceed 0.5%. For porous scaffolds the differences between CAD files and the produced pores have been described to be larger, ranging from 0.2% for the large pores to 8.3% for the very small pores[65].

Amongst the pitfalls in STL are diluting the polymers before the polymerization process and the use of non-reacted chemicals after polymerization[66]. Diluting the polymers negatively influences the mechanical properties of the produced structures[67]. Non-reacted chemicals inside the scaffold can potentially cause problems if they are not adequately removed from the fabricated structures. Particularly non-reacted

photo-initiator might be cytotoxic[68]. The use of biocompatible non-reacted polymers and non-reactive diluents would be a solution[66].

Functional studies on STL scaffolds are scarce. Engelmayer *et al*. have shown that pore dimensions influence collagen orientation and deposition by rat skin fibroblasts[69]. Using 2PP STL, sub-micron needle like structures have been produced on which the reaction of fibroblast cells (NIH-3T3) and epithelial cells (MDCK) has been shown to be dependent on the pattern of actin microfilament bundles in the cells. For bone TE scaffolds with channels were produced to study the optimal channel diameter to facilitate cell ingrowth[70]. Functional animal studies related to the in-vivo tissue reactions are very scarce. The group of Jansen studied the soft and hard tissue response to photo-crosslinked PPF scaffolds in a rabbit model[58]. These scaffolds appeared to induce a mild inflammatory reaction in both tissue types. A powerful future application might be the blending of cells into SLT scaffolds during photopolymerization[56].

MODIFIED CONVENTIONAL TECHNIQUES

Conventional methods for manufacturing scaffolds include particle leaching[9,10], gas (CO2) foaming[11], freeze-drying[12], thermal induced phase separation (TIPS)[13,14], liquid/liquid phase separation in combination with freeze extraction[15], electrospinning[16], and particle sintering[17,18]. However, there are inherent limitations in these processing methods. These methods offer little capability to control pore size, pore geometry, pore interconnectivity, spatial distribution of pores and construction of internal channels within the scaffold[71]. Consequently, it has been tried to modify the conventional techniques to overcome these inherent process limitations[17,72-75]. The following sections will focus on modified conventional techniques that have been used to fabricate anisotropic scaffolds.

Modified thermal induced phase separation (TIPS)

A commonly used procedure to create porous polymer scaffolds is TIPS. This technique is based on the principle that a homogeneous polymer solution made at elevated temperature is converted via the removal of thermal energy (cooling) into two-phase separated domains. Through extraction, evaporation or sublimation the solvent containing phase will be removed and give rise to the pores of the scaffold. Two different phase separations have been described, namely solid-liquid and liquidliquid phase separation. In solid-liquid phase separation the temperature is lowered to solidify the polymer solution. The solvent will form crystals and thereby separate the polymer from the solvent. Finally, the crystals are removed which exposes the pores. In the second method, liquid-liquid phase separation, phase separation is based on a polymer-rich and a polymer-lean phase. The solvent part will be present in the polymer lean phase which will be processed further to create the pores in the scaffold[14,76]. For example, polymers such as PLA and PLGA are diluted in dioxane/ water in the desired polymer concentration and subsequently cooling down of the

polymer induces the phase separation. A porous foam-like scaffold is available after removal of the solvent in a freeze-dryer. The formed scaffolds have a randomly distributed isotropic pore structure[77-79].

In the modified TIPS a uni-axial thermal gradient is applied between top and bottom instead of uniformly cooling during the phase separation step (Figures 1E, 1F)[80]. Via insulation of the walls of the polymer/solvent container a longitudinal temperature gradient is created resulting in longitudinal crystal formation. The result is a scaffold containing micro-channels instead of pores, which are orientated in a top to bottom direction. The diameter of these micro-channels can range between 15–240 μm[72,81,82]. The diameter can be controlled by changing the thermal gradient and/or the proportion polymer/solvent. Using a higher thermal gradient and higher polymer concentration the diameter of the channels has been shown to decrease. The micro-architecture of the channels can be influenced by the type of solvent used. Using benzene as a solvent, microtubules will be open, while with dioxane the channels have ladder-like structures[72,80]. The anisotropic structural properties of the scaffold is reflected in higher compressive modulus and yield strength in the longitudinal direction compared to the transverse direction[72,80]. Culture studies show that cells grow along the direction of the microtubules and synthesize oriented neo-tissue[83]. Modified TIPS has also been applied to natural polymers such as collagen. A temperature gradient between bottom and top of the container, according to the Bridgman technique[84], resulted in an ice front growth in an opposite direction than the temperature gradient[85]. Applying this temperature gradient to collagen suspensions resulted in unidirectional collagen scaffolds, also with some ladder-like characteristics[86-88]. The channels were in the range 20-40 μm and were predominantly controlled by the temperature gradient and solvent type (either ethanol or acetic acid). The scaffolds can be molded in discs or tube like shapes. It should be noticed that after polymerization skin formation can occur on the edge, thereby limiting cell penetration into the scaffold.

Electrospinning

A conventional method for fiber deposition is electrospinning. Using a high voltage/low current a very thin fiber (tenths of nanometers) can be produced from a polymer droplet, which is directed toward a grounded counter plate electrode, the so-called collector plate. On a static collector plate the fibers will be displayed in a random orientation. Scaffolds can be fabricated in various different tubular configurations with different surface patterning using different shaped, static 3D, columnar patterned collectors[89]. With help of a rotating cylinder or rotating disc type collector it is possible to produce orientated/aligned fibers (Figures 1G, 1H)[90,91]. It has been shown that fiber diameter and degree of fiber alignment can determine the behavior of cells[16]. Cells orientate themselves and migrate into the direction of the fiber orientation with higher proliferation and synthetic rates[92,93]. Aligned nanofibers seeded with ligament fibroblasts induced more elongated fibroblasts compared to randomly orientated fibers, and these cells also produced more collagen compared to

cells on non-aligned scaffolds[94]. Multiple spinneret tips with different polymers can create multilayer scaffolds[95]. These layers can also be separated by seeded cells. Using different cell types in between layers, complex 3D structures with living cells have been produced[96]. With a set-up using a syringe-inside-a-syringe core/shell nanofibers

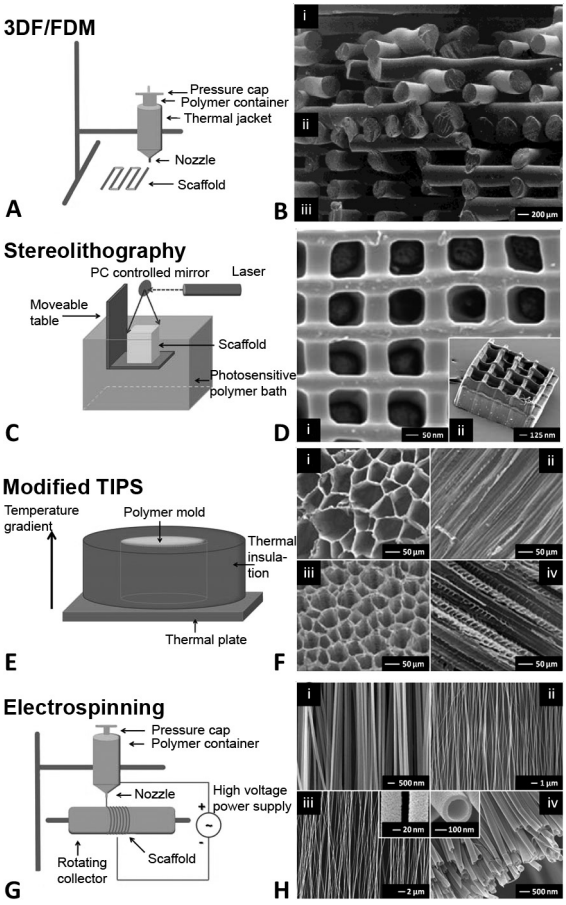

Figure 1. (A) Schematic representation of 3D fiber deposition (3DF)/Fused deposition modeling (FDM). (B) SEM micrographs of a PCL scaffold with varying multiple-layer design prepared using 3DF/FDM, showing a scaffold architecture with (i) a 0/60/120° laydown pattern for the top part, (ii) a nonporous structure for the middle part, and (iii) a 0/90° lay-down pattern of the bottom part of the scaffold. Reproduced and modified with permission from Hutmacher et al. [99]. Copyright John Wiley & Sons, Inc. (C) Schematic representation of stereolithography (STL). (D) SEM micrographs of a STL prepared scaffold, showing (i) a single-layer scaffold, and (ii) a multilayered scaffold. Reproduced and modified with permission from Mapili et al. [59]. Copyright John Wiley & Sons, Inc. (E) Schematic representation of modified thermal induced phased separation (TIPS). (F) SEM micrographs of the uniaxial microtubular scaffolds prepared using modified TIPS, showing (i) a cross-section of a scaffold prepared from 2.5% (w/v) polymer/benzene under liquid nitrogen, (ii) a longitudinal section of this scaffold, (iii) a cross-section of a scaffold prepared from 3.0% (w/v) polymer/benzene under liquid nitrogen, and (iv) a longitudinal section of this scaffold. Reproduced and modified with permission from Chen et al. [72]. Copyright John Wiley & Sons, Inc. (G) Schematic representation of modified electrospinning. (H) SEM micrographs of scaffolds prepared with electrospinning, showing (i-iii) aligned nanofibers, and (iv) uniaxially aligned nanotubes. Reproduced and modified with permission from Li et al. [100]. Copyright Wiley-VCH Verlag GmbH & Co. KGaA.

have been created[97]. This technique is has also been used to produce aligned collagen nanofiber scaffolds with a similar cellular response to fiber orientation as described above[98].

ALTERNATIVE METHODS TO CREATE ANISOTROPIC SCAFFOLDS

Using the techniques outlined above, the production of aligned channels in a scaffold has been realized. However, most of the above mentioned techniques are technically demanding. Alternative methods might be cheaper, more easy to use, or useful if the size of features in the scaffolds is limited by the resolution of the technique. Therefore, a number of alternative methods have been proposed to incorporate aligned channels into the general structure of the scaffold. Some of these alternative methods can be applied directly during scaffold polymerization, while others are applied after polymerization as a post-processing step.

Direct methods

Most polymers are in the liquid phase before molding. Using arrays of needles and/or wires placed in the mold, porous scaffolds with aligned channels can easily be fabricated. The diameter of these channels depends on the thickness of the needles and/or wires used. The architecture can vary on the needle array applied[99,100]. Unfortunately, removal of the needles and/or wires after polymerization has been shown to damage these scaffolds. To prevent damage, coated wires and/or needles have been used[101]. After polymerization of the scaffold, the coating on the wires or needles can be dissolved, facilitating the removal of the wires and/or needles. An alternative approach is to use wires that can dissolve completely[18,101]. Nazhat *et al*. incorporated unidirectional aligned soluble 30–40 μm diameter phosphate glass fibers (PGFs) into dense compacted collagen scaffolds[102]. The degradation time of PGFs can range from minutes to years depending on their chemistry. Their biocompatibility has been demonstrated with a number of cell types[103,104]. In addition, the use of phosphate glass particles as reinforcing agents, and eventually as porogens through their degradation in synthetic biodegradable composites, has been carried out in PCL[105,106] and lactide[107,108] matrices developed for drug delivery and tissue engineering. Therefore, PGFs might also be used as channel-creating devices in synthetic biodegradable composites. Besides solvable wires or retracting wires, it is also possible to leave the wires inside the scaffold but then the effect of creating access for mass transport is lost[109].

Another direct method to create anisotropic scaffolds is the use of conventional porogens, such as sugar, salt, alginate, or bovine serum albumin micro-bubbles[110-113]. Capes *et al*. have managed to arrange sugar strands in a mold[114]. Subsequently, the polymer solution was casted over the sugar strands, and after polymerization the strands were washed out. Similar methods can be applied using other porogens like paraffin, sodium alginate and/or gelatine[115].

Various methods have been described to create channels in scaffolds after polymerization. Silva *et al*. produced an array of aligned 400 μm thick channels into a random, porous PDLLA scaffold structures using a computer controlled drill system[100]. Using relatively thin polymer sheet, excimer laser ablation has been used to create specifically sized channels in polymer scaffolds[116-119]. For musculoskeletal tissue engineering purposes stacking these single-layer sheets might be an option. Recently, Vishnubhatla *et al*. have fabricated micro-channels in fused silica by femto-second laser irradiation[120]. They have created cylindrical micro-channels with uniform cross-sections and a length of 4 mm. As mentioned above, Capes *et al*. used a traditional solid porogen technique for the fabrication of PGLA scaffolds[114]. Besides the use of close-packed sugar strands to create a 3D polymer scaffold with multiple aligned channels, they also created single-layer scaffolds using sugar spheres. Multi-layer scaffolds were created by stacking the single-layer to form a 3D structure. Also known porogens such as, paraffin, sodium alginate, and gelatine might be used to create anisotropic scaffolds using single-layer stacking. Using phase separation micromolding, Papenburg *et al*. reported a one-step method to fabricate highly porous micro-patterned polymer 2D scaffold sheets[121]. These 2-D micropatterned sheets can be built into a 3-D scaffold by multi-layer stacking immediately after casting. Residues of the solvent still present in the sheets enabling the layers to bond. Stacking was achieved through two different methods: by either clamping several films between glass-plates or rolling up one or more sheets around a tube. By tuning size of the channels and the sheet thickness, the scaffold architecture can be designed.

DISCUSSION

Tissue engineered biomaterials should ideally bear close resemblance to the in vivo mechanical and structural properties of the tissues that they are intended to replace. Since mechanical loads can vary spatially and temporally within the tissues of an organ, they exhibit complex, mechanically anisotropic behaviors optimized for their respective physiological functions[122].

Many tissues in the musculoskeletal system, particularly those that bear mechanical loads in a defined direction, exhibit preferential fiber alignment[123]. This alignment endows such tissues to functional properties that vary depending on the testing direction. For example, in tendons and ligaments, tensile properties are 200-500 times higher along, compared to perpendicular to, the fiber direction[124]. In articular cartilage, tensile properties are greatest in the superficial zone along the split line direction[125,126]. In the meniscus, circumferentially oriented collagen fibers predominate[127], resulting in higher tensile properties in the circumferential compared to the radial direction[128-130]. When damage occurs, the architecture is interrupted and the ability of the tissue to withstand load is compromised. As such, the architecture must be one of the first considerations when engineering replacement constructs[131].

Using conventional scaffolds, it has been shown that the tissues formed had

no relationship with the native tissue but were oriented into the direction of the isotropic distributed pores[23]. Differentiation of the newly formed tissue directly into the anisotropic organization of the native tissue would be much more efficacious. Therefore, one of the considerable challenges remaining in the field of tissue engineering is to produce a construct with an anatomically correct architectural framework, both in terms of cell morphology and matrix deposition[123].

The use of SFF techniques will allow control over localized pore morphologies and porosities to suit the requirements of different cell types within the same scaffold volume. This is achieved by incorporating different controllable macroscopic and microscopic design features on different regions of the same scaffold. Depending on the TE strategy used, this can be realized either using negative anisotropic scaffolds, positive anisotropic scaffolds, or a combination of both. Negative anisotropic scaffolds, often referred to as "mirror imaged" scaffolds, are fabricated based on guidance or entubulization TE strategies. Newly formed tissues growing into the scaffold will be guided and subsequentially differentiate directly into the anisotropic organization of the native tissues (indirect) [72,80,82,83,88,101]. On the other hand, positive anisotropic constructs are fabricated directly into the anisotropic organization of the native tissue, resembling the hierarchical structure of multiple cell types, and/or ECM compounds, such as collagen and elastin[34,45,96,132]. Scaffolds consisting of aligned fibers were found to possess controllable anisotropic mechanical properties and to dictate cellular morphology, with cell polarity following the prevailing fiber direction[123]. Under conditions of maximal fiber alignment, meniscal chondrocytes attached to these scaffolds and their directionality was prescribed in both the short and long term culture. It has previously been shown in organized monolayer cultures that fibroblasts deposit an organized ECM according to cell orientation[133], and that ligament fibroblasts on an aligned fiber meshes produce more collagen than on random meshes[94].

A common problem encountered when using conventional scaffolds for tissue engineering is the rapid formation of tissue on the outer edge, leading to the development of a necrotic core due to limitations of cell penetration and nutrient exchange[100,134,135]. Most tissues possess a network of blood and capillary vessels that perform this function in vivo, but engineering such a complex construct in vitro has been shown to be quite challenging[136,137]. Even avascular tissue, such as cartilage, has been shown challenging to engineer since the in vivo nutrient supply still cannot be adequately simulated in vitro[134]. A common approach used to overcome this issue is to utilize sophisticated culture systems or bioreactors to perfuse culture media around and/or through the scaffold[138-140]. Although these bioreactors have been successful, even in an optimized in vitro culture system, there is still a need to ensure tissue growth occurs evenly throughout the construct. Furthermore, for strategies where the scaffold alone will be implanted and the body is used as bioreactor, it is important to ensure that native tissue can infiltrate the whole scaffold to ensure adequate integration of the construct[141]. Another strategy to encourage tissue formation and cell differentiation within scaffolds, in vitro or in vivo, is to incorporate biological

factors, such as growth factors, ECM compounds, or pharmaceutical agents which can also act as chemotactic factors to encourage cell migration and differentiation[142].

Patient specific data and scaffold structural properties required for regenerating specific tissues can be incorporated into scaffold design via CAD, often referred to as 'reverse engineering'[22]. SFF techniques can be easily automated and integrated with these imaging techniques to produce scaffolds that are customized in size and shape allowing tissue engineered grafts to be tailored for specific applications or even for individual patients[143]. In musculoskeletal applications, so far, these patient specific scaffolds have been used for the reconstruction of cranial[144,145], calvarial[146], and maxillofacial defects[147].

A key factor used to enhance the versatility of scaffold fabrication by SFF is construction of a scaffold matrix using a wide variety of biomaterials[143]. One emerging method is to fabricate a negative mold based on the scaffold design and cast the scaffold using desired polymeric and/or ceramic biomaterials. This alternative technique is known as 'indirect' SFF. Based on a lost mold technique by combining epoxy resin molds made by stereolithography and CAD data HA scaffolds with interconnecting pores have been created[148]. Despite a few fabrication inaccuracies, in-vivo experiments demonstrated osteoconductivity and biocompatibility in a minipig model. In addition, a series of biomimetic scaffolds have been fabricated by mold removal in combination with conventional sponge fabrication[149]. The fabricated scaffolds had interconnected pores ranging from 500–800 μm as specified by the prefabricated mold, and when local pores were formed they ranged from 10–300 μm depending on the local pore creating method. Similarly, an indirect SFF method for ceramic scaffolds with a defined and reproducible 3D porous architecture has been developed[150]. They reported ectopic bone formation for all scaffold and cell constructs. Manufacturing of collagen based scaffolds by using the SFF technique to fabricate a mold has also been reported[151].

The main restriction on casting with the conventional techniques was the inability to create molds to produce complex geometries and internal architecture but with indirect SFF conventional casting processes with these molds can meet specific tissue engineering requirements[143]. Indirect SFF allows use of a wider range of biomaterials or combinations of materials, such as composites and/or copolymers. However, some drawbacks still exist with this technology, including the use of organic solvents and the resolution of the SFF method. For example, the cast model copies errors and defects from the mold, such as cracks and dimensional changes. In addition, a method has to be developed to remove the mold precisely while preserving the cast scaffold intact without compromising its properties[143].

CONCLUSIONS

Although many options are available to fabricate anisotropic scaffolds for musculoskeletal tissue engineering, each method has its own set of strengths and weaknesses. For all techniques described, the choice of scaffold material seems to be

endless since almost every polymer, natural or synthetic, can be used in combination with the desired technique. However, it has to be ensured that choice of materials for the scaffold is compatible with the selected method. Important considerations that should be made during the selection of materials used for musculoskeletal tissue engineering include mechanical properties of the material, scaffold design, degradation profile, bioactivity and biodegradability, as well as issues of cell seeding and vascularization

REFERENCE LIST

1. Jurgens WJ, Oedayrajsingh-Varma MJ, Helder MN, Zandiehdoulabi B, Schouten TE, Kuik DJ, Ritt MJ, van Milligen FJ. Effect of tissue-harvesting site on yield of stem cells derived from adipose tissue: implications for cell-based therapies. Cell Tissue Res 2008;332(3):415-426.
2. Buma P, Ramrattan NN, van Tienen TG, Veth RP. Tissue engineering of the meniscus. Biomaterials 2004;25(9):1523-1532.
3. Dhariwala B, Hunt E, Boland T. Rapid prototyping of tissue-engineering constructs, using photopolymerizable hydrogels and stereolithography. Tissue Eng 2004;10(9-10):1316-1322.
4. Boccaccini AR, Blaker JJ. Bioactive composite materials for tissue engineering scaffolds. Expert Rev Med Devices 2005;2(3):303-317.
5. Buma P, Pieper JS, van TT, van Susante JL, van der Kraan PM, Veerkamp JH, van den Berg WB, Veth RP, van Kuppevelt TH. Cross-linked type I and type II collagenous matrices for the repair of full-thickness articular cartilage defects--a study in rabbits. Biomaterials 2003;24(19):3255-3263.
6. Heijkants RG, van Calck RV, de Groot JH, Pennings AJ, Schouten AJ, van Tienen TG, Ramrattan N, Buma P, Veth RP. Design, synthesis and properties of a degradable polyurethane scaffold for meniscus regeneration. J Mater Sci Mater Med 2004;15(4):423-427.
7. Hutmacher DW, Schantz JT, Lam CX, Tan KC, Lim TC. State of the art and future directions of scaffold-based bone engineering from a biomaterials perspective. J Tissue Eng Regen Med 2007;1(4):245-260.
8. Raghunath J, Rollo J, Sales KM, Butler PE, Seifalian AM. Biomaterials and scaffold design: key to tissue-engineering cartilage. Biotechnol Appl Biochem 2007;46(Pt 2):73-84.
9. Hou Q, Grijpma DW, Feijen J. Preparation of interconnected highly porous polymeric structures by a replication and freeze-drying process. J Biomed Mater Res B Appl Biomater 2003;67(2):732-740.
10. Shin K, Jayasuriya AC, Kohn DH. Effect of ionic activity products on the structure and composition of mineral self assembled on three-dimensional poly(lactide-co-glycolide) scaffolds. J Biomed Mater Res A 2007;83(4):1076-1086.
11. Nam YS, Yoon JJ, Park TG. A novel fabrication method of macroporous biodegradable polymer scaffolds using gas foaming salt as a porogen additive. J Biomed Mater Res 2000;53(1):1-7.
12. Madihally SV, Matthew HW. Porous chitosan scaffolds for tissue engineering. Biomaterials 1999;20(12):1133-1142.
13. Guan J, Fujimoto KL, Sacks MS, Wagner WR. Preparation and characterization of highly porous, biodegradable polyurethane scaffolds for soft tissue applications. Biomaterials 2005;26(18):3961-3971.
14. van de Witte P, Dijkstra PJ, van den Berg JWA, Feijen J. Phase behavior of polylactides in solvent-nonsolvent mixtures. J Polym Sci B Pol Phys 1996;34(15):2553-2568.
15. Budyanto L, Goh YQ, Ooi CP. Fabrication of porous poly(L-lactide) (PLLA) scaffolds for tissue engineering using liquid-liquid phase separation and freeze extraction. J Mater Sci Mater Med 2009;20(1):105-111.
16. Bashur CA, Shaffer RD, Dahlgren LA, Guelcher SA, Goldstein AS. Effect of Fiber Diameter and Alignment of Electrospun Polyurethane Meshes on Mesenchymal Progenitor Cells. Tissue Eng Part A 2009;15(9):2435-2445.
17. Murphy WL, Dennis RG, Kileny JL, Mooney DJ. Salt fusion: an approach to improve pore interconnectivity within tissue engineering scaffolds. Tissue Eng 2002;8(1):43-52.
18. Williams JM, Adewunmi A, Schek RM, Flanagan CL, Krebsbach PH, Feinberg SE, Hollister SJ, Das S. Bone tissue engineering using polycaprolactone scaffolds fabricated via selective laser sintering. Biomaterials 2005;26(23):4817-4827.
19. Heijkants RG, van Calck RV, van Tienen TG, de Groot JH, Pennings AJ, Buma P, Veth RP, Schouten AJ. Polyurethane scaffold formation via a combination of salt leaching and thermally induced phase separation. J Biomed Mater Res A 2008;87(4):921-932.
20. Chang KY, Cheng LW, Ho GH, Huang YP, Lee YD. Fabrication and characterization of poly(gamma-glutamic acid)-graft-chondroitin sulfate/polycaprolactone porous scaffolds for cartilage tissue engineering. Acta Biomater 2009;5(6):1937-1947.
21. Chang KY, Hung LH, Chu IM, Ko CS, Lee YD. The application of type II collagen and chondroitin sulfate grafted PCL porous scaffold in cartilage tissue engineering. J Biomed Mater Res A 2009.
22. Leong KF, Cheah CM, Chua CK. Solid freeform fabrication of three-dimensional scaffolds for engineering replacement tissues and organs. Biomaterials 2003;24(13):2363-2378.
23. Welsing RT, van Tienen TG, Ramrattan N, Heijkants R, Schouten AJ, Veth RP, Buma P. Effect on tissue differentiation and articular cartilage degradation of a polymer meniscus implant: A 2-year follow-up study in dogs. Am J Sports Med 2008;36(10):1978-1989.
24. Coward TJ, Watson RM, Wilkinson IC. Fabrication of a wax ear by rapid-process modeling using

stereolithography. Int J Prosthodont 1999;12(1):20-27.
25. Meakin JR, Shepherd DE, Hukins DW. Short communication: fused deposition models from CT scans. Br J Radiol 2004;77(918):504-507.
26. D'Urso PS, Earwaker WJ, Barker TM, Redmond MJ, Thompson RG, Effeney DJ, Tomlinson FH. Custom cranioplasty using stereolithography and acrylic. Br J Plast Surg 2000;53(3):200-204.
27. Sanghera B, Amis A, McGurk M. Preliminary study of potential for rapid prototype and surface scanned radiotherapy facemask production technique. J Med Eng Technol 2002;26(1):16-21.
28. Leong KF, Phua KK, Chua CK, Du ZH, Teo KO. Fabrication of porous polymeric matrix drug delivery devices using the selective laser sintering technique. Proc Inst Mech Eng H 2001;215(2):191-201.
29. Cheah CM, Leong KF, Chua CK, Low KH, Quek HS. Characterization of microfeatures in selective laser sintered drug delivery devices. Proc Inst Mech Eng H 2002;216(6):369-383.
30. Leong KF, Wiria FE, Chua CK, Li SH. Characterization of a poly-epsilon-caprolactone polymeric drug delivery device built by selective laser sintering. Biomed Mater Eng 2007;17(3):147-157.
31. Moroni L, de Wijn JR, van Blitterswijk CA. 3D fiber-deposited scaffolds for tissue engineering: influence of pores geometry and architecture on dynamic mechanical properties. Biomaterials 2006;27(7):974-85.
32. Moroni L, Schotel R, Sohier J, de Wijn JR, van Blitterswijk CA. Polymer hollow fiber three-dimensional matrices with controllable cavity and shell thickness. Biomaterials 2006;27(35):5918-26.
33. Woodfield TB, van Blitterswijk CA, De WJ, Sims TJ, Hollander AP, Riesle J. Polymer scaffolds fabricated with pore-size gradients as a model for studying the zonal organization within tissue-engineered cartilage constructs. Tissue Eng 2005;11(9-10):1297-1311.
34. Fedorovich NE, de W, Jr., Verbout AJ, Alblas J, Dhert WJ. Three-dimensional fiber deposition of cell-laden, viable, patterned constructs for bone tissue printing. Tissue Eng Part A 2008;14(1):127-133.
35. Moroni L, Curti M, Welti M, Korom S, Weder W, de Wijn JR, van Blitterswijk CA. Anatomical 3D fiber-deposited scaffolds for tissue engineering: designing a neotrachea. Tissue Eng 2007;13(10):2483-2493.
36. Moroni L, de Wijn JR, van Blitterswijk CA. Integrating novel technologies to fabricate smart scaffolds. J Biomater Sci Polym Ed 2008;19(5):543-572.
37. Moroni L, Hendriks JA, Schotel R, de Wijn JR, van Blitterswijk CA. Design of biphasic polymeric 3-dimensional fiber deposited scaffolds for cartilage tissue engineering applications. Tissue Eng 2007;13(2):361-371.
38. Li JP, de Wijn JR, van Blitterswijk CA, de Groot K. The effect of scaffold architecture on properties of direct 3D fiber deposition of porous Ti6Al4V for orthopedic implants. J Biomed Mater Res A 2009.
39. Zein I, Hutmacher DW, Tan KC, Teoh SH. Fused deposition modeling of novel scaffold architectures for tissue engineering applications. Biomaterials 2002;23(4):1169-1185.
40. Moroni L, Lambers FM, Wilson W, van Donkelaar CC, de Wijn J, Huiskes R, van Blitterswijk CA. Finite Element Analysis of Meniscal Anatomical 3D Scaffolds: Implications for Tissue Engineering. Open Biomed Eng J 2007;1:23-34.
41. Moroni L. A mechanistic approach to design smart scaffolds for tissue engineering. Thesis; 2006.
42. Den Buijs JO, Dragomir-Daescu D, Ritman EL. Cyclic deformation-induced solute transport in tissue scaffolds with computer designed, interconnected, pore networks: experiments and simulations. Ann Biomed Eng 2009;37(8):1601-1612.
43. Wilson WC, Jr., Boland T. Cell and organ printing 1: protein and cell printers. Anat Rec A Discov Mol Cell Evol Biol 2003;272(2):491-496.
44. Cohen DL, Malone E, Lipson H, Bonassar LJ. Direct freeform fabrication of seeded hydrogels in arbitrary geometries. Tissue Eng 2006;12(5):1325-1335.
45. Boland T, Mironov V, Gutowska A, Roth EA, Markwald RR. Cell and organ printing 2: fusion of cell aggregates in three-dimensional gels. Anat Rec A Discov Mol Cell Evol Biol 2003;272(2):497-502.
46. Boland T, Xu T, Damon B, Cui X. Application of inkjet printing to tissue engineering. Biotechnol J 2006;1(9):910-917.
47. Xu T, Jin J, Gregory C, Hickman JJ, Boland T. Inkjet printing of viable mammalian cells. Biomaterials 2005;26(1):93-99.
48. Lutolf MP, Hubbell JA. Synthetic biomaterials as instructive extracellular microenvironments for morphogenesis in tissue engineering. Nat Biotechnol 2005;23(1):47-55.
49. Peltola SM, Melchels FP, Grijpma DW, Kellomaki M. A review of rapid prototyping techniques for tissue engineering purposes. Ann Med 2008;40(4):268-280.
50. Jansen J, Melchels FP, Grijpma DW, Feijen J. Fumaric acid monoethyl ester-functionalized poly(D,L-lactide)/N-vinyl-2-pyrrolidone resins for the preparation of tissue engineering scaffolds by stereolithography. Biomacromolecules 2009;10(2):214-220.
51. Sachlos E, Czernuszka JT. Making tissue engineering scaffolds work. Review: the application of solid freeform fabrication technology to the production of tissue engineering scaffolds. Eur Cell Mater 2003;5:29-39.
52. Doraiswamy A, Jin C, Narayan RJ, Mageswaran P, Mente P, Modi R, Auyeung R, Chrisey DB, Ovsianikov A,

Chichkov B. Two photon induced polymerization of organic-inorganic hybrid biomaterials for microstructured medical devices. Acta Biomater 2006;2(3):267-275.
53. Hidai H, Jeon H, Hwang DJ, Grigoropoulos CP. Self-standing aligned fiber scaffold fabrication by two photon photopolymerization. Biomed Microdevices 2009;11(3):643-652.
54. Ovsianikov A, Schlie S, Ngezahayo A, Haverich A, Chichkov BN. Two-photon polymerization technique for microfabrication of CAD-designed 3D scaffolds from commercially available photosensitive materials. J Tissue Eng Regen Med 2007;1(6):443-449.
55. Schlie S, Ngezahayo A, Ovsianikov A, Fabian T, Kolb HA, Haferkamp H, Chichkov BN. Three-dimensional cell growth on structures fabricated from ORMOCER by two-photon polymerization technique. J Biomater Appl 2007;22(3):275-287.
56. Arcaute K, Mann BK, Wicker RB. Stereolithography of three-dimensional bioactive poly(ethylene glycol) constructs with encapsulated cells. Ann Biomed Eng 2006;34(9):1429-1441.
57. Cooke MN, Fisher JP, Dean D, Rimnac C, Mikos AG. Use of stereolithography to manufacture critical-sized 3D biodegradable scaffolds for bone ingrowth. J Biomed Mater Res B Appl Biomater 2003;64(2):65-69.
58. Fisher JP, Vehof JW, Dean D, van der Waerden JP, Holland TA, Mikos AG, Jansen JA. Soft and hard tissue response to photocrosslinked poly(propylene fumarate) scaffolds in a rabbit model. J Biomed Mater Res 2002;59(3):547-556.
59. Mapili G, Lu Y, Chen S, Roy K. Laser-layered microfabrication of spatially patterned functionalized tissue-engineering scaffolds. J Biomed Mater Res B Appl Biomater 2005;75(2):414-424.
60. Matsuda T, Mizutani M. Liquid acrylate-endcapped biodegradable poly(epsilon-caprolactone-co-trimethylene carbonate). II. Computer-aided stereolithographic microarchitectural surface photoconstructs. J Biomed Mater Res 2002;62(3):395-403.
61. Naumann A, Aigner J, Staudenmaier R, Seemann M, Bruening R, Englmeier KH, Kadegge G, Pavesio A, Kastenbauer E, Berghaus A. Clinical aspects and strategy for biomaterial engineering of an auricle based on three-dimensional stereolithography. Eur Arch Otorhinolaryngol 2003;260(10):568-575.
62. Sodian R, Fu P, Lueders C, Szymanski D, Fritsche C, Gutberlet M, Hoerstrup SP, Hausmann H, Lueth T, Hetzer R. Tissue engineering of vascular conduits: fabrication of custom-made scaffolds using rapid prototyping techniques. Thorac Cardiovasc Surg 2005;53(3):144-149.
63. Sodian R, Loebe M, Hein A, Martin DP, Hoerstrup SP, Potapov EV, Hausmann H, Lueth T, Hetzer R. Application of stereolithography for scaffold fabrication for tissue engineered heart valves. ASAIO J 2002;48(1):12-16.
64. Lan PX, Lee JW, Seol YJ, Cho DW. Development of 3D PPF/DEF scaffolds using micro-stereolithography and surface modification. J Mater Sci Mater Med 2009;20(1):271-279.
65. Lee KW, Wang S, Fox BC, Ritman EL, Yaszemski MJ, Lu L. Poly(propylene fumarate) bone tissue engineering scaffold fabrication using stereolithography: effects of resin formulations and laser parameters. Biomacromolecules 2007;8(4):1077-1084.
66. Melchels FP, Feijen J, Grijpma DW. A poly(D,L-lactide) resin for the preparation of tissue engineering scaffolds by stereolithography. Biomaterials 2009;30(23-24):3801-3809.
67. Lee JW, Lan PX, Kim B, Lim G, Cho DW. Fabrication and characteristic analysis of a poly(propylene fumarate) scaffold using micro-stereolithography technology. J Biomed Mater Res B Appl Biomater 2008;87(1):1-9.
68. Bryant SJ, Anseth KS. Hydrogel properties influence ECM production by chondrocytes photoencapsulated in poly(ethylene glycol) hydrogels. J Biomed Mater Res 2002;59(1):63-72.
69. Engelmayr GC, Jr., Papworth GD, Watkins SC, Mayer JE, Jr., Sacks MS. Guidance of engineered tissue collagen orientation by large-scale scaffold microstructures. J Biomech 2006;39(10):1819-1831.
70. Chu TM, Halloran JW, Hollister SJ, Feinberg SE. Hydroxyapatite implants with designed internal architecture. J Mater Sci Mater Med 2001;12(6):471-478.
71. Yeong WY, Chua CK, Leong KF, Chandrasekaran M. Rapid prototyping in tissue engineering: challenges and potential. Trends Biotechnol 2004;22(12):643-652.
72. Chen S, Wang PP, Wang JP, Chen GQ, Wu Q. Guided growth of smooth muscle cell on poly(3-hydroxybutyrate-co-3-hydroxyhexanoate) scaffolds with uniaxial microtubular structures. J Biomed Mater Res A 2008;86(3):849-856.
73. Gross KA, Rodriguez-Lorenzo LM. Biodegradable composite scaffolds with an interconnected spherical network for bone tissue engineering. Biomaterials 2004;25(20):4955-4962.
74. Ho MH, Kuo PY, Hsieh HJ, Hsien TY, Hou LT, Lai JY, Wang DM. Preparation of porous scaffolds by using freeze-extraction and freeze-gelation methods. Biomaterials 2004;25(1):129-138.
75. Kim BS, Mooney DJ. Engineering smooth muscle tissue with a predefined structure. J Biomed Mater Res 1998;41(2):322-332.
76. Goh YQ, Ooi CP. Fabrication and characterization of porous poly(L-lactide) scaffolds using solid-liquid phase separation. J Mater Sci Mater Med 2008;19(6):2445-2452.
77. Schugens C, Maquet V, Grandfils C, Jerome R, Teyssie P. Polylactide macroporous biodegradable implants for

cell transplantation. II. Preparation of polylactide foams by liquid-liquid phase separation. J Biomed Mater Res 1996;30(4):449-461.
78. van Minnen B, van Leeuwen MB, Stegenga B, Zuidema J, Hissink CE, van Kooten TG, Bos RR. Short-term in vitro and in vivo biocompatibility of a biodegradable polyurethane foam based on 1,4-butanediisocyanate. J Mater Sci Mater Med 2005;16(3):221-227.
79. Zhang R, Ma PX. Poly(alpha-hydroxyl acids)/hydroxyapatite porous composites for bone-tissue engineering. I. Preparation and morphology. J Biomed Mater Res 1999;44(4):446-455.
80. Ma PX, Zhang R. Microtubular architecture of biodegradable polymer scaffolds. J Biomed Mater Res 2001;56(4):469-477.
81. Guan J, Fujimoto KL, Wagner WR. Elastase-sensitive elastomeric scaffolds with variable anisotropy for soft tissue engineering. Pharm Res 2008;25(10):2400-2412.
82. Yang F, Qu X, Cui W, Bei J, Yu F, Lu S, Wang S. Manufacturing and morphology structure of polylactide-type microtubules orientation-structured scaffolds. Biomaterials 2006;27(28):4923-4933.
83. Hu X, Shen H, Yang F, Bei J, Wang S. Preparation and cell affinity of microtubular orientation-structured PLGA(70/30) blood vessel scaffold. Biomaterials 2008;29(21):3128-3136.
84. Braescu L. Shape of menisci in terrestrial dewetted Bridgman growth. J Colloid Interface Sci 2008;319(1):309-315.
85. Beckmann J, Korber C, Rau G, Hubel A, Cravalho EG. Redefining cooling rate in terms of ice front velocity and thermal gradient: first evidence of relevance to freezing injury of lymphocytes. Cryobiology 1990;27(3):279-287.
86. Faraj KA, van Kuppevelt TH, Daamen WF. Construction of collagen scaffolds that mimic the three-dimensional architecture of specific tissues. Tissue Eng 2007;13(10):2387-2394.
87. O'Brien FJ, Harley BA, Yannas IV, Gibson L. Influence of freezing rate on pore structure in freeze-dried collagen-GAG scaffolds. Biomaterials 2004;25(6):1077-1086.
88. Schoof H, Apel J, Heschel I, Rau G. Control of pore structure and size in freeze-dried collagen sponges. J Biomed Mater Res 2001;58(4):352-357.
89. Zhang D, Chang J. Electrospinning of three-dimensional nanofibrous tubes with controllable architectures. Nano Lett 2008;8(10):3283-3287.
90. Baker SC, Atkin N, Gunning PA, Granville N, Wilson K, Wilson D, Southgate J. Characterisation of electrospun polystyrene scaffolds for three-dimensional in vitro biological studies. Biomaterials 2006;27(16):3136-3146.
91. Murugan R, Ramakrishna S. Design strategies of tissue engineering scaffolds with controlled fiber orientation. Tissue Eng 2007;13(8):1845-1866.
92. Lu H, Feng Z, Gu Z, Liu C. Growth of outgrowth endothelial cells on aligned PLLA nanofibrous scaffolds. J Mater Sci Mater Med 2009;20(9):1937-1944.
93. Xu CY, Inai R, Kotaki M, Ramakrishna S. Aligned biodegradable nanofibrous structure: a potential scaffold for blood vessel engineering. Biomaterials 2004;25(5):877-886.
94. Lee CH, Shin HJ, Cho IH, Kang YM, Kim IA, Park KD, Shin JW. Nanofiber alignment and direction of mechanical strain affect the ECM production of human ACL fibroblast. Biomaterials 2005;26(11):1261-1270.
95. Kidoaki S, Kwon IK, Matsuda T. Mesoscopic spatial designs of nano- and microfiber meshes for tissue-engineering matrix and scaffold based on newly devised multilayering and mixing electrospinning techniques. Biomaterials 2005;26(1):37-46.
96. Yang X, Shah JD, Wang H. Nanofiber enabled layer-by-layer approach toward three-dimensional tissue formation. Tissue Eng Part A 2009;15(4):945-956.
97. Liao IC, Chew SY, Leong KW. Aligned core-shell nanofibers delivering bioactive proteins. Nanomed 2006;1(4):465-471.
98. Zhong S, Teo WE, Zhu X, Beuerman RW, Ramakrishna S, Yung LY. An aligned nanofibrous collagen scaffold by electrospinning and its effects on in vitro fibroblast culture. J Biomed Mater Res A 2006;79(3):456-463.
99. Bagnaninchi PO, Yang Y, Zghoul N, Maffulli N, Wang RK, Haj AJ. Chitosan microchannel scaffolds for tendon tissue engineering characterized using optical coherence tomography. Tissue Eng 2007;13(2):323-331.
100. Silva MM, Cyster LA, Barry JJ, Yang XB, Oreffo RO, Grant DM, Scotchford CA, Howdle SM, Shakesheff KM, Rose FR. The effect of anisotropic architecture on cell and tissue infiltration into tissue engineering scaffolds. Biomaterials 2006;27(35):5909-5917.
101. Bender MD, Bennett JM, Waddell RL, Doctor JS, Marra KG. Multi-channeled biodegradable polymer/CultiSpher composite nerve guides. Biomaterials 2004;25(7-8):1269-1278.
102. Nazhat SN, Neel EA, Kidane A, Ahmed I, Hope C, Kershaw M, Lee PD, Stride E, Saffari N, Knowles JC and others. Controlled microchannelling in dense collagen scaffolds by soluble phosphate glass fibers. Biomacromolecules 2007;8(2):543-551.
103. Bitar M, Salih V, Mudera V, Knowles JC, Lewis MP. Soluble phosphate glasses: in vitro studies using human cells of hard and soft tissue origin. Biomaterials 2004;25(12):2283-2292.

104. Knowles JC. Phosphate based glasses for biomedical applications. Journal of Materials Chemistry 2003;13(10):2395-2401.
105. Kim HW, Lee EJ, Jun IK, Kim HE, Knowles JC. Degradation and drug release of phosphate glass/polycaprolactone biological composites for hard-tissue regeneration. J Biomed Mater Res B Appl Biomater 2005;75(1):34-41.
106. Prabhakar RL, Brocchini S, Knowles JC. Effect of glass composition on the degradation properties and ion release characteristics of phosphate glass--polycaprolactone composites. Biomaterials 2005;26(15):2209-2218.
107. Georgiou G, Mathieu L, Pioletti DP, Bourban PE, Manson JA, Knowles JC, Nazhat SN. Polylactic acid-phosphate glass composite foams as scaffolds for bone tissue engineering. J Biomed Mater Res B Appl Biomater 2007;80(2):322-331.
108. Navarro M, Ginebra MP, Planell JA, Zeppetelli S, Ambrosio L. Development and cell response of a new biodegradable composite scaffold for guided bone regeneration. J Mater Sci Mater Med 2004;15(4):419-422.
109. Veth RP, Jansen HW, Leenslag JW, Pennings AJ, Hartel RM, Nielsen HK. Experimental meniscal lesions reconstructed with a carbon fiber-polyurethane-poly(L-lactide) graft. Clin Orthop Relat Res 1986;202(202):286-293.
110. Izquierdo R, Garcia-Giralt N, Rodriguez MT, Caceres E, Garcia SJ, Gomez Ribelles JL, Monleon M, Monllau JC, Suay J. Biodegradable PCL scaffolds with an interconnected spherical pore network for tissue engineering. J Biomed Mater Res A 2008;85(1):25-35.
111. Kim J, Yaszemski MJ, Lu L. Three-Dimensional Porous Biodegradable Polymeric Scaffolds Fabricated with Biodegradable Hydrogel Porogens. Tissue Eng Part C Methods 2009.
112. Tyson T, Finne-Wistrand A, Albertsson AC. Degradable porous scaffolds from various L-lactide and trimethylene carbonate copolymers obtained by a simple and effective method. Biomacromolecules 2009;10(1):149-154.
113. Yu G, Fan Y. Preparation of poly(D,L-lactic acid) scaffolds using alginate particles. J Biomater Sci Polym Ed 2008;19(1):87-98.
114. Capes JS, Ando HY, Cameron RE. Fabrication of polymeric scaffolds with a controlled distribution of pores. J Mater Sci Mater Med 2005;16(12):1069-1075.
115. Liu X, Ma PX. Polymeric scaffolds for bone tissue engineering. Ann Biomed Eng 2004;32(3):477-486.
116. Aguilar CA, Lu Y, Mao S, Chen S. Direct micro-patterning of biodegradable polymers using ultraviolet and femtosecond lasers. Biomaterials 2005;26(36):7642-7649.
117. Brayfield CA, Marra KG, Leonard JP, Tracy CX, Gerlach JC. Excimer laser channel creation in polyethersulfone hollow fibers for compartmentalized in vitro neuronal cell culture scaffolds. Acta Biomater 2008;4(2):244-255.
118. Nakayama Y, Nishi S, Ishibashi-Ueda H, Matsuda T. Surface microarchitectural design in biomedical applications: in vivo analysis of tissue ingrowth in excimer laser-directed micropored scaffold for cardiovascular tissue engineering. J Biomed Mater Res 2000;51(3):520-528.
119. Tiaw KS, Goh SW, Hong M, Wang Z, Lan B, Teoh SH. Laser surface modification of poly(epsilon-caprolactone) (PCL) membrane for tissue engineering applications. Biomaterials 2005;26(7):763-769.
120. Vishnubhatla KC, Bellini N, Ramponi R, Cerullo G, Osellame R. Shape control of microchannels fabricated in fused silica by femtosecond laser irradiation and chemical etching. Opt Express 2009;17(10):8685-8695.
121. Papenburg BJ, Vogelaar L, Bolhuis-Versteeg LA, Lammertink RG, Stamatialis D, Wessling M. One-step fabrication of porous micropatterned scaffolds to control cell behavior. Biomaterials 2007;28(11):1998-2009.
122. Courtney T, Sacks MS, Stankus J, Guan J, Wagner WR. Design and analysis of tissue engineering scaffolds that mimic soft tissue mechanical anisotropy. Biomaterials 2006;27(19):3631-3638.
123. Li WJ, Mauck RL, Cooper JA, Yuan X, Tuan RS. Engineering controllable anisotropy in electrospun biodegradable nanofibrous scaffolds for musculoskeletal tissue engineering. J Biomech 2007;40(8):1686-1693.
124. Lynch HA, Johannessen W, Wu JP, Jawa A, Elliott DM. Effect of fiber orientation and strain rate on the nonlinear uniaxial tensile material properties of tendon. J Biomech Eng 2003;125(5):726-731.
125. Huang CY, Stankiewicz A, Ateshian GA, Mow VC. Anisotropy, inhomogeneity, and tension-compression nonlinearity of human glenohumeral cartilage in finite deformation. J Biomech 2005;38(4):799-809.
126. Mow VC, Guo XE. Mechano-electrochemical properties of articular cartilage: their inhomogeneities and anisotropies. Annu Rev Biomed Eng 2002;4:175-209.
127. Petersen W, Tillmann B. Collagenous fibril texture of the human knee joint menisci. Anat Embryol (Berl) 1998;197(4):317-324.
128. Fithian DC, Kelly MA, Mow VC. Material properties and structure-function relationships in the menisci. Clin Orthop Relat Res 1990;252(252):19-31.
129. Proctor CS, Schmidt MB, Whipple RR, Kelly MA, Mow VC. Material properties of the normal medial bovine

meniscus. J Orthop Res 1989;7(6):771-782.
130. Setton LA, Guilak F, Hsu EW, Vail TP. Biomechanical factors in tissue engineered meniscal repair. Clin Orthop Relat Res 1999;367 Suppl(367 Suppl):S254-S272.
131. Baker BM, Mauck RL. The effect of nanofiber alignment on the maturation of engineered meniscus constructs. Biomaterials 2007;28(11):1967-1977.
132. Roth EA, Xu T, Das M, Gregory C, Hickman JJ, Boland T. Inkjet printing for high-throughput cell patterning. Biomaterials 2004;25(17):3707-3715.
133. Wang JH, Jia F, Gilbert TW, Woo SL. Cell orientation determines the alignment of cell-produced collagenous matrix. J Biomech 2003;36(1):97-102.
134. Freed LE, Martin I, Vunjak-Novakovic G. Frontiers in tissue engineering. In vitro modulation of chondrogenesis. Clin Orthop Relat Res 1999;367 Suppl(367 Suppl):S46-S58.
135. Ishaug SL, Crane GM, Miller MJ, Yasko AW, Yaszemski MJ, Mikos AG. Bone formation by three-dimensional stromal osteoblast culture in biodegradable polymer scaffolds. J Biomed Mater Res 1997;36(1):17-28.
136. Kannan RY, Salacinski HJ, Sales K, Butler P, Seifalian AM. The roles of tissue engineering and vascularisation in the development of micro-vascular networks: a review. Biomaterials 2005;26(14):1857-1875.
137. Patel ZS, Mikos AG. Angiogenesis with biomaterial-based drug- and cell-delivery systems. J Biomater Sci Polym Ed 2004;15(6):701-726.
138. Bancroft GN, Sikavitsas VI, van den DJ, Sheffield TL, Ambrose CG, Jansen JA, Mikos AG. Fluid flow increases mineralized matrix deposition in 3D perfusion culture of marrow stromal osteoblasts in a dose-dependent manner. Proc Natl Acad Sci U S A 2002;99(20):12600-12605.
139. Martin I, Wendt D, Heberer M. The role of bioreactors in tissue engineering. Trends Biotechnol 2004;22(2):80-86.
140. Pazzano D, Mercier KA, Moran JM, Fong SS, DiBiasio DD, Rulfs JX, Kohles SS, Bonassar LJ. Comparison of chondrogensis in static and perfused bioreactor culture. Biotechnol Prog 2000;16(5):893-896.
141. Stevens MM, Marini RP, Schaefer D, Aronson J, Langer R, Shastri VP. In vivo engineering of organs: the bone bioreactor. Proc Natl Acad Sci U S A 2005;102(32):11450-11455.
142. Rose FR, Hou Q, Oreffo RO. Delivery systems for bone growth factors - the new players in skeletal regeneration. J Pharm Pharmacol 2004;56(4):415-427.
143. Hutmacher DW, Sittinger M, Risbud MV. Scaffold-based tissue engineering: rationale for computer-aided design and solid free-form fabrication systems. Trends Biotechnol 2004;22(7):354-362.
144. Maravelakis E, David K, Antoniadis A, Manios A, Bilalis N, Papaharilaou Y. Reverse engineering techniques for cranioplasty: a case study. J Med Eng Technol 2008;32(2):115-121.
145. Solaro P, Pierangeli E, Pizzoni C, Boffi P, Scalese G. From computerized tomography data processing to rapid manufacturing of custom-made prostheses for cranioplasty. Case report. J Neurosurg Sci 2008;52(4):113-116.
146. Chim H, Schantz JT. New frontiers in calvarial reconstruction: integrating computer-assisted design and tissue engineering in cranioplasty. Plast Reconstr Surg 2005;116(6):1726-1741.
147. Ekstrand K, Hirsch JM. Malignant tumors of the maxilla: virtual planning and real-time rehabilitation with custom-made R-zygoma fixtures and carbon-graphite fiber-reinforced polymer prosthesis. Clin Implant Dent Relat Res 2008;10(1):23-29.
148. Chu TM, Orton DG, Hollister SJ, Feinberg SE, Halloran JW. Mechanical and in vivo performance of hydroxyapatite implants with controlled architectures. Biomaterials 2002;23(5):1283-1293.
149. Taboas JM, Maddox RD, Krebsbach PH, Hollister SJ. Indirect solid free form fabrication of local and global porous, biomimetic and composite 3D polymer-ceramic scaffolds. Biomaterials 2003;24(1):181-194.
150. Wilson CE, de Bruijn JD, van Blitterswijk CA, Verbout AJ, Dhert WJ. Design and fabrication of standardized hydroxyapatite scaffolds with a defined macro-architecture by rapid prototyping for bone-tissue-engineering research. J Biomed Mater Res A 2004;68(1):123-132.
151. Sachlos E, Reis N, Ainsley C, Derby B, Czernuszka JT. Novel collagen scaffolds with predefined internal morphology made by solid freeform fabrication. Biomaterials 2003;24(8):1487-1497.

Chapter 6

Effect of polyurethane scaffold architecture on ingrowth speed and collagen orientation in a subcutaneous rat pocket model

BioMedical Materials, 2013

Eric de Mulder
Gerjon Hannink
Nico Verdonschot
Pieter Buma

ABSTRACT

Clinically used scaffolds are suboptimal in regenerating the highly oriented meniscus fiber structure in full meniscal defects. The objective of this study was to test whether anisotropic porous scaffolds with channels resulted in a more meniscus like matrix organization compared to isotropic porous scaffolds.

Isotropic polyurethane scaffolds were made via standard solvent leaching techniques. Anisotropic porous scaffolds with channels were made via modified thermal induced phase separation. Both scaffold types were analyzed with light microscopy, scanning electron microscopy and computed nano-tomography. Finally, isotropic and anisotropic scaffolds were bilateral subcutaneous implanted on the back of 32 Wistar rats for 1, 4, 8 and 24 weeks to assess tissue ingrowth and matrix organization.

Isotropic scaffolds had a pore diameter of 35±14.7μm and a degree of anisotropy of 0.18, while anisotropic scaffolds had a channel diameter of 20±6.0μm and a degree of anisotropy of 0.39. After implantation full tissue ingrowth was achieved after 8 and 24 weeks for isotropic and anisotropic, respectively. Isotropic scaffolds had a random tissue infiltration with unorganized collagen deposition, whereas anisotropic scaffolds showed tissue infiltration and collagen alignment in the direction of the channels.

Anisotropic scaffolds resulted in a matrix organization that resembled the tissue in the vascularized zone of the meniscus, while isotropic scaffolds resembled the tissue in the avascular zone of the meniscus.

INTRODUCTION

Most tissues in the human body have anisotropic characteristics. Mainly musculoskeletal tissues, such as articular cartilage and the fibro-cartilage of the meniscus, show well-defined anisotropic properties. Generally, the anisotropy is presented in the organization of the extracellular matrix. With respect to the meniscus, large collagen type I fibers, which make up to 75% of the total protein content of the extracellular matrix, are oriented circumferentially[1]. Due to the anisotropic fiber arrangement, the meniscus is able to withstand high compressive forces and redirect them into tensile stresses with limited strains in circumferential direction[2,3]. This makes the meniscus efficient shock absorbers in the knee joint.

The meniscus has a poor vascularization, thereby its healing capacity is impaired depending on the location and the type of tear[4]. Therefore, surgeons will often proceed to (partial) removal of the injured meniscus if repair is unlikely. It is well understood that with an increasing amount of tissue being removed, peak forces on the articular cartilage increase, and thereby the risk of cartilage damage[5-7]. To prevent cartilage damage the resected part of the meniscus can be replaced with a scaffold. This meniscus scaffold will allow new tissue ingrowth into the resected part of the meniscus[8,9]. The ultimate aim of these scaffolds is that, after resorption of the scaffold, the newly formed tissue can restore the original functional behavior of the meniscus tissue. Two types of scaffolds for partial meniscus replacement/repair are now available for treatment of patients[8,10]. In case of a total meniscus replacement, the only available treatment option would be a transplantation of a donor meniscus. However, due to size matching issues these donor menisci have a limited availability.

In a previous study, a polymer scaffold was tested as a material for total meniscus replacement[11]. The organization of the neo-tissue in this polymer scaffold was not similar to that in the native meniscus. The collagen bundles formed were orientated in a random way guided by the isotropic pore architecture of the scaffold[11]. The morphology was far different from the highly organized and anisotropic morphology, mainly present in the vascularized zone of the native meniscus. It is not known if the unorganized neo-tissue can re-differentiate into the anisotropic organized tissue of the native meniscus and how long this process would take[12]. To optimally replace a total meniscus a scaffold should promote anisotropic tissue formation similar to the tissue organization in the vascularized zone of the native meniscus.

It has been shown that scaffolds with an anisotropic microgrooves promote cell alignment in culture[13,14]. Furthermore, these aligned cells are able to synthesize aligned extracellular matrix[15]. To enable the formation of aligned collagen bundles *in vivo*, as in the vascularized zone of the native meniscus, the first requisite is a scaffold with an anisotropic orientated pore structure. Preferentially the anisotropic channels inside the porous scaffolds should have diameters similar to that of the collagen fiber bundles in the meniscus. Numerous techniques are available to obtain anisotropic scaffolds depending on the material properties of the scaffold[16]. A scaffold material with promising characteristics for meniscus tissue engineering is polyurethane (PU)

made from P(D/L)LA and PCL[7].

In this study we tested whether *in vivo* extracellular matrix orientation could be guided by scaffold pore architecture. We hypothesized that neo-tissue produced in channel-like porous anisotropic scaffolds would resemble meniscus tissue present in the vascularized zone.

MATERIAL AND METHODS

Scaffold preparation

Scaffolds were composed of 50% DL(50/50)-lactide (PDLLA, Purac) and 50% ε-caprolactone (PCL, Acros Organics) by ring opening polymerization with 1,4-butanediol (BDO) as initiator. The final macrodiol prepolymer had a molecular weight (MN) of 2000 g/mole. Subsequently, this was end-capped with 1,4-butanediisocyanate (BDI). Chain extension was performed with a BDO-BDI-BDO urethane block which resulted in a hard block urethane segment with a uniform length of five urethane moieties. The final PU consisted of 22.5 w/w % hard urethane segments and 77.5 w/w % amorphous polyester soft segments. Polymer solutions were made of 5% polymer and 95% solvent to obtain 95% porous scaffold at the final stage. Isotropic scaffolds were prepared via solvent leaching as previously reported [18]. In short, polymer solution was casted in malls and subsequently frozen at -18^{O}C. The frozen polymers were lyophilized at -18^{O}C, 1 mbar, overnight to remove water and dioxane crystals. Anisotropic scaffolds were produced using thermal induced phase separation (TIPS)[19-22]. Polymers were solvent casted in a glass container with an isolating wall (Chapter 5, Figure 1E). This setup was placed on an alumina disc which was pre-cooled with liquid N_2 and kept cooled with N_2 during polymerization to create a temperature gradient. After the polymer was frozen, samples were lyophilized similar to the isotropic scaffolds.

Both porous materials were frozen in liquid nitrogen and cut with a surgical blade into rectangular blocks of 5x5x10mm. The anisotropic scaffolds had the channel orientation parallel to the longest axis of the rectangular blocks.

To evaluate the internal pore structure of the scaffold, scaffolds were inspected macroscopically with light microscopy. In addition, isotropic and anisotropic scaffolds were further analyzed with scanning electron microscopy (n=2) (JEOL JSM 6310, JEOL Ltd, Herts, UK) and computed nano-tomography (n=1) (nano-CT; SkyScan 2011, SkyScan, Kontich, Belgium). High-resolution (0.85 μm) scanning was performed at an energy of 40 kV and intensity of 180 μA. Specimens were attached to a stage that rotated 180° with images acquired every 0.3°. After scanning, cross-sectional slices were reconstructed (NRecon 1.6.3.2, SkyScan, Kontich, Belgium) and the degree of anisotropy (DA) and pore diameters were calculated from 250x250x250μm VOIs from the center of each specimen using BoneJ v1.3.5 software[23].

Collagen fiber measurement

Menisci were isolated from 3 skeletal mature male New Zeeland White rabbits, 3 skeletal mature female Dutch milk goats (Capra Hircus Sana), and 1 human male and 2 female knees (mean age 75yr). From each knee the lateral and medial menisci were isolated and fixated in 4% buffered formaldehyde. Animals were available from non-related research projects. Human knees were obtained from the Department of Anatomy of the Radboud University Nijmegen Medical Centre (Nijmegen, The Netherlands). All menisci used were from healthy knees without macroscopical signs of osteoarthritis. Subsequently, tissues were embedded in PMMA plastic for sectioning in the transversal plane. Sections were stained with picrosirius red staining and analyzed with polarized light microscopy. Of each meniscus three transversal sections were photographed and the diameters of ten circumferential collagen fiber bundles per section were measured using computer aided image analysis software (analySIS Soft Imaging System, GmbH, Münster, Germany).

Analysis of tissue ingrowth and polymer behavior

Isotropic and anisotropic scaffolds were inspected with light microscopy to verify the isotropic/anisotropic architecture. These scaffolds were disinfected three times with 70% ethanol and subsequently rinsed with sterile PBS. To rule out the influence of load on tissue orientation, the scaffolds were implanted subcutaneously. One isotropic and one anisotropic scaffold (with alternating location) were implanted bilaterally on the back of 32 male Wistar rats (weight range: 200-220gr). Rats were anesthetized with isoflurane and individual subcutaneous pockets were made with blunt scissors. Scaffolds were inserted and pockets were closed with surgical staples. Rats were housed under standard conditions with *ad libitum* food and water. After 1, 4, 8 and 24 weeks follow-up, the rats were killed by CO_2, the samples were retrieved and fixated in 4% buffered formaldehyde (n=8 per time point for both scaffold types). The animal experiment was approved by the institutional Animal Ethics Committee of the Radboud University.

Ex vivo histology

Fixated samples were embedded in PMMA and cut in half. One half was sectioned (7µm thickness) in the coronal plane, the other half in the sagittal plane. Sections were stained with heamatoxilin/eosin (HE), Masson's trichrome and picrosirius red. Sections were analyzed with normal and polarized light microscopy, respectively. To calculate the percentage of tissue ingrowth, photographs of one HE stained sagittal mid section per sample were recorded with an Olympus digital camera and analyzed using computer aided image analysis software. Tissue ingrowth was measured using a method previously described by Ramrattan *et al.*[24]. In short, the total scaffold surface area and tissue ingrowth surface area were measured to calculate the percentage of tissue ingrowth.

Statistics

A two way ANOVA was used on all datasets with factors time (1, 4, 8, 24 weeks) and scaffold (isotropic, anisotropic). All data were expressed as mean ± SEM unless stated otherwise. For all experiments, differences were considered statistically significant for P values <0.05. Statistical analysis was performed using SPSS v18.0 software (SPSS Inc., Chicago, IL, USA).

RESULTS

SEM and nano-CT

SEM imaging showed a difference in pore structure between isotropic and anisotropic scaffolds (Figures 1A, 1C). The isotropic scaffold had random pores with small interconnective pores, whereas the anisotropic scaffolds showed a more channel-like pore structure with ladder like appearance. Nano-CT images confirmed these observations (Figures 1B, 1D). The DA was calculated to be 0.18 and 0.39 for isotropic and anisotropic scaffolds, respectively. A lower value indicating a more isotropic structure while a higher value indicates a more anisotropic structure. Isotropic scaffolds had a mean pore diameter of 35.4 ± 14.7 (SD) µm with a maximum diameter of 68.9 µm, while anisotropic scaffolds had a mean pore diameter of 20.0 ± 6.0 (SD) µm with a maximum diameter of 39.7 µm.

Collagen fiber bundles

Diameter of collagen fiber bundles varied between species. Rabbit meniscus collagen fibers had a diameter of 25 ± 1.3 µm. For goat and human, collagen fiber bundle diameter was 65 ± 1.5 µm and 88 ± 4.0 µm respectively (Figure 2).

Histology

After one week a thin capsule had already been formed around the scaffolds. The first signs of tissue ingrowth into the scaffolds were seen. In isotropic scaffolds ingrowth was circumferentially present in larger pores which showed in many cases direct access to the capsule (Figure 3A). In the anisotropic scaffolds ingrowth was mainly seen in longer channels that were in direct contact with the capsule interface which was perpendicular to the long axis of the channel structure (Figure 3B). In the surface perpendicular to the channel structure no or very little ingrowth of tissue was found. Ingrown tissue consisted of fibroblasts that surrounded small capillary blood vessels (Figure 3B, 3C). In the channels in the anisotropic scaffolds fibroblast, and the synthesized matrix, were already aligned in the direction of the channel. (Figure 3C). In the isotropic scaffolds a more randomly organized tissue was found.

After four and eight weeks more tissue was found inside the scaffolds. In the isotropic scaffold tissue penetrated the scaffold in a rather random way. In the anisotropic scaffolds tissue penetrated along the long channels and then filled small pores adjacent to each main channel (Figures 3D, 3E). A similar pattern of main

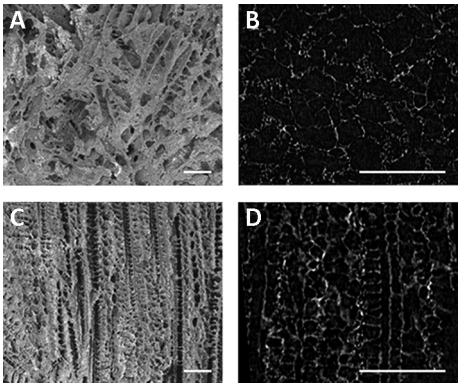

Figure 1: Scanning electron microscopy and nano-CT images of isotropic and anisotropic scaffold in sagittal plane. Isotropic scaffold show a more random distribution of pores in both SEM (A) and nano-CT (B) images. Anisotropic scaffolds have a channel-like pore distribution. The walls of the channels have a ladder-like appearance visible in both SEM (C) and nano-CT (D) images. Scale bars represent 250µm.

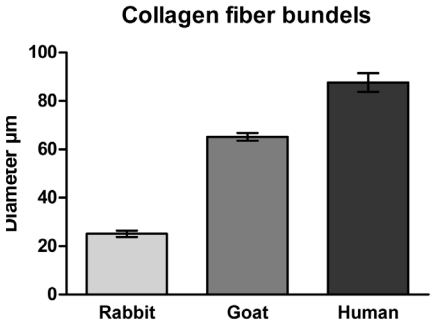

Figure 2: Diameter of circumferential meniscal collagen fiber bundles from rabbits, goats and humans.

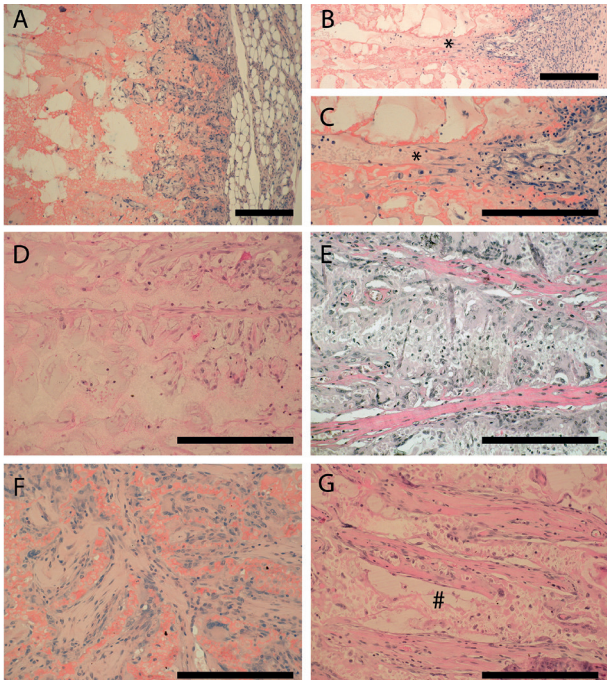

Figure 3: Histological HE sections of scaffolds after subcutaneous implantation. A: isotropic scaffold after 1wk implantation. B, C: anisotropic scaffolds after 1wk implantation with tissue infiltration via channels (*). D: anisotropic scaffold after 8wk of implantation showing tissue infiltration of the channels. E: anisotropic scaffold after 8wk implantation with collagen alignment. F: isotropic scaffold after 8wk of implantation with infiltration of pores with side-pockets. G: anisotropic scaffold after 24wk implantation with scaffold degradation(#). Scale bars represent 250µm.

channels that branched in a regular way was found in the isotropic channels but here the main channels were not aligned as in the anisotropic scaffolds (Figure 3F). After 8 weeks of implantation macrophages and giant cells were visible on the surface of the scaffold. Macrophage and giant cells were present in both isotropic and anisotropic scaffolds in same intensity but scaffold material was not located inside the giant cells. The capsule consisted of a thin layer of fibroblasts surrounded by fat tissue.

After 24 weeks of implantation the scaffold shape integrity at a macroscopic scale was lost for both isotropic and anisotropic scaffolds as shown by a more flattened scaffold shape in sagittal sections. Both scaffold types were completely filled with tissue. The collagen structure was still present in both types of scaffolds and seemed not to be degraded by the macrophages (Figure 3G). More macrophages and giant cells were present in the tissue that had engulfed the degraded scaffold which was seen as foamy material in their cytoplasm.

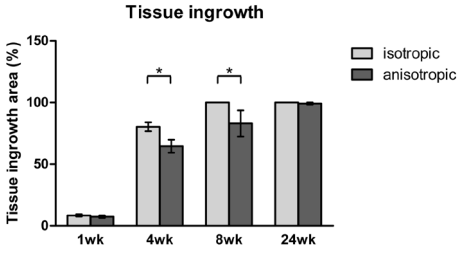

Figure 4: Tissue ingrowth in isotropic and anisotropic scaffolds after 1, 4, 8 and 24 week of subcutaneous implantation in rats. Sagittal sections were used to measure the tissue ingrowth area and the total scaffold area to calculate percentage of tissue ingrowth. After 4 and 8 wks of implantation percentage of tissue ingrowth was bigger in isotropic scaffolds compared to anisotropic scaffolds (= p<0.005).*

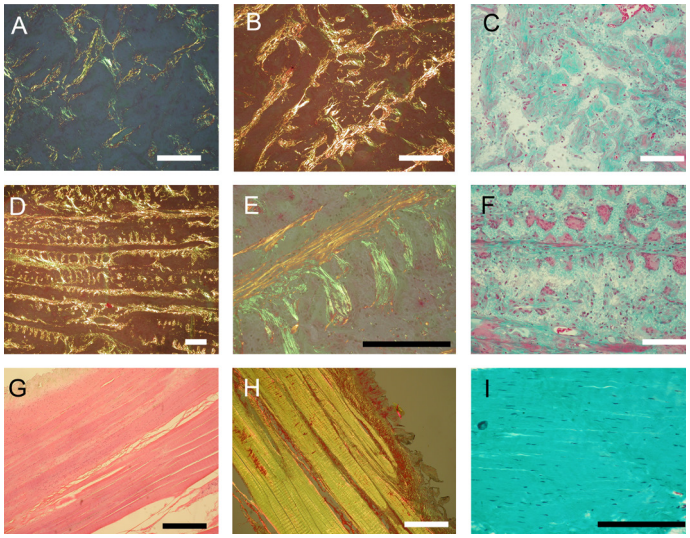

Figure 5. Picrosirius red stained (A, B, D, E, H), HE stained (G) and Masson trichrome stained (C, F, I) sections of scaffolds (A)–(F), follow-up period 24 weeks and of human meniscus (G)–(I). (A–C) Unorganized collagen formation in isotropic scaffolds. (D) Collagen alignment in anisotropic scaffold. (E) Collagen alignment in channels of anisotropic scaffolds with side-pockets. (F) Section of similar group but Masson trichrome stained. (G–I) Sections of the inner avascular part of a human meniscus. Notice the poor cellularity compared to the 24-week scaffold (compare I with C and F). Scale bars represent 250 µm.

After 1 week of implantation no difference in tissue ingrowth surface area was measured between the isotropic and anisotropic scaffold. After 4 weeks of implantation, tissue ingrowth surface area was 80% ± 3.6 versus 65% ± 5.2 for isotropic and anisotropic respectively (Figure 4). After 8 weeks all samples of the isotropic type have full tissue ingrowth while in the anisotropic scaffolds tissue ingrowth surface area was 83% ± 10.6. At 24 weeks of follow up both scaffold types showed complete tissue ingrowth.

Collagen fiber formation was visualized by polarized light microscopy of the picrosirius red staining and compared with the Masson trichrome staining of scaffold and human native meniscus tissue (Figure 5). No clear birifringent matrix was seen in the tissue that was formed after 1 week. The isotropic scaffolds contained collagen fibers from 4 weeks onward and appeared in random orientation following the random pore structure (Figures 5A–5C). The anisotropic scaffolds showed collagen fiber content from 8 weeks onward and the collagen fibers followed the typical pattern of the channels. In the main branches, the collagen orientation was aligned along the channels, whereas in the adjacent pores, the collagen was more randomly aligned in the pore structures (Figures 5D–5F). The collagen in the scaffolds was less organized and dense compared to the collagen in the inner avascular part of the human meniscus (Figures 5G–5I).

DISCUSSION

The goal of this study was to produce and test anisotropic scaffolds for future total meniscus tissue engineering purposes. The PU composition of the scaffold used in this study has a number of novel aspects compared to other polymer scaffolds previously used for meniscus tissue engineering purposes or in clinical practice. The advantage of synthetic polymers above natural polymers such as collagen, is that the latter could induce an immunologic response[25]. In addition, the scaffold described in the present study has a 95% porosity compared to an approximately 80% porosity of most other scaffolds[11,26]. The high porosity and permeability is required to increase the surface area for cell attachment, tissue ingrowth, and to facilitate adequate transport of nutrients and cellular waste products[27]. With decreasing porosity and permeability, nutrient and waste exchange of cells in the deeper regions is limited, leading to necrotic sites in the center of the scaffold[11]. Another advantage of a high porosity is that it, in general, will lead to a higher speed of resorption as less polymer material has to be degraded. Reducing the time foreign materials remain present in the body has been shown to lower immunological responses. Furthermore, with smaller amounts of polymer material to be degraded, lower acidic levels will be reached. Higher acidity levels are known to reduce tissue regeneration speed[28]. The high porosity of the material used in our study thus aims to ensure a faster resorption rate, a low immunological risk, and a high tissue regeneration speed. In addition, the use of a co-polymer from caprolactone and both isomers of lactic acid

exclude crystalline regions in this material. It has been described that the presence of crystalline regions results in highly stable remnants and an increased inflammatory risk in a late degradation stage[29].

With this PU material scaffolds were produced using modified TIPS to obtain anisotropic scaffolds with a channel like structure. Channels showed a ladder-like structure. Channel structure has been shown to be production technique dependent. The use of different solvent types results in different channel structures. In the present study, dioxane was used as a solvent. Dioxane is known to produce ladder-like channels. In contrast, open channels can be created when benzene is used as a solvent, however, using benzene the channel walls do not contain pores[19]. Further studies with solvent types are needed to optimize channel wall structure.

The channels obtained had a diameter in the range of 20 µm as measured on nano-CT images. These channels are smaller compared to the diameter of the circumferential collagen fiber bundles in the vascularized zone of human menisci. However, in the mean diameter calculations also the abundant smaller interconnective pores were included. Therefore the mean diameter size is skewed towards the smaller size. When comparing to the maximum channel size diameter, 40 µm, it was more close to that of the human collagen fiber bundles, 88 µm, but still smaller. The significance of this observation is not yet clear. Smaller diameter collagen bundles which are formed inside the scaffold would indicate that the formed tissue might have inferior mechanical properties compared to the native meniscus tissue. However, with the scaffolds used, this study does not allow the formation of thicker bundles since the maximal fiber bundle diameter is determined by the diameter of the channels in the anisotropic scaffold. Though we speculate that if the scaffold degrades, the cell rich and vascularized tissues in the scaffold will allow growth of the bundles into more mature collagen bundles. This effect could be enhanced by the increased loading during the degradation of the scaffold. If a further differentiation does not occur during degradation of the scaffold, scaffold properties should be redefined related to the channel diameter. A possible method to increase channel diameter would be decreasing the temperature gradient or changing polymer to solvent ratio[19,20,22].

It was shown that the isotropic scaffolds, with larger pore diameter, were fully filled with ingrown tissue at an earlier time point. The anisotropic scaffolds took 4 weeks longer till full tissue ingrowth was realized. Difference in ingrowth speed is well explained by the smaller pore size of the anisotropic scaffold. Smaller pores are known to reduce tissue infiltration speed[30].

Most importantly, this study showed that pore architecture indeed guided collagen deposition and orientation. The isotropic scaffold showed a random collagen organization. This organization closely resembles the avascular zone of the meniscus [1]. The channels of the anisotropic scaffold guided alignment of the collagen fibers, similar to collagen fibers in the vascularized zone of the meniscus. This process was not being limited by the diameter of the channels . These differences in neo-tissue formation in isotropic and anisotropic scaffolds could be of great potential for tissue engineering of a total meniscus when both isotropic and anisotropic architectures

will be combined in one scaffold. In addition to meniscus tissue engineering, this scaffold could potentially be used for tissues with highly anisotropic properties such as cartilage, bone, tendon and ligament tissue[31].

At 8 weeks macrophages and giant cells were visible, presumable digesting the polymer, however, the scaffolds retained their shape. After 24 weeks of implantation both scaffold types lost their mechanical integrity and appeared deformed. Literature shows that scaffold integrity should be retained for at least 8 weeks to facilitate fibrocartilage differentiation[32,33]. The newly formed collagen fibers were not able to provide shape integrity at 24 weeks. This means that the construct is too weak for load bearing applications, such as total meniscus replacement. However, in this animal experiment loads were virtually absent, whereas in meniscus tissue engineering applications, the scaffold may be exposed to considerable loads and deformations. It is known that meniscus cells increase collagen synthesis and that matrix differentiation increases as a response to mechanical forces[34,35]. These mechanical stimuli together with the scaffold architecture could induce an oriented meniscus-like tissue which is optimized towards its (mechanical) function and should be the focus of future studies.

CONCLUSION

This study showed that collagen formation can be guided by scaffold architecture in a non load bearing environment. Isotropic and anisotropic architectures resulted in neo-tissue closely resembling the meniscus avascular and vascularized zones respectively.

REFERENCE LIST

1. Petersen W, Tillmann B. Collagenous fibril texture of the human knee joint menisci. Anat Embryol (Berl) 1998;197(4):317-24.
2. Fithian DC, Kelly MA, Mow VC. Material properties and structure-function relationships in the menisci. Clin Orthop Relat Res 1990(252):19-31.
3. Walker PS, Erkman MJ. The role of the menisci in force transmission across the knee. Clin Orthop Relat Res 1975(109):184-92.
4. Arnoczky SP, Warren RF. The microvasculature of the meniscus and its response to injury. An experimental study in the dog. Am J Sports Med 1983;11(3):131-41.
5. Cox JS, Nye CE, Schaefer WW, Woodstein IJ. The degenerative effects of partial and total resection of the medial meniscus in dogs' knees. Clin Orthop Relat Res 1975(109):178-83.
6. Fairbank TJ. Knee joint changes after meniscectomy. J Bone Joint Surg Br 1948;30B(4):664-70.
7. McDermott ID, Amis AA. The consequences of meniscectomy. J Bone Joint Surg Br 2006;88(12):1549-56.
8. Steadman JR, Rodkey WG. Tissue-engineered collagen meniscus implants: 5- to 6-year feasibility study results. Arthroscopy 2005;21(5):515-25.
9. van Tienen TG, Heijkants RG, de Groot JH, Pennings AJ, Schouten AJ, Veth RP, Buma P. Replacement of the knee meniscus by a porous polymer implant: a study in dogs. Am J Sports Med 2006;34(1):64-71.
10. de Groot JH. Polyurethane scaffolds for meniscal tissue regeneration. Med Device Technol 2005;16(7):18-20.
11. Welsing RT, van Tienen TG, Ramrattan N, Heijkants R, Schouten AJ, Veth RP, Buma P. Effect on tissue differentiation and articular cartilage degradation of a polymer meniscus implant: A 2-year follow-up study in dogs. Am J Sports Med 2008;36(10):1978-89.
12. Buma P, Ramrattan NN, van Tienen TG, Veth RP. Tissue engineering of the meniscus. Biomaterials 2004;25(9):1523-32.
13. Coutinho DF, Gomes ME, Neves NM, Reis RL. Development of micropatterned surfaces of poly(butylene succinate) by micromolding for guided tissue engineering. Acta Biomater 2012;8(4):1490-7.
14. English A, Azeem A, Gaspar DA, Keane K, Kumar P, Keeney M, Rooney N, Pandit A, Zeugolis DI. Preferential cell response to anisotropic electro-spun fibrous scaffolds under tension-free conditions. J Mater Sci Mater Med 2012;23(1):137-48.
15. Wang JH, Jia F, Gilbert TW, Woo SL. Cell orientation determines the alignment of cell-produced collagenous matrix. J Biomech 2003;36(1):97-102.
16. de Mulder EL, Buma P, Hannink G. Anisotropic Porous Biodegradable Scaffolds for Musculoskeletal Tissue Engineering. Materials 2009;2(4).
17. de Mulder EL, Hannink G, Giele M, Verdonschot N, Buma P. Proliferation of meniscal fibrochondrocytes cultured on a new polyurethane scaffold is stimulated by TGF-ss. J Biomater Appl 2011.
18. van Minnen B, van Leeuwen MB, Stegenga B, Zuidema J, Hissink CE, van Kooten TG, Bos RR. Short-term in vitro and in vivo biocompatibility of a biodegradable polyurethane foam based on 1,4-butanediisocyanate. J Mater Sci Mater Med 2005;16(3):221-7.
19. Chen S, Wang PP, Wang JP, Chen GQ, Wu Q. Guided growth of smooth muscle cell on poly(3-hydroxybutyrate-co-3-hydroxyhexanoate) scaffolds with uniaxial microtubular structures. J Biomed Mater Res A 2008;86(3):849-56.
20. Guan J, Fujimoto KL, Wagner WR. Elastase-sensitive elastomeric scaffolds with variable anisotropy for soft tissue engineering. Pharm Res 2008;25(10):2400-12.
21. Ma PX, Zhang R. Microtubular architecture of biodegradable polymer scaffolds. J Biomed Mater Res 2001;56(4):469-77.
22. Yang F, Qu X, Cui W, Bei J, Yu F, Lu S, Wang S. Manufacturing and morphology structure of polylactide-type microtubules orientation-structured scaffolds. Biomaterials 2006;27(28):4923-33.
23. Doube M, Klosowski MM, Arganda-Carreras I, Cordelieres FP, Dougherty RP, Jackson JS, Schmid B, Hutchinson JR, Shefelbine SJ. BoneJ: Free and extensible bone image analysis in ImageJ. Bone 2010;47(6):1076-9.
24. Ramrattan NN, Heijkants RG, van Tienen TG, Schouten AJ, Veth RP, Buma P. Assessment of tissue ingrowth rates in polyurethane scaffolds for tissue engineering. Tissue Eng 2005;11(7-8):1212-23.
25. Lynn AK, Yannas IV, Bonfield W. Antigenicity and immunogenicity of collagen. J Biomed Mater Res B Appl Biomater 2004;71(2):343-54.
26. Moroni L, Poort G, Van Keulen F, de Wijn JR, van Blitterswijk CA. Dynamic mechanical properties of 3D fiber-deposited PEOT/PBT scaffolds: an experimental and numerical analysis. J Biomed Mater Res A 2006;78(3):605-14.
27. Karande TS, Ong JL, Agrawal CM. Diffusion in musculoskeletal tissue engineering scaffolds: design issues

related to porosity, permeability, architecture, and nutrient mixing. Ann Biomed Eng 2004;32(12):1728-43.
28. van Minnen B, Stegenga B, van Leeuwen MB, van Kooten TG, Bos RR. A long-term in vitro biocompatibility study of a biodegradable polyurethane and its degradation products. J Biomed Mater Res A 2006;76(2):377-85.
29. Bergsma JE, de Bruijn WC, Rozema FR, Bos RR, Boering G. Late degradation tissue response to poly(L-lactide) bone plates and screws. Biomaterials 1995;16(1):25-31.
30. van Tienen TG, Heijkants RG, Buma P, de Groot JH, Pennings AJ, Veth RP. Tissue ingrowth and degradation of two biodegradable porous polymers with different porosities and pore sizes. Biomaterials 2002;23(8):1731-8.
31. Surrao DC, Waldman SD, Amsden BG. Biomimetic poly(lactide) based fibrous scaffolds for ligament tissue engineering. Acta Biomater 2012.
32. Klompmaker J, Jansen HW, Veth RP, Nielsen HK, de Groot JH, Pennings AJ. Porous implants for knee joint meniscus reconstruction: a preliminary study on the role of pore sizes in ingrowth and differentiation of fibrocartilage. Clin Mater 1993;14(1):1-11.
33. Klompmaker J, Veth RP, Jansen HW, Nielsen HK, de Groot JH, Pennings AJ, Kuijer R. Meniscal repair by fibrocartilage in the dog: characterization of the repair tissue and the role of vascularity. Biomaterials 1996;17(17):1685-91.
34. Kjaer M. Role of extracellular matrix in adaptation of tendon and skeletal muscle to mechanical loading. Physiol Rev 2004;84(2):649-98.
35. Huey DJ, Athanasiou KA. Tension-compression loading with chemical stimulation results in additive increases to functional properties of anatomic meniscal constructs. PLoS One 2011;6(11):e27857.

Chapter 7

Isotropic and anisotropic collagen scaffolds induce similar hyaline-like cartilage repair in subchondral defects in rabbits

Submitted

Eric de Mulder
Gerjon Hannink
Toin van Kuppevelt
Willeke Daamen
Pieter Buma

ABSTRACT

Lesions in knee joint articular cartilage have limited repair capacity. Many clinically available treatments induce a fibrous-like cartilage repair instead of hyaline cartilage. To induce hyaline cartilage repair we hypothesized that type I collagen scaffolds with fibers aligned perpendicular to the articular cartilage surface would result in qualitatively better tissue repair due to improved cellular influx from the subchondral bone.

By specific freezing protocols, type I collagen scaffolds with isotropic and anisotropic fiber architectures were produced. Rabbits were operated on bilaterally and two full-thickness defects were created in each knee joint. The defect was left empty or inserted with isotropic, anisotropic with pores parallel or perpendicular to the cartilage surface. After 4 (n=13) and 12 (n=13) weeks, regeneration was scored qualitatively and quantitatively using histological analysis and a modified O'Driscoll score.

After 4 weeks all defects were completely filled with partially differentiated hyaline cartilage tissue. No differences in O'Driscoll scores were measured between empty defects and scaffold types. After 12 weeks all treatments led to hyaline cartilage repair visualized by increased glycosaminoglycan staining. Total scores were significantly increased for parallel anisotropic and empty defects over time ($p<0.05$). Remarkably, after both 4 and 12 weeks trabecular bone was formed orientated parallel to the surface of the articular cartilage in a limited number of defects treated with perpendicular anisotropic scaffolds.

The results indicate that collagen scaffolds induce hyaline-like cartilage repair. Fiber architecture had no effect on cartilage repair, however, perpendicular anisotropic scaffolds showed a tendency for improved subchondral bone formation.

INTRODUCTION

Articular cartilage (AC) is a highly organized avascular tissue composed of chondrocytes embedded within an extracellular matrix of collagens, proteoglycans (PGs) and non-collagenous proteins. Type II collagen forms the structural skeleton of the tissue, which resists both the pressure from the PGs and the shear stresses produced during joint movement. In the deep or radial zone of AC, collagen fibers run perpendicular in orientation in respect to the AC surface, before arching over in the intermediate or transitional zone. In the regions closest to the surface of the cartilage, the superficial or tangential zone, the fibers lie in a parallel orientation to the articular surface[1,2].

Focal chondral and osteochondral defects are common injuries with a great impact on the patient's life. Most defects are located on the medial femoral condyle with a mean defect size of ca. 2 mm^2 [3]. Repair of these AC defects is limited due to the low mitotic activity levels of chondrocytes and their dense extracellular matrix surrounding, limiting chondrocyte migration from adjacent healthy articular cartilage to the defect site[4]. In addition, articular cartilage lacks vascularization, limiting repair from non-chondrocytic cells. The general concept in the orthopedic community is that if injuries to the articular cartilage remain untreated, these injuries will progress into more generalized osteoarthritis.

The most frequently used repair technique for focal articular cartilage defects is microfracturing (MF)[5]. With this technique small drill holes are made in the subchondral bone, which creates a route for stem cells to enter into the defect site. These cells can subsequently differentiate and produce a fibro-cartilage or hyaline-like cartilage tissue type. This technique is cheap, simple and can be applied by all surgeons. However, studies with midterm follow-up periods, showed that the repair tissue after MF is of a fibrous instead of a hyaline tissue type[6-8]. From animal studies it is known that this fibrous tissue is mechanically inferior to native hyaline cartilage[9]. Moreover, it might result in poor physical and chemical bonding to the adjacent healthy AC. Both might result in progressive failure at longer follow-up periods[4]. Therefore, better repair strategies are urgently needed.

The quality of repair tissue might be improved with tissue engineering and/or regenerative medicine applications. A minimal invasive, cost effective optimization could be to fill defects with 'smart' scaffolds[10]. In this approach the subchondral bone should be penetrated as in microfracturing and thereafter defects could be filled with a scaffold optimized to attract, guide, stimulate and differentiate bone marrow derived stem cells originating from the subchondral bone. In this way, defects could be filled more rapidly with a higher quality repair tissue compared to MF[11,12]. Previously, scaffolds, based on type I or II collagen, have been described that guide cell migration from the bone marrow into the defect and stimulate cartilage matrix production[13]. Buma *et al*. showed that attachment of chondroitin sulphate to isotropic type I and II based collagen scaffolds could facilitate cartilage repair when implanted in the knee joint of rabbits. However, tissue migration was limited, particularly in the

type II scaffolds, and did not reach the full defect thickness even after 12 weeks[14]. Since it has been shown that tissue formation is guided by the orientation of collagen fibers of the scaffold[15,16], we speculated that by filling defects with anisotropic scaffolds, the defects would be filled more rapidly. Moreover, if collagen is produced along the pore orientation of these anisotropic scaffolds, the quality of the articular repair tissue could be improved.

The aim of this study was to investigate the effect of anisotropic type I collagen scaffolds on articular cartilage repair. We hypothesized that anisotropic scaffolds implanted with the fiber orientation perpendicular to the surface of the cartilage would result in a more native like cartilage repair compared to random, isotropic, collagen scaffolds in a full-thickness articular cartilage defect in rabbits.

MATERIALS & METHODS

Scaffold production

Isotropic porous collagenous scaffolds were prepared by freezing and lyophilizing an acidic dispersion of insoluble bovine type I collagen in 0.25 M acetic acid [15,17]. After lyophilisation, vapor fixation was performed with 38% formaldehyde under vacuum for 30 min. Vapor cross-linking reaction was stopped by quenching remaining aldehydes with 30 mM $NaBH_4$ in 1 M sodium phosphate buffer pH 6.5 for 1 hour at 4^{O}C. Subsequently, scaffolds were crosslinked using 1- ethyl-3-(3-dimethyl aminopropyl) carbodiimide (EDC) (Fluka Chemie, Buchs, Switzerland) and N-hydroxysuccinimide (NHS) (Fluka Chemie)[18].

Anisotropic collagenous scaffolds were prepared using a freezing gradient, resulting in an orientation of the collagen lamellae parallel to the temperature gradient[19,20]. These scaffolds were also crosslinked using formaldehyde vapor, quenched and EDC/NHS crosslinked as described above. Scaffolds were cut parallel and perpendicular to the orientation of the scaffold lamellae to obtain anisotropic scaffolds with fibers running perpendicular and parallel to the top surface respectively. Scaffolds were analyzed with scanning electron microscopy (SEM) to visualize the iso- and anisotropic architectures in collagen scaffolds, and crosslinking efficiency was measured using 2,4,6-trinitrobenzene sulphonic acid with a glycine calibration curve[21,22].

Animal experiment

For the *in vivo* experiment 26 skeletal mature female New Zealand white rabbits were used (mean weight 4.1kg; SEM ±0.12). All procedures were approved by the institutional animal ethics committee. Under general anesthesia a medial skin incision was made over the knee joint. The joint was opened with a medial para-patellar incision, where after the patella was dislocated with the leg in full extension. Two cylindrical full thickness defects (4 mm diameter, 3 mm deep) were created in the patellar groove using a high-speed drill with manual physiological salt irrigation. A spacer was placed onto the 4 mm diameter drill and fixed 3 mm from the end

to standardize defect size. The two defects were separated by 4 mm of cartilage. Each defect was filled with one of the three scaffolds, i.e. isotropic, perpendicular anisotropic and parallel anisotropic. Empty defects were used as controls. Rabbits were bilaterally operated, thereby each rabbit received one scaffold of each experimental group and a control. The positions of the scaffolds were alternated with a random start. After insertion of the scaffolds, the patella was relocated and the knee was bend 3 times until 90^0 of flexion after which the patella was luxated again to check for proper insertion of the scaffolds. Finally, the wound was carefully closed in layers and the animals were allowed full weight bearing and normal daily activity in large rooms with saw dust coverage of the floor. After 4 (n=13) and 12 weeks (n=13) the animals were sacrificed by an overdose of pentobarbital.

Histology

After sacrifice of the rabbits, the knees were inspected macroscopically and synovial tissue was visually analyzed for inflammatory changes. Tissue blocks containing the defects and directly surrounding bone, were dissected with an oscillating saw with irrigation of physiological saline to avoid heat production, fixed in 4% phosphate buffered (pH 7.4) formalin, and after decalcification with EDTA embedded in paraffin. Serial sections of 7 μm were stained with Hematoxylin/Eosin, picrosirius red and Safranin O/fast green. Representative sections through the center of the defect were scored blindly by three of the authors (EdM, GH and PB). Sections were described qualitatively in which special attention was given to the location of the new cartilage-like tissue, the presence of fissures and the remodeling of the subchondral bone. Using a modification of the scoring system developed by O'Driscoll *et al*. a semi-quantitative score of the repair was made[14,23].

Statistical analysis

All data were expressed as mean ± SEM. Statistical analysis were performed with a Two-Way ANOVA with factors treatment/scaffold and time and a post-hoc LSD (SPSS v18, Chicago, IL, USA). P-values <0.05 were considered significant.

RESULTS

A total of 27±4% and 24±6% of the available amine groups were used in the cross-linking process for anisotropic and isotropic porous scaffolds, respectively. After lyophilization, isotropic scaffolds showed rounded pores surrounded by collagen sheets (Figure 1A). Anisotropic scaffolds made with the temperature gradient showed alignment of the collagen sheets with smaller crossing fibers (Figure 1B parallel anisotropic and 1C perpendicular anisotropic). The orientation of the collagen sheets was parallel to the heat gradient.

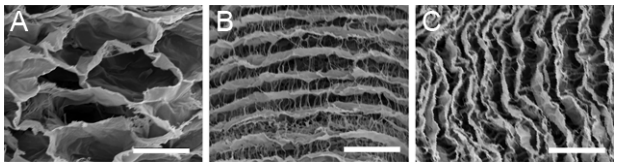

Figure 1: Scanning electron microscopy images of (A) isotropic, (B) parallel anisotropic and (C) perpendicular anisotropic collagen scaffolds. Scale bars represent 100 µm.

After opening the joints no significant adhesions were found. In general, the synovial tissue had a normal appearance without signs of inflammation. The synovial fluid was clear and had a normal viscosity and consistency. Both joints of one rabbit of the 4-week group showed severe signs of infection (redness, pus, etc). This animal was excluded from the study. The host cartilage around defect sites showed macroscopically the normal transparent white/bluish color of control cartilage. After 4-week follow up, macroscopic inspection showed that all defects, including the controls, could be clearly discerned from the adjacent host cartilage and were all completely filled with material with a variable color, varying from white to transparent red. No difference was observed between scaffold types. The surface of the defect site was level with the adjacent host cartilage and had a similar contour. Defects of the 12-week groups were in general more white and resembled adjacent host cartilage more closely than those of the four-week group. In five perpendicular anisotropic scaffolds the transition between host and defect was clearly visible. In other cases this transition was difficult to see macroscopically.

4 weeks

After 4 weeks, the collagen scaffolds could still be seen embedded in newly formed tissues (Figures 2A, 2C, 2E, 2G and Figures. 3A, 3B). The collagen sheets were thicker in the isotropic scaffolds compared to anisotropic scaffolds (compare red fibers in Figs. 3A with 3B). All defects were almost completely filled with partial differentiated cartilage-like tissue as shown by the moderate GAG staining with Safranin O (Fig. 2 left panel). Between the different scaffold types or between controls and scaffolds there was no difference in repair as scored with the modified O'Driscoll method. Total scores ranged between 10.2 ± 1.3 for perpendicular anisotropic and 11.5 ± 1.4 for empty defects (Figure 4). The contour of the implant surface was similar to that of the native trochlea (Figure 2 left panel). The surface of the implant site showed occasionally some mild superficial fibrillation (Figure 3C). The tissue at the surface contained lower cells numbers and was more fibrous compared to the tissues in the deeper parts, which was more chondrogenic. Integration between implant and host tissue was occasionally observed at the superficial articular cartilage side. However, no direct connection was present between the implants and the lateral borders of the subchondral bone (Figure 3D). A tight tissue connection between subchondral bone and the lower implant side seemed present in all defects (Figure 3E), but bone remodeling at the bottom of the defect was still very limited or even

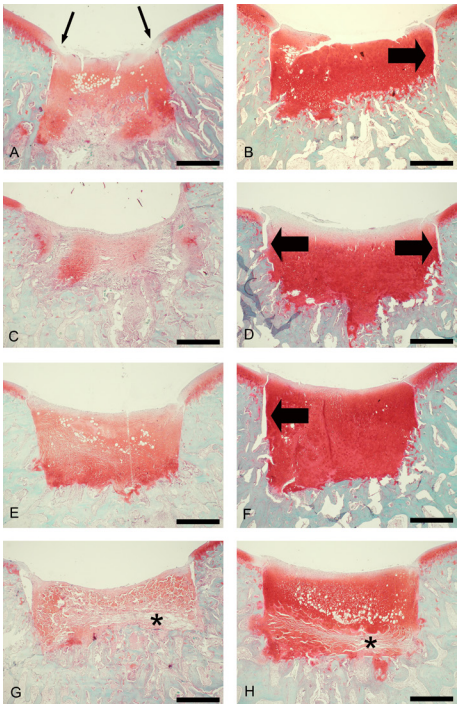

Figure 2: Safranin-O staining of empty defects (A, B), parallel anisotropic implants (C, D), perpendicular anisotropic implants (E, F), and isotropic implants (G, H) after 4 and 12 weeks respectively. In a number of samples integration of host articular cartilage with neo-tissue was observed (small arrows). Integration between scaffold and subchondral bone was absent in most samples (large arrows). In defects filled with isotropic scaffolds, locations with less intense staining inside the scaffold were observed (*). Scale bars represent 1 mm.

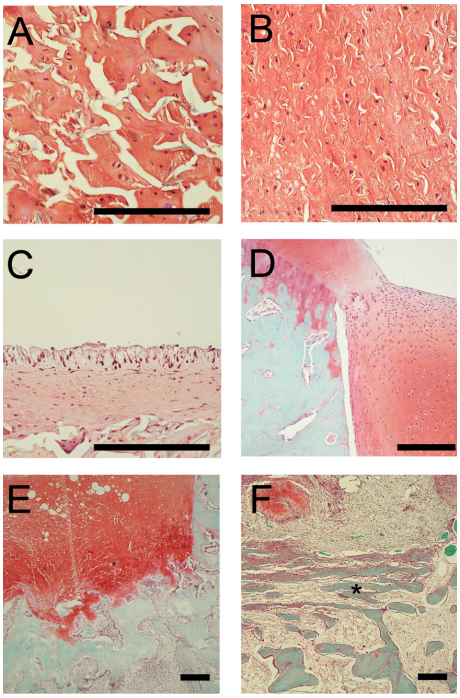

Figure 3: Safranin-O stained sections after 4 weeks of implantations. Isotropic implant (A) and a parallel anisotropic implant (B) with stained collagen fibers. Occasionally superficial cartilage fibrillation was observed (C; isotropic). Integration between implant and host tissue was observed at the superficial cartilage surface (D; perpendicular isotropic) and at the lower contact area with the subchondral bone (E; perpendicular anisotropic) while not at the lateral contact sides with the subchondral bone (D). Similar cases were observed in all implants types and controls. In some cases of the perpendicular anisotropic implant trabecular bone (*) regeneration was parallel to the articular cartilage surface (F; perpendicular anisotropic). Scale bars represent 250µm.

completely absent after four weeks. In three of the defects filled with perpendicular anisotropic scaffolds a very specific pattern of new bone formation in the bottom of the defects was observed. Trabecular bone was formed with long thin trabeculae orientated parallel to surface of the articular cartilage in the direction perpendicular to the anisotropy of the scaffold (Figure 3F). The new bone seemed to originate from the exposed lateral aspect of the subchondral bone (Figure 3B). In defects filled with isotropic scaffolds, locations with less intense staining inside the scaffold were observed (Figure 2G).

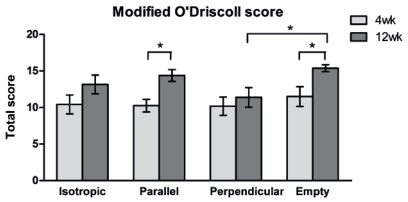

Figure 4: Mean total modified O'Driscoll score (± SEM) of isotropic, parallel anisotropic, perpendicular anisotropic and empty defects (= p<0.05; 4 weeks n=12, and 12 weeks n=13).*

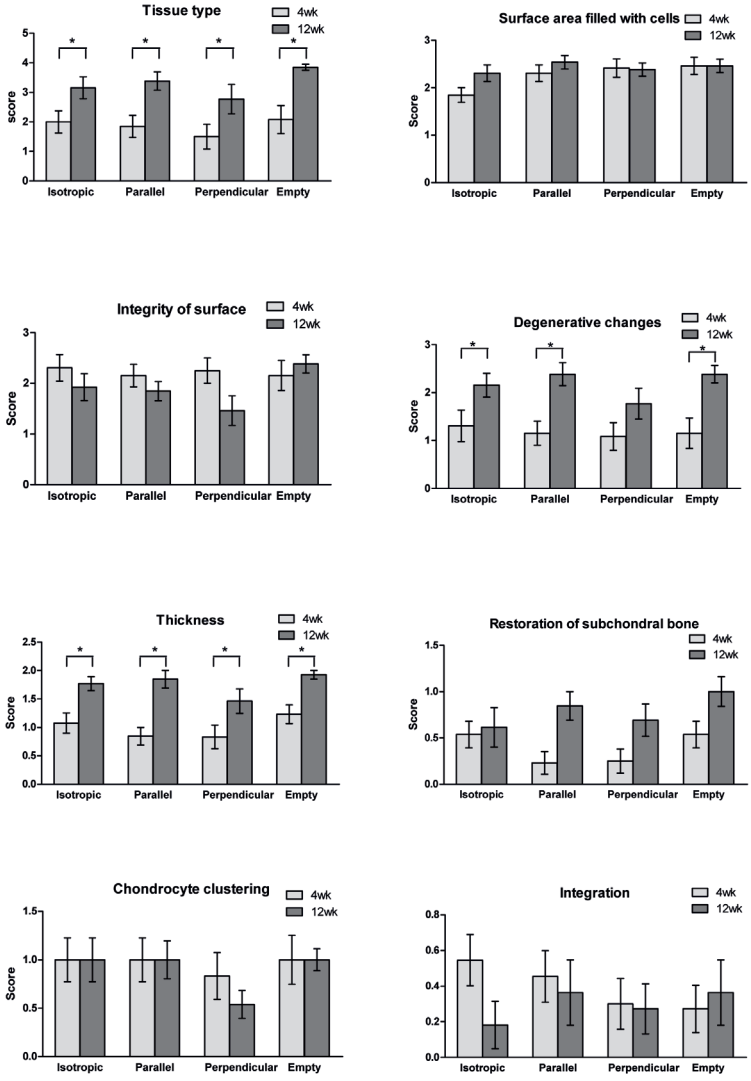

Figure 5: Mean of the individual items of the modified O'Driscoll score (± SEM) of isotropic, parallel anisotropic, perpendicular anisotropic and empty defects (= p<0.05; 4 weeks n=12, and 12 weeks n=13).*

12 weeks

All defects were completely filled with cartilage-like tissue (Figs. 2B, D, F, H). The intensity of the GAG staining was increased compared to the 4 weeks groups (Figure 2: compare left (4 weeks) and right (12 weeks) panel) as visualized by the increased intense red staining in the Safranin O stained sections. Quantitative scores for repair had significantly increased in time for parallel anisotropic and empty defects by 4.1 and 3.9 points respectively (Figure 4). For all treatments, the individual O'Driscoll score items showed a time dependant significant increase for *Tissue type* and *Thickness* (Figure 5). This significant increase was also measured for *Degenerative changes*, but not significantly for perpendicular anisotropic scaffolds. Cells in the repair tissue were mainly rounded single cells (occasionally in small clusters) surrounded by an intense metachromatically stained extracellular matrix (Figure 6A). The tissue thus more closely resembled hyaline cartilage-like tissue compared to the 4 weeks group. The surface of the defect was generally smooth, and followed the original contour of the trochlea (Figure 6B). On occasion a small partial thickness fissure was found. This fissure was always located in the central region of the defects and extended into the direction of the subchondral bone (Figure 6C). Two defects of the perpendicular anisotropic scaffolds showed new subchondral bone formation up to the original contour of the cartilage with a thin layer of fibrous tissue only on top (Figure 6D). After 12 weeks the isotropic scaffolds were still clearly visible in the defects while the anisotropic scaffolds were not recognizable after 12 weeks (Figure2 right panel). Furthermore, isotropic scaffold did show locations with minor GAG staining (Figure 2H).

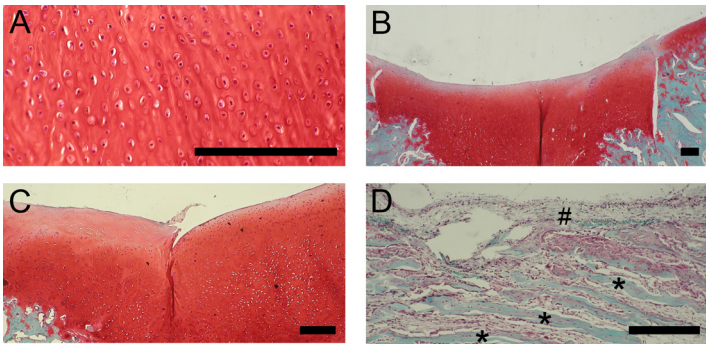

Figure 6: Mean of the individual items of the modified O'Driscoll score (± SEM) of isotropic, parallel anisotropic, perpendicular anisotropic and empty defects (= p<0.05; 4 weeks n=12, and 12 weeks n=13).*

DISCUSSION

In general, we found no large effects of fiber orientation on cartilage regeneration and that all repair reactions were similar to that of the empty controls. Even though rabbits were skeletally mature, their relative young age could have had a beneficial effect on the self-repair capacity in the empty defects. Wei and Messner found that

spontaneous healing of osteochondral defects in the knee joints of non skeletal mature rabbits resulted in a faster filling and earlier tissue specialization than in adolescent or older skeletal mature animals[24]. However, this model of a full thickness articular cartilage defect in the femur of rabbits remains a suitable model to study differences in cartilage repair between scaffold types[14]. For implantation we used collagenous scaffolds that guide the infiltration, proliferation, and differentiation of progenitor cells, and improve the healing response[14]. We chose cross-linked type I collagen scaffolds above type II collagen scaffolds since in our previous studies type II collagen scaffolds only revealed cartilaginous tissue at the superficial zone and at the interface of the matrix with the subchondral bone, leaving large areas of the matrix devoid of new tissue. We speculated that this was induced by rapid differentiation of stem cells into the cartilage phenotype before the defect was filled completely. Therefore, type I collagen scaffolds with an isotropic or anisotropic pore orientation were made and implanted into the defects. We hypothesized that a perpendicular orientation of collagen fibers to the articular cartilage surface enables improved guidance of the cells from the subchondral bone for improved complete thickness repair.

In this study no blood vessels were found in the area of the original defect. This indicates that indeed cells from the subchondral bone populated the matrix without vascular invasion. The observation that cells can migrate quite easily in such type I collagenous matrices is not completely surprising since this was already demonstrated in a previous study[14]. The cells involved in matrix population are probably mainly derived from the bone marrow. Shapiro *et al*. demonstrated that chondrocytes from the residual adjacent cartilage did not participate in the re-population of full-thickness articular cartilage defects[4]. Repair was completely mediated by the proliferation and differentiation of mesenchymal cells from the marrow. We assume similar repair in this study. The contribution of repair cells from a synovial origin, however, cannot be ruled out. Hunziker *et al*. performed a study with partial thickness defects in rabbits in which the defects were filled with fibrin. Mesenchymal cells derived from the synovial membrane migrated across the articular cartilage surface into the defect, where they repaired the cavity with fibrous connective tissue[25]. With this in mind, we speculate that in our model also some repair along the latter route might have taken place. In all defects, particularly at the surface of the implants, bridges were formed between the new tissue in the defect and the host cartilage. In addition, only the bottom side, not the lateral sides, showed integration with host tissue indicating that the repair cells that fill the defect probably originated from the deeper parts of the subchondral bone directly under the defect site and did not originate from more laterally located subchondral bone.

All defects had hyaline-like cartilage repair tissue after 4 and 12 weeks of implantation although in general the GAG staining was more intense after 12 weeks. We found no large effects of fiber orientation on cartilage regeneration. All scaffolds induced similar hyaline like cartilage repair. Surprisingly, it seemed as if the distribution of cells and matrix was more homogeneous in the empty defects

and the anisotropic scaffolds compared to the isotropic scaffolds. The influence of pore size, known to influence cell behavior [26], might have played a role since in this study the morphology of the scaffolds is quite different between the isotropic random and anisotropic scaffolds. Pore sizes of the isotropic scaffolds appeared to be larger and the collagen walls surrounding the pores were also thicker. Potentially, this could have had an effect on the penetration capacity of the cells into the pores of the scaffold. After 12 weeks the isotropic scaffolds were still clearly visible in the defects while the anisotropic scaffolds were not recognizable after 12 weeks, probably due to differences in resorption speed. Rapid degradation in anisotropic scaffolds may have resulted in a reduced effect of the collagen fiber alignment. When scaffolds are quickly degraded, they may not have had the time to guide the cells fully. Development of anisotropic scaffolds with thicker collagen walls may result in increased cell guidance and better cartilage formation.

In the present study the tissue repair was in general better than found in clinical studies where a more fibrous tissue type was found after MF and ACI[6-8]. Further optimization of the developed scaffolds could induce an even better tissue repair. Instead of a homogenous architecture, scaffolds can be made with multiple architectures[27]. Such scaffolds, with an isotropic lower part and a parallel anisotropic upper part have only been tested *in vitro* with cultured chondrocytes, and resulted in engineered cartilage tissue that mimicked hyaline cartilage[28,29]. An interesting observation in the current study was that a limited number of perpendicular anisotropic scaffolds resulted in organized bone formation at 4 and 12 weeks post operation parallel to the AC surface and perpendicular to the direction of the collagen fibers. This is the first *in vivo* indication that based on the orientation of collagen, scaffolds could be designed which induce organized bone in the deeper parts or the defect and cartilage-like tissue in the more superficial areas of the defect. This type of scaffold might offer a new treatment option for deeper osteochondral defects (ICRS grade V defects). These defects are now treated with the sandwich technique in which first the bone defect is filled with bone graft and sealed from the rest of the defect with a Chondroguide collagen membrane as in the M-ACI technique[30]. A second collagen membrane is then placed over the cartilage defect and can be treated with conventional ACI techniques.

Besides changing the architecture of collagen scaffolds, others have been mixing it with other macromolecules, such as GAGs to direct stem cell differentiation. Buma *et al*. showed a positive effect on chondrogenic differentiation of chondroitin sulphate[14]. Matsiko *et al.* showed that addition of hyaluronic acid to collagen increased mesenchymal stem cell infiltration, higher SOX9 expression and more cartilage matrix production *in vitro* when compared to collagen and chondroitin sulphate blends[31]. In addition to blending with matrix components, growth factors could be added to stimulate tissue regeneration[32,33].

To increase regenerative capacity of the scaffold further, research could focus on cell seeded scaffold implantation. Scaffolds could be seeded with a variety of cells such as autologous or allologous chondrocytes, stem cells or co-cultures of these

two, with co-cultures being the most promising[34]. When implanted in osteochondral knee defects in rabbits cell-less scaffolds showed good repair tissue, however, tissue repair was even better when scaffolds were pre-seeded with cells[35]. Nonetheless, cost effectiveness of these cell seeding techniques remains unknown until long term studies are finished[36].

CONCLUSION

Collagen scaffolds are able to regenerate articular cartilage with hyaline-like cartilage. Differences in collagen scaffold fiber architecture resulted in similar cartilage repair. However, in a limited number of cases perpendicular anisotropic scaffolds seemed to have a positive effect on subchondral bone repair.

REFERENCE LIST

1. Broom ND, Marra DL. Ultrastructural evidence for fibril-to-fibril associations in articular cartilage and their functional implication. J Anat 1986;146:185-200.
2. Minns RJ, Steven FS. The collagen fibril organization in human articular cartilage. J Anat 1977;123(Pt 2):437-57.
3. Hjelle K, Solheim E, Strand T, Muri R, Brittberg M. Articular cartilage defects in 1,000 knee arthroscopies. Arthroscopy 2002;18(7):730-4.
4. Shapiro F, Koide S, Glimcher MJ. Cell origin and differentiation in the repair of full-thickness defects of articular cartilage. J Bone Joint Surg Am 1993;75(4):532-53.
5. Steadman JR, Rodkey WG, Rodrigo JJ. Microfracture: surgical technique and rehabilitation to treat chondral defects. Clin Orthop Relat Res 2001;391(391 Suppl):S362-9.
6. Gudas R, Kalesinskas RJ, Kimtys V, Stankevicius E, Toliusis V, Bernotavicius G, Smailys A. A prospective randomized clinical study of mosaic osteochondral autologous transplantation versus microfracture for the treatment of osteochondral defects in the knee joint in young athletes. Arthroscopy 2005;21(9):1066-75.
7. Kreuz PC, Steinwachs MR, Erggelet C, Krause SJ, Konrad G, Uhl M, Sudkamp N. Results after microfracture of full-thickness chondral defects in different compartments in the knee. Osteoarthritis Cartilage 2006;14(11):1119-25.
8. Mithoefer K, Williams RJ, 3rd, Warren RF, Potter HG, Spock CR, Jones EC, Wickiewicz TL, Marx RG. The microfracture technique for the treatment of articular cartilage lesions in the knee. A prospective cohort study. J Bone Joint Surg Am 2005;87(9):1911-20.
9. Briggs TW, Mahroof S, David LA, Flannelly J, Pringle J, Bayliss M. Histological evaluation of chondral defects after autologous chondrocyte implantation of the knee. J Bone Joint Surg Br 2003;85(7):1077-83.
10. Gomoll AH. Microfracture and augments. J Knee Surg 2012;25(1):9-15.
11. Iwasa J, Engebretsen L, Shima Y, Ochi M. Clinical application of scaffolds for cartilage tissue engineering. Knee Surg Sports Traumatol Arthrosc 2009;17(6):561-77.
12. Kock L, van Donkelaar CC, Ito K. Tissue engineering of functional articular cartilage: the current status. Cell Tissue Res 2012;347(3):613-27.
13. Stoddart MJ, Grad S, Eglin D, Alini M. Cells and biomaterials in cartilage tissue engineering. Regen Med 2009;4(1):81-98.
14. Buma P, Pieper JS, van Tienen T, van Susante JL, van der Kraan PM, Veerkamp JH, van den Berg WB, Veth RP, van Kuppevelt TH. Cross-linked type I and type II collagenous matrices for the repair of full-thickness articular cartilage defects--a study in rabbits. Biomaterials 2003;24(19):3255-63.
15. Faraj KA, van Kuppevelt TH, Daamen WF. Construction of collagen scaffolds that mimic the three-dimensional architecture of specific tissues. Tissue Eng 2007;13(10):2387-94.
16. Wang JH, Jia F, Gilbert TW, Woo SL. Cell orientation determines the alignment of cell-produced collagenous matrix. J Biomech 2003;36(1):97-102.
17. Pieper JS, Oosterhof A, Dijkstra PJ, Veerkamp JH, van Kuppevelt TH. Preparation and characterization of porous crosslinked collagenous matrices containing bioavailable chondroitin sulphate. Biomaterials 1999;20(9):847-58.
18. Faraj KA, Brouwer KM, Geutjes PJ, Versteeg EM, Wismans RG, Deprest JA, Chajra H, Tiemessen DM, Feitz WFJ, Oosterwijk E and others. The Effect of Ethylene Oxide Sterilisation, Beta Irradiation and Gamma Irradiation on Collagen Fibril-Based Scaffolds. Tissue Eng Regen Med 2011;8(5):460-470.
19. Faraj KA, Cuijpers VM, Wismans RG, Walboomers XF, Jansen JA, van Kuppevelt TH, Daamen WF. Micro-computed tomographical imaging of soft biological materials using contrast techniques. Tissue Eng Part C Methods 2009;15(3):493-9.
20. de Mulder EL, Buma P, Hannink G. Anisotropic Porous Biodegradable Scaffolds for Musculoskeletal Tissue Engineering. Materials 2009;2(4):1674-96.
21. Gilbert DL, Kim SW. Macromolecular release from collagen monolithic devices. J Biomed Mater Res 1990;24(9):1221-39.
22. Olde Damink LH, Dijkstra PJ, van Luyn MJ, van Wachem PB, Nieuwenhuis P, Feijen J. Cross-linking of dermal sheep collagen using a water-soluble carbodiimide. Biomaterials 1996;17(8):765-73.
23. O'Driscoll SW, Keeley FW, Salter RB. The chondrogenic potential of free autogenous periosteal grafts for biological resurfacing of major full-thickness defects in joint surfaces under the influence of continuous passive motion. An experimental investigation in the rabbit. J Bone Joint Surg Am 1986;68(7):1017-35.
24. Wei X, Messner K. Maturation-dependent durability of spontaneous cartilage repair in rabbit knee joint. J Biomed Mater Res 1999;46(4):539-48.
25. Hunziker EB, Rosenberg LC. Repair of partial-thickness defects in articular cartilage: cell recruitment from

the synovial membrane. J Bone Joint Surg Am 1996;78(5):721-33.
26. Chen FS, Frenkel SR, Di Cesare PE. Chondrocyte transplantation and experimental treatment options for articular cartilage defects. Am J Orthop (Belle Mead NJ) 1997;26(6):396-406.
27. Qi Y, Zhao T, Xu K, Dai T, Yan W. The restoration of full-thickness cartilage defects with mesenchymal stem cells (MSCs) loaded and cross-linked bilayer collagen scaffolds on rabbit model. Mol Biol Rep 2012;39(2):1231-7.
28. McCullen S, Autefage H, Callanan A, Gentleman E, Stevens M. Anisotropic fibrous scaffolds for articular cartilage regeneration. Tissue Eng Part A 2012.
29. Klein TJ, Malda J, Sah RL, Hutmacher DW. Tissue engineering of articular cartilage with biomimetic zones. Tissue Eng Part B Rev 2009;15(2):143-57.
30. Bartlett W, Gooding CR, Carrington RW, Skinner JA, Briggs TW, Bentley G. Autologous chondrocyte implantation at the knee using a bilayer collagen membrane with bone graft. A preliminary report. J Bone Joint Surg Br 2005;87(3):330-2.
31. Matsiko A, Levingstone TJ, O'Brien FJ, Gleeson JP. Addition of hyaluronic acid improves cellular infiltration and promotes early-stage chondrogenesis in a collagen-based scaffold for cartilage tissue engineering. J Mech Behav Biomed Mater 2012;11:41-52.
32. Reyes R, Delgado A, Sanchez E, Fernandez A, Hernandez A, Evora C. Repair of an osteochondral defect by sustained delivery of BMP-2 or TGFbeta1 from a bilayered alginate-PLGA scaffold. J Tissue Eng Regen Med 2012.
33. Mullen LM, Best SM, Brooks RA, Ghose S, Gwynne JH, Wardale J, Rushton N, Cameron RE. Binding and release characteristics of insulin-like growth factor-1 from a collagen-glycosaminoglycan scaffold. Tissue Eng Part C Methods 2010;16(6):1439-48.
34. Meretoja VV, Dahlin RL, Kasper FK, Mikos AG. Enhanced chondrogenesis in co-cultures with articular chondrocytes and mesenchymal stem cells. Biomaterials 2012;33(27):6362-9.
35. Shao X, Goh JC, Hutmacher DW, Lee EH, Zigang G. Repair of large articular osteochondral defects using hybrid scaffolds and bone marrow-derived mesenchymal stem cells in a rabbit model. Tissue Eng 2006;12(6):1539-51.
36. Clar C, Cummins E, McIntyre L, Thomas S, Lamb J, Bain L, Jobanputra P, Waugh N. Clinical and cost-effectiveness of autologous chondrocyte implantation for cartilage defects in knee joints: systematic review and economic evaluation. Health Technol Assess 2005;9(47):iii-iv, ix-x, 1-82.

Chapter 8

Summary of the thesis

CHAPTER ONE

Menisci are crescent shaped fibro-cartilage structures located in pairs in the knee joint. Lesions, such as meniscus tears, are one of the most frequently occurring orthopedic traumas. Tears in the white zone of the meniscus have limited repair capacity due to the avascular nature of this part of the meniscus. Current clinical strategies to repair the damaged meniscus start with preservation of as much of meniscus tissue as possible by suturing the loose fragment to the main body of the meniscus. If fixation is unsuccessful, a partial meniscectomy will be performed. However, the inferior biomechanics of the remaining meniscus tissue will lead to the onset of osteoarthritis in a high percentage of patients. Two partial meniscus implants, Menaflex™ and Actifit®, are currently clinically available to replace the lost meniscus tissue with successful short term results. In case of a severely damaged peripheral rim, mechanical integrity of the meniscus is lost and a total meniscectomy is the preferred treatment. The current available treatment after total meniscectomy is implantation of a donor meniscus. However, the availability is limited and correct sizing is problematic. New approaches for total meniscus replacement therefore strongly focus on tissue engineering. Scaffolds should have sufficient mechanical strength to allow tissue ingrowth and permit fibro-cartilage formation. Furthermore, an anisotropic channel-like porosity might be beneficial for the direct formation of anisotropic extracellular matrix mimicking that of the native meniscus. Subsequently, two options can be used. One is *in vivo* tissue engineering by implantation of an empty scaffold directly into the defect. The body will repair the defect. The second option is *in vitro* tissue engineering. By seeding cells prior to implantation of the scaffolds, implants show improved biological properties and repair after implantation.

CHAPTER TWO

In this chapter we studied whether a previously developed polyurethane (PU) scaffold is applicable for *in vitro* meniscus tissue engineering purposes. The PU scaffold was composed of poly (D/L) lactic acid and polycaprolactone, considered as “soft” segments, and 1,4-butanidiisocyanate to obtain “hard” urethane segments. A 95% porous isotropic scaffold was produced using solvent leaching. Subsequently, goat meniscal fibrochondrocytes (MFCs) were isolated from goat menisci, seeded and cultured in these 3D porous scaffolds. Proliferation and matrix synthesis in the constructs were studied in standard medium and in TGF-beta supplemented medium. It was shown that the MFCs were able to adhere to the scaffold. In standard medium, proliferation and matrix synthesis did not increase in time. However, if TGF-beta was added to the culture medium proliferation increased almost four times while collagen production was increased over 15 times compared to cultures in standard medium. Furthermore, increased production of glycosaminoglycans was observed. Despite this increase in collagen and glycosaminoglycan production, the compressive stiffness of the constructs did not increase during these cultures.

In conclusion, the PU scaffold can be used for *in vitro* meniscus tissue engineering but surface optimization is recommended since the scaffold itself did not stimulate proliferation or matrix synthesis. A coating with bioactive molecules could increase the biological properties of the scaffold. Addition of TGF-beta to the culture medium had a positive effect on proliferation of MFCs and meniscus specific matrix production. Based on these results, it is recommended to further optimize the scaffold used for future meniscus tissue engineering.

CHAPTER THREE

As proposed in chapter two, coating of scaffolds could be useful to increase its biological properties. In this chapter, we aimed to coat the surface of a porous PU scaffold with heparin. Heparin is a bioactive macromolecule that can bind and gradually release growth factors, such as TGF-beta, VEGF and FGF. Moreover, heparin inhibits degradation of these growth factors. A two step reaction was developed to coat the PU surface with a layer of heparin. The first step was aminolysis of the porous scaffold with diamines resulting in a covalent bond of one of the amines onto the scaffold with the other amine free for further reaction. Subsequently, it was demonstrated that heparin could be cross-linked to this free amine via standard carbodiimide cross-linking. Immuno-histochemistry confirmed that there was a heparin coating on the entire surface throughout the complete 3D porous scaffold. Without the first aminolysis step, no heparin coating was detectable. Furthermore, the final heparin coating increased surface hydrophilicity, but the reaction reduced mechanical stiffness by almost 50% to 12.2kPa.

This two-step coating procedure resulted in complete coating of the porous PU scaffold with heparin. In future applications, the heparin coating will potentially enable the binding of bioactive growth factors onto the PU scaffold. In addition, an increased surface hydrophilicity indicates that both cell adherence and migration into the scaffold could be improved. The reduction in mechanical stiffness might limit the application in an *in vivo* load-bearing environment. However, in an *in vitro* tissue engineering approach, meniscus cells cultured inside the construct can produce matrix and by that the mechanical properties of the construct during the culture period will increase before implantation. However, protocols to enable this should be further optimized.

CHAPTER FOUR

The most favorable long term option for patients with a heavily damaged meniscus would be to replace this meniscus by a tissue engineered implant based on slowly resorbable polymers in combination with cells that produce new matrix. However, one of the reasons that these *in vitro* tissue engineered constructs are not clinically applied yet is the addition of fetal bovine serum (FBS) to most tissue culture media as growth stimulating supplement. FBS potentially contains bovine pathogens, thereby

increasing the risk of disease transfer or xeno-immunization. FBS is supplemented to culture media because of the positive effect on proliferation and matrix synthesis, mainly ascribed to its rich pool of growth factors. A potential effective replacement for FBS could be platelet rich plasma (PRP). These platelets can secrete a variety of growth factors which play an important role in inducing tissue regeneration. After informed consent was obtained, PRP was isolated from the blood of three healthy adult donors and human meniscus fibrochondrocytes were isolated from meniscus tissue which was removed during an arthroscopically performed partial meniscectomy in a young adult patient. Cells were cultured in monolayer and different culture media were tested. DMEM/F12+1%PSF was used as basal medium and supplemented with one of the following additives: 10% FBS, 5%, 10% or 20% PRP, or 5%, 10% or 20% of PPP (platelet poor plasma) (v/v). After 24hrs and 3 days of culture no differences were found in proliferation and gene expressions of extracellular matrix proteins. After 7 days of culture all PPP cultures showed a strongly reduced proliferation rate while medium supplemented with 10% and 20% PRP showed significantly higher cell numbers compared to all PPP concentrations and slightly higher cell numbers compared to the standard medium supplements with 10% FBS. Collagen type I gene expression was similar to the control FBS, while collagen type II was undetermined in all culture conditions. Aggrecan expression was increased in 10% and 20% PRP and in all PPP supplements compared to the FBS.

These experiments showed that medium supplemented with 10% and 20% PRP can fully replace FBS in meniscus fibrochondrocyte cell cultures with similar proliferation and matrix gene expressions. This could probably ease the clinical application of *in vitro* tissue engineered constructs for meniscus replacement but is also of value for tissue engineering of other tissues.

CHAPTER FIVE

It has been generally accepted that tissue engineered constructs should closely resemble the *in vivo* mechanical and structural properties of the tissues they are intended to replace. Most native meniscus tissues have significant anisotropic extracellular matrix components and concomitant mechanical properties. However, most scaffolds produced so far were isotropic porous scaffolds. Tissues that are formed in these scaffolds are quite different from the anisotropic native meniscus tissue. Collagen is not orientated anisotropically and probably mechanical properties are also quite different. Thus, the formed tissues have no structural and functional relationships with the native tissues. Therefore, to obtain complete regeneration of tissues resembling anisotropic native tissues, a second differentiation step after resorption of the isotropic scaffold would be required. It is doubtful whether the required plasticity for this second differentiation step is still present in already final differentiated tissues. It would be much more efficacious if the newly formed tissues in the scaffold could differentiate directly into the anisotropic organization of the native tissues being replaced. Therefore, anisotropic scaffolds that enable such a

direct differentiation might be extremely helpful to realize this goal. Up to now, anisotropic scaffolds have been fabricated using modified conventional techniques, solid free-form fabrication techniques, and a few alternative methods. In this chapter an overview of current anisotropic scaffold fabrication techniques was presented and discussed.

CHAPTER SIX

Scaffolds which are currently used to treat patients are not suitable for the regeneration of a complete meniscus after a total meniscectomy. The organization of the regenerated meniscus tissue appeared to be different from that in the native meniscus. The collagen bundles formed were orientated in a random direction guided by the isotropic pore architecture of the scaffold. The morphology is therefore far different from the highly organized and anisotropic morphology, which is mainly present in the vascularized peripheral rim of the native meniscus. Moreover, these scaffolds are too weak. As proposed in chapters one and five, anisotropic scaffolds may induce anisotropic repair tissue. To test the effect of scaffold pore architecture on the ability to guide organized extracellular matrix formation, isotropic and anisotropic PU scaffolds were produced with two different solvent leaching procedures. In chapter two, a standard solvent leaching procedure (i.e. isotropic freezing condition) was used to obtain isotropic porous scaffolds. To obtain anisotropic porous scaffolds with channels inside, a thermal freezing gradient was applied (chapter 5, modified TIPS). These two different freezing techniques resulted in isotropic and anisotropic scaffolds with a degree of anisotropy of 0.39 and 0.18, respectively. Anisotropic scaffolds had a channel diameter of 20 ± 6.0µm while isotropic scaffolds had a larger pore diameter of 35 ± 14.7µm. Subsequently, these scaffolds were implanted subcutaneously in rats for 1, 4, 8 or 24 weeks. Since in this model mechanical loading is minimal, it allowed us to test the sole effect of scaffold pore architecture on extracellular matrix differentiation. Isotropic scaffolds obtained full tissue ingrowth after 8 weeks while anisotropic scaffolds showed full ingrowth after 24 weeks. Extracellular matrix infiltration in isotropic scaffolds was of an unorganized fibro-collagenous type. The anisotropic scaffolds showed tissue infiltration which was more organized with parallel aligned collagen fibers. The tissue of the anisotropic scaffold closely resembled the meniscal vascularized peripheral rim, while the isotropic scaffolds resembled tissue of the inner zone. This tissue orientation was only due to scaffold architecture and this showed to be an important factor in the regeneration of an isotropic organized extracellular matrix. Therefore we propose that a total meniscus implant should have an anisotropic peripheral rim and an isotropic inner zone. Whether these effects remain present in a load-bearing situation should be further investigated.

CHAPTER SEVEN

Anisotropic scaffolds can be applied not only to induce meniscus tissue repair, but also to facilitate the repair of other, related tissues such as articular cartilage. In case of small size articular cartilage damage, in current clinical practice small holes are drilled into the subchondral bone to allow mesenchymal stem cells to enter the cartilage defect to induce repair. This technique is now known as micro-fracturing. However, this leads to the generation of a fibrous cartilage-like repair tissue, mechanically inferior to the native hyaline cartilage. Previous studies in which isotropic collagen scaffolds were re-inserted into the drilled defect resulted in hyaline-like cartilage repair, however, the defect remained partly unhealed. Therefore, we tested if the insertion of anisotropic collagen scaffolds, with fibers perpendicular to the cartilage surface, could induce complete repair by improving cellular influx from the subchondral bone. Isotropic and anisotropic collagen type I scaffolds were produced via similar freezing protocols as described in chapter six. Isotropic scaffolds showed to have larger pores and thicker walls compared to the anisotropic scaffolds. Subsequently, two full thickness articular cartilage defects were created in both knees of rabbits. These defects were left empty, filled with the isotropic scaffold or with the anisotropic scaffold. In the latter case the scaffold was placed with the main direction of the pores parallel or perpendicular to the cartilage surface. After 4 weeks, all defects were completely filled with partially differentiated hyaline cartilage tissue. Sections were scored via a modified O'Driscoll score and showed no differences between empty defects and scaffold types. After 12 weeks of implantation, all treatments led to hyaline cartilage repair visualized by increased glycosaminoglycan staining. Total O'Driscoll scores were significantly increased for parallel anisotropic and empty defects over time ($p<0.05$). Furthermore, isotropic scaffolds were still visible in the defect while anisotropic scaffolds seemed to be completely resorbed after 12 weeks. Remarkably, after both 4 and 12 weeks trabecular bone was formed parallel to the surface of the articular cartilage in a limited number of defects treated with perpendicular anisotropic scaffolds.

The results indicate that collagen scaffolds can induce hyaline-like cartilage repair. Fiber architecture had no effect on cartilage repair. This could be due to differences in pore sizes and wall thickness reducing the effect of anisotropic scaffolds.

8

Chapter 9

Discussion and future perspectives

Repair of damaged meniscus tissue remains challenging. The main goal after a meniscus tear is preservation of as much meniscus tissue as possible to prevent articular cartilage degradation. Tears can be sutured in order to fixate the loose fragment stable to the main body of the meniscus. It was also investigated whether tears can be glued with fibrin glue, resulting in mixed outcomes [1]. The main problem with fibrin glue is the inadequate strength of the glue. Therefore, our department is developing stronger glues for enhanced meniscus repair. An additional improvement can be mixing stem cells inside the glue to promote healing [2]. If fixation fails or in case of complex tears, (partial) meniscectomy will be the logical next procedure to follow. For partial meniscus replacement, two scaffolds, Actifit® and Menaflex™, are currently available to treat patients with reported positive effects on tissue repair and function [3]. In case of total meniscus replacement, donor meniscus tissue is the single clinical option [4]. However, the correct size of a donor meniscus is of great importance on proper knee joint biomechanics [5,6]. Due to insufficient sizing of the donor menisci, and in addition the risk of disease transfer, the number of donor transplantations remains limited. Nowadays, roughly two different options for total meniscus replacement are being evaluated. One focuses on a solid permanent implant, the other on a tissue engineered construct. By omitting biologic aspects, solid permanent implants can be obtained and produced faster and clinical approval is more easy. These implants can be attractive for elderly patients with mild osteoarthritis and in which tissue regeneration is limited. However, correct sizing of the implant is crucial since it cannot remodel or adapt itself in case of a mismatch in geometrical parameters with the native meniscus. Furthermore, it remains unknown if these implants will endure the large and repetitive strains and forces applied by *in vivo* activities for a number of decades. So positive effects should be found in the older patient category before such implants can be applied in younger patients. Therefore, younger patients potentially benefit more from implants able to fully form and replace the defect with native tissue and reduce the effect of long term foreign body reaction. In addition, cost effectiveness of a treatment remains crucial as well. In general, tissue engineering is a more expensive approach compared to using a permanent implant. To be cost effective, these tissue engineered constructs need to increase quality of life of the patient for a large number of years.

In this thesis, a new potential polyurethane (PU) meniscus scaffold based on D/L lactic acid and caprolactone with urethane blocks has been described and tested. This PU scaffold has a 95% porosity and thereby has a higher porosity compared to the Menaflex™ scaffold (80% porosity). Higher porosities are known to improve cell penetration and matrix synthesis [7,8]. Another advantage of a high porosity is that it, in general, will lead to a faster resorption as less polymer material has to be degraded. Reducing the time foreign materials remain present in the body has been shown to lower the risk on immunological responses. In addition, with smaller amounts of polymer material to be degraded, lower acidic levels of tissue in the direct vicinity will be reached. It has been described that higher acidity levels reduce the tissue regeneration speed [9]. The PU scaffold has been shown to allow meniscus cell culture.

However, proliferation in our studies was limited, but, stimulation with TGF-beta increased proliferation. Heparin, a glycosaminoglycan, is able to bind a variety of growth factors, such as TGF-beta, VEGF and FGF, thereby enabling a retained bioactivity and gradual release of the growth factor [10,11]. This release can potentially stimulate cells over longer periods of time, but needs to be investigated in more detail. In theory, the developed coating procedure based on aminolysis and subsequent cross-linking of heparin, could be applicable to a wide variety of polymer scaffolds, not only to the one described in this thesis. However, further research is needed to show its efficacy. Furthermore, other macromolecules, besides heparin, could be cross-linked to the free amine, e.g. collagens and chondroitin sulphate [12,13]. The main pitfall with this coating technique is cleavage of polymer chains during the aminolysis, resulting in reduced mechanical stiffness. This would not be a problem if the scaffold would be used in non load-bearing tissues. However, when applied as replacement for load-bearing meniscus tissue, the mechanical properties might become inferior and chondroprotection cannot be maintained [14]. To maintain mechanical properties the aminolysis step might be performed with a shorter incubation period, but this will also reduce the amount of macromolecules available for cross-linking on the surface. Another option could be to incorporate free amines during synthesis of a new polymer. This would make aminolysis step superfluous and thereby not alter the mechanical properties of the new construct. However, in the application foreseen by us, an *in vitro* tissue engineered meniscus construct, the initial reduced mechanical properties of the scaffold might be less significant. If cells are pre-cultured in optimal conditions, matrix synthesized by these cells will improve mechanical properties in time [15]. However, it remains under investigation if optimization of culture conditions will lead to a tissue engineered meniscus construct that will enable the replacement of the complete meniscus. We showed that in our scaffold seeded with meniscal fibrochondrocytes, matrix synthesis increased under influence of TGF-beta, but this did not lead to increased mechanical properties. A low seeding density can be the cause why we did not find improved mechanical properties. Another reason could be that these used meniscal fibrochondrocytes are differentiated cells which might be less potent for regeneration. Others investigated additional cell types for improved meniscus tissue engineering, such as chondrocytes, mesenchymal stem cells or co-cultures of these cell types [16]. They showed that co-cultures of stem cells with MFCs induced better meniscus tissue regeneration than MFCs alone and should therefore be the focus of future research. Besides chemical stimulation, mechanical stimulation could be investigated for improved tissue regeneration. It is known that cells behave differently under mechanical stimulation [17]. Various bioreactors have been fabricated to copy *in vivo* biomechanics/loading situations during *in vitro* culture conditions. These bioreactors can apply compression, tensile, shear stress or even combinations of these stresses [17,18]. These studies showed that mechanical stimulations result in cell differentiation, proliferation and matrix synthesis, thereby improving the quality of the final *in vitro* tissue engineered meniscus construct.

When pre-culturing cells for a clinically used tissue engineered construct, a

number of hurdles have to be taken. One of these hurdles is to avoid the issue of fetal bovine serum. FBS is a mix of potent growth factors able to stimulate a wide variety of cell types, hence it is widely used in scientific research. However, due to its bovine origin, FBS could contain bovine pathogens thereby increasing the risk of disease transfer [19]. We showed that replacing bovine serum by platelet rich plasma could maintain similar proliferation and matrix gene expression in case of meniscus cell cultures. This increases the potential for clinical application of meniscus cell cultured implants. Furthermore, this platelet rich plasma could be easily and safely obtained from patients own blood or from donors.

Significant improvements are made in optimizing culture conditions (e.g. serum, growth factors, coatings and bioreactors), however, additional alterations should be considered, especially when aiming for total meniscus regeneration. Both Menaflex™ and Actifit® are isotropic porous scaffolds. Plain isotropic scaffolds are not ideal for complete meniscus tissue regeneration [20]. These scaffolds result in unorganized tissue differentiation thereby unable to cope with the high mechanical stresses the menisci endure. When analyzing the meniscus' extracellular matrix, well defined topographies are observed. The inner zone may have an isotropic matrix organization, but the vascularized peripheral rim has a clear anisotropic matrix organization with large collagen fibers oriented in a parallel, circumferential orientation [21]. These fibers redirect the forces necessary for shock absorption. We showed that anisotropic porous scaffolds are of great importance to guide similar anisotropic matrix regeneration. Therefore, to create a total meniscus implant, we hypothesize that the scaffold should consist of an anisotropic outer rim and an isotropic inner zone. These complex structures are difficult to obtain via the freeze drying procedure used in this thesis. However, improved fabrication techniques, such as 3D fiber depositioning and stereolithography became available. The latter would be the preferred option since this technique enables complex structures via computer aided design models [22]. Using these models, complex anisotropic porous architectures can be produced and the final constructs can be resized into patient specific anatomical geometries. Subsequently, these constructs can be used for *in vitro* cell culture and finally be implanted into the patient.

An important factor not addressed yet is scaffold degradation. Degradation of the scaffold should be in balance with tissue infiltration and differentiation. If degradation of the scaffold is too fast, new tissue cannot cope with the high stresses inside the knee joint. In our study about articular cartilage defects we hypothesize that the lack of difference in repair might be a result of relatively fast degradation of the anisotropic collagen scaffolds. After 12 weeks, only the isotropic scaffolds were still visible in histology, whereas the anisotropic scaffolds already disappeared. When anisotropic scaffolds degrade, they might lose their anisotropic properties resulting in similar outcomes as isotropic scaffolds. To investigate critical time for pore structure to influence cell migration and cartilage repair, slower degrading scaffolds should be created and tested in the future. This can be achieved by increasing the amount of cross-links in case of collagen scaffolds.

Tissue engineering of a total meniscus remains challenging. The experiments described in this thesis resulted in tools to improve properties of a total tissue engineered meniscus implant. Future research should focus on meniscus scaffolds with porosities similar to the meniscus collagen fiber architecture, i.e. an anisotropic outer rim and an isotropic inner zone. To improve surface hydrophilicity, and thereby cell migration, these scaffolds can be coated with heparin to which additional growth factors such as TGF-beta can be coupled. This will enhance biological properties of the tissue engineered construct during *in vitro* cell culture. Further improvements of the construct can be achieved by investigating the effects of co-cultures and mechanical stimulation on tissue proliferation and differentiation. The final tissue engineered construct should be tested in an *in vivo* total meniscus transplantation model to study its chondroprotective capacity.

The last two decades the Orthopedic Research Lab investigated and improved meniscus tissue engineering. This resulted in enhanced research techniques necessary to reach the ultimate goal of total meniscus replacement. The improvements shown in this thesis will contribute to this development and the development of a tissue engineered meniscus construct.

REFERENCE LIST

1. Ishimura M, Ohgushi H, Habata T, Tamai S, Fujisawa Y. Arthroscopic meniscal repair using fibrin glue. Part II: Clinical applications. Arthroscopy 1997;13(5):558-63.
2. Ferris D, Frisbie D, Kisiday J, McIlwraith CW. In vivo healing of meniscal lacerations using bone marrow-derived mesenchymal stem cells and fibrin glue. Stem Cells Int 2012;2012:691605.
3. Spencer SJ, Saithna A, Carmont MR, Dhillon MS, Thompson P, Spalding T. Meniscal scaffolds: Early experience and review of the literature. Knee 2012.
4. McDermott I. Meniscal tears, repairs and replacement: their relevance to osteoarthritis of the knee. Br J Sports Med 2011;45(4):292-7.
5. Alhalki MM, Hull ML, Howell SM. Contact mechanics of the medial tibial plateau after implantation of a medial meniscal allograft. A human cadaveric study. Am J Sports Med 2000;28(3):370-6.
6. Dienst M, Greis PE, Ellis BJ, Bachus KN, Burks RT. Effect of lateral meniscal allograft sizing on contact mechanics of the lateral tibial plateau: an experimental study in human cadaveric knee joints. Am J Sports Med 2007;35(1):34-42.
7. van Tienen TG, Heijkants RG, Buma P, de Groot JH, Pennings AJ, Veth RP. Tissue ingrowth and degradation of two biodegradable porous polymers with different porosities and pore sizes. Biomaterials 2002;23(8):1731-8.
8. Klompmaker J, Jansen HW, Veth RP, Nielsen HK, de Groot JH, Pennings AJ. Porous implants for knee joint meniscus reconstruction: a preliminary study on the role of pore sizes in ingrowth and differentiation of fibrocartilage. Clin Mater 1993;14(1):1-11.
9. van Minnen B, Stegenga B, van Leeuwen MB, van Kooten TG, Bos RR. A long-term in vitro biocompatibility study of a biodegradable polyurethane and its degradation products. J Biomed Mater Res A 2006;76(2):377-85.
10. Stringer SE, Gallagher JT. Heparan sulphate. Int J Biochem Cell Biol 1997;29(5):709-14.
11. Nillesen ST, Geutjes PJ, Wismans R, Schalkwijk J, Daamen WF, van Kuppevelt TH. Increased angiogenesis and blood vessel maturation in acellular collagen-heparin scaffolds containing both FGF2 and VEGF. Biomaterials 2007;28(6):1123-31.
12. Chang KY, Cheng LW, Ho GH, Huang YP, Lee YD. Fabrication and characterization of poly(gamma-glutamic acid)-graft-chondroitin sulfate/polycaprolactone porous scaffolds for cartilage tissue engineering. Acta Biomater 2009;5(6):1937-47.
13. Zhu Y, Gao C, Liu X, Shen J. Surface modification of polycaprolactone membrane via aminolysis and biomacromolecule immobilization for promoting cytocompatibility of human endothelial cells. Biomacromolecules 2002;3(6):1312-9.
14. Hannink G, van Tienen TG, Schouten AJ, Buma P. Changes in articular cartilage after meniscectomy and meniscus replacement using a biodegradable porous polymer implant. Knee Surg Sports Traumatol Arthrosc 2011;19(3):441-51.
15. Talukdar S, Nguyen QT, Chen AC, Sah RL, Kundu SC. Effect of initial cell seeding density on 3D-engineered silk fibroin scaffolds for articular cartilage tissue engineering. Biomaterials 2011;32(34):8927-37.
16. Matthies NF, Mulet-Sierra A, Jomha NM, Adesida AB. Matrix formation is enhanced in co-cultures of human meniscus cells with bone marrow stromal cells. J Tissue Eng Regen Med 2012.
17. Upton ML, Chen J, Guilak F, Setton LA. Differential effects of static and dynamic compression on meniscal cell gene expression. J Orthop Res 2003;21(6):963-9.
18. Grad S, Lee CR, Gorna K, Gogolewski S, Wimmer MA, Alini M. Surface motion upregulates superficial zone protein and hyaluronan production in chondrocyte-seeded three-dimensional scaffolds. Tissue Eng 2005;11(1-2):249-56.
19. Hodgson J. To treat or not to treat: that is the question for serum. Biotechnology (N Y) 1995;13(4):333-4, 337-8, 342-3.
20. Welsing RT, van Tienen TG, Ramrattan N, Heijkants R, Schouten AJ, Veth RP, Buma P. Effect on tissue differentiation and articular cartilage degradation of a polymer meniscus implant: A 2-year follow-up study in dogs. Am J Sports Med 2008;36(10):1978-89.
21. Petersen W, Tillmann B. Collagenous fibril texture of the human knee joint menisci. Anat Embryol (Berl) 1998;197(4):317-24.
22. Melchels FP, Feijen J, Grijpma DW. A review on stereolithography and its applications in biomedical engineering. Biomaterials 2010;31(24):6121-30.

9

Chapter 10

Nederlandse samenvatting van het proefschrift

HOOFDSTUK 1

De meniscus is een halvemaanvormige structuur en bestaat uit fibreus kraakbeen. De menisci liggen in paren in het kniegewricht en spelen een belangrijke rol in de schokdemping. Een veel voorkomend klinisch probleem is het optreden van scheuren de menisci. Scheuren die optreden in het doorbloede deel van de meniscus kunnen meestal hersteld worden met hechtingen. Echter, wanneer de scheur gelegen is in het niet-doorbloede deel van de meniscus falen hechtingen vaker. Via een kijkoperatie kan het "los" zittende stuk van de meniscus worden verwijderd. Het resterende meniscusweefsel biedt hierdoor een slechtere schokdemping met als gevolg een grotere kans op kraakbeenschade. Momenteel zijn er twee implantaten beschikbaar, Menaflex™ en Actifit®, die kunnen worden gebruikt om het verwijderde meniscusweefsel te vervangen. Beide implantaten zijn gemaakt van poreuze materialen die worden ingehecht op de plek waar meniscusweefsel is verwijderd. Nieuw weefsel kan vervolgens in de poriën van dit implantaat ingroeien en zo het beschadigde en verwijderde deel van de meniscus vervangen. Deze techniek biedt goede uitkomsten op de korte termijn. Echter wanneer de buitenste rand van de meniscus is ingescheurd, kan de meniscus niet meer goed herstellen en zal deze vaak in zijn geheel moeten worden verwijderd. Een donormeniscus is dan nog de enig resterende optie. Een donormeniscus is echter moeilijk te verkrijgen en met name het vinden van een meniscus met de juiste afmetingen blijkt in de praktijk erg lastig. Om deze redenen worden er veel studies gedaan naar het maken van meniscusweefsel in het laboratorium ter vervanging van de donormeniscus. Om een meniscus in het laboratorium te kunnen maken is een dragermateriaal, een zogenaamde "scaffold", nodig die stevig genoeg is om de krachten in het kniegewricht te kunnen weerstaan, de ingroei van weefsel in de scaffold toelaat, en vervolgens de omvorming van dit ingegroeide weefsel in fibreus kraakbeen kan stimuleren. Middels een tweetal opties kan dit proces worden bewerkstelligd. De eerste optie is het implanteren van een lege scaffold in het kniegewricht, waarna het lichaam zelf voor weefselingroei en oriëntatie van de nieuw gevormde weefsel zal zorgen. De tweede methode is om de scaffold in het laboratorium te voorzien van cellen en deze cellen vervolgens te stimuleren om weefsel te maken. Hierdoor zou na implantatie een sneller herstel kunnen plaatsvinden.

HOOFDSTUK 2

Allereerst is bestudeerd of een reeds bestaande polyurethaanscaffold (PU) geschikt is om in het laboratorium meniscuscellen op te zaaien en te laten groeien. Deze PU scaffold is een combinatie van poly (D/L) lactaat, een zogenaamd "zachte" segment, en 1,4-butaandiisocyanaat, een zogenaamd "hard" segment. Er werd een 95% poreuze PU scaffold gemaakt met een willekeurige structuur van de poriën. Vervolgens werden meniscuscellen geïsoleerd uit geitenmenisci, gezaaid op deze 3D scaffolds en gekweekt in het laboratorium in een "normaal" kweekmedium en in een

kweekmedium waaraan de groeifactor TGF-beta was toegevoegd. De proliferatie en eiwitproductie van de gekweekte cellen werd bestudeerd. Deze studie liet zien dat de meniscuscellen in staat zijn om aan de PU scaffold te hechten. Na zes weken werd gevonden dat cellen die waren gekweekt in het "normale" kweekmedium nauwelijks waren geprolifereerd en geen eiwit te hebben geproduceerd. Echter, in de groep waar TGF-beta aan het medium was toegevoegd was het aantal cellen 4x zo hoog geworden. Verder was de productie van collageen, een van de belangrijkste eiwitten in de meniscus, zelfs 15x zo hoog in deze groep. De productie van glycosaminoglycanen, een andere belangrijke component van de meniscus, werd ook gestimuleerd door de toevoeging van TGF-beta aan het kweekmedium. Ondanks de toename in eiwitproductie bleven de mechanische eigenschappen van de scaffold echter onveranderd.

Geconcludeerd kan worden dat deze PU scaffold geschikt is om meniscuscellen in te kweken. De toevoeging van TGF-beta aan het medium liet een duidelijk positief effect zien op meniscuscelkweken. Op basis van deze resultaten wordt aangeraden het oppervlakte van deze PU scaffold te voorzien van een bioactieve coating die cellen kan stimuleren te prolifereren en tevens de productie van meniscuseiwitten aanzet.

HOOFDSTUK 3

Een voorbeeld van een dergelijke bioactieve coating is heparine. Heparine is een molecuul dat in staat is om groeifactoren te binden en daarna geleidelijk weer los te laten. Ook is heparine in staat om afbraak van deze groeifactoren te voorkomen. Om heparine aan de PU scaffold te binden onderzochten we een twee-stapsreactie. De eerste stap is een aminolysestap, die ervoor zorgt dat er vrije aminogroepen aan het oppervlakte van de scaffold komen. Vervolgens wordt in de tweede stap heparine aan deze vrije aminogroepen gekoppeld. We zijn erin geslaagd het gehele oppervlakte van de 3D PU scaffolds te coaten met heparine. Het coatingsproces zorgde ervoor dat de oppervlakte minder waterafstotend werd, maar tevens verlaagde het de stijfheid van de scaffold. Het veranderde oppervlakte van de scaffolds zorgt ervoor dat cellen makkelijker kunnen hechten en dieper in de scaffold kunnen ingroeien. De lagere stijfheid kan echter de toepasbaarheid van de uiteindelijke scaffolds beperken voor het gebruik in meniscusdefecten. Een mogelijke oplossing voor dit probleem zou kunnen zijn om in het laboratorium cellen in de scaffolds te kweken en de eiwitproductie van deze cellen te stimuleren en daarmee verbeterde mechanische eigenschappen te creëren.

HOOFDSTUK 4

Bij het maken van een gekweekt meniscusimplantaat wordt er standaard koeienserum aan het kweekmedium toegevoegd. Dit serum bevat onder andere groeifactoren die een stimulerende werking hebben op de gekweekte cellen. Echter,

vanwege de dierlijke afkomst en het daarbij horende risico op overdracht van ziektekiemen is het niet toegestaan met koeienserum gekweekte meniscusscaffolds te implanteren bij patiënten. Een mogelijke vervanging voor dit serum is plasma dat verrijkt is met bloedplaatjes (PRP). De plaatjes in dit plasma kunnen een variatie aan groeifactoren afgeven. Het PRP kan geïsoleerd worden uit eigen bloed van een patiënt of uit bloed van donoren. Om te onderzoeken of PRP het koeienserum kan vervangen tijdens het opkweken van meniscusfibroblasten is van drie gezonde donoren bloed afgenomen en hieruit het PRP geïsoleerd. Uit een tijdens een kijkoperatie verwijderd loszittend stukje meniscusweefsel van een patiënt zijn meniscuscellen geïsoleerd. Deze cellen zijn opgekweekt in kweekmedium met PRP, plaatjesarm plasma (PPP) of koeienserum. Vervolgens is onderzocht of de cellen goed groeien en of er op mRNA niveau een aanzet wordt gemaakt belangrijke meniscuseiwitten te produceren. Er werd geen verschil gevonden tussen de celkweken tot 3 dagen. Na 7 dagen groeiden de cellen in het PRP medium net zo goed als in koeienserum, terwijl de groei in het PPP medium was gestopt. De eiwitproductie was in alle groepen gelijk aan die in het koeienserum. Hiermee is aangetoond dat koeienserum volledig vervangen kan worden door PRP. Door koeienserum te vervangen door PRP is het gebruik van een in het laboratorium gekweekte meniscus een stap dichter bij de klinische toepassing gekomen.

HOOFDSTUK 5

Het is belangrijk dat implantaten vergelijkbare mechanische en weefseleigenschappen hebben met het weefsel dat ze moeten gaan vervangen. De meniscus zelf heeft een duidelijk georiënteerde structuur. In de buitenste zone liggen grote collageenbundels parallel aan elkaar in de halve maan vorm van de meniscus. Het is dan ook van belang dat de scaffold deze weefseloriëntatie stimuleert. Dit kan worden bereikt door een scaffold te vervaardigen met eenzelfde poriestructuur als de “echte” meniscus. Echter, scaffolds die nu gebruikt worden zijn nog niet voorzien van een dergelijke georiënteerde poriestructuur. In dit hoofdstuk geven we een overzicht van productiemethoden waarmee scaffolds kunnen worden gemaakt met een vooraf bepaalde poriestructuur. De voor- en nadelen van elke productiemethode komen uitgebreid aan bod.

HOOFDSTUK 6

Een methode om georiënteerde scaffolds te maken is het materiaal tijdens het invriezen bloot te stellen aan een koudegradiënt. Deze methode is toegepast op de PU scaffolds die gebruikt zijn in hoofdstuk 2 en 3. Door middel van deze invriesmethode met koudegradiënt werden scaffolds met kanalen die parallel aan elkaar lopen vervaardigd. Via de standaard invriesmethode werden scaffolds verkregen met een random poriestructuur zoals ook gebruikt in de hoofdstukken 2 en 3. Vervolgens is onderzocht hoe weefsel ingroeit in beide typen scaffolds. Een goede methode om

dit te bestuderen is het implanteren van deze scaffolds onder de huid van ratten. Hierdoor kan de invloed van de poriestructuur op weefselingroei worden bestudeerd in afwezigheid van mechanische belasting. Na 8 weken waren de scaffolds met een random poriestructuur volledig ingegroeid met nieuw weefsel terwijl de scaffolds met parallelle kanalen pas na 24 weken volledig waren ingegroeid. De scaffolds met parallelle kanalen lieten echter wel eenzelfde weefseloriëntatie zien als de buitenste zone van de meniscus. De scaffolds met de random poriestructuur lieten een ongeorganiseerde weefseloriëntatie zien die meer op de binnenste zone van de meniscus lijkt. Op basis van deze resultaten zou een meniscusscaffold met een buitenste zone met kanalen en een binnenste zone met random poriën moeten worden gecreëerd. Dit construct zou uiteindelijk verder onderzocht moeten worden in een omgeving waarin krachten op de scaffold werken om te kunnen bestuderen wat de invloed van deze krachten op de weefselingroei is.

HOOFDSTUK 7

De meniscus is niet het enige weefsel waar de oriëntatie van de scaffold van belang is. Dit is bijvoorbeeld ook het geval bij kraakbeenweefsel. Een klein kraakbeendefect kan worden hersteld middels een operatie waarbij kleine gaatjes in het subchondrale bot worden geboord. Dit stimuleert stamcellen om zich vanuit het onderliggende beenmerg te verplaatsen naar het kraakbeen waar ze dan nieuw kraakbeenachtig weefsel te gaan maken. Het nieuw gemaakte kraakbeen is echter wel van een minder goede kwaliteit in vergelijk met "originele" kraakbeen. In eerdere studies van de afdeling Orthopedie samen met de afdeling Matrix Biochemie is kraakbeenherstel na implantatie van verschillende collageenscaffolds met een random poriestructuur onderzocht. Met name scaffolds op basis van type II collageen induceerden een beter kraakbeenherstel. Echter, het oppervlakte van het nieuwe kraakbeen bestond voornamelijk uit fibreus weefsel. In dit hoofdstuk is gekeken naar het effect van collageenscaffolds met een georiënteerde poriestructuur op het kraakbeenherstel. De hypothese was dat door de georiënteerde poriestructuur de stamcellen zich beter kunnen verplaatsen naar het oppervlakte van het kraakbeendefect wat vervolgens zou kunnen resulteren in een beter of mogelijk zelfs volledig kraakbeenherstel. De georiënteerde scaffolds zijn met een vergelijkbare methode gemaakt, zoals beschreven in hoofdstuk 6, namelijk door gebruik te maken van een temperatuurgradiënt tijdens invriezen. De scaffolds met een random poriestructuur bleken grotere poriën en dikkere poriewanden te hebben in vergelijking met de scaffolds met een georiënteerde poriestructuur. Vervolgens werden deze scaffolds bestudeerd in een konijnen kraakbeenmodel. Er werden kleine gaatjes geboord in het kraakbeen van de knie van deze konijn, waarna deze gaatjes werden opgevuld met een scaffold met random of met georiënteerde poriën, of werden leeg gelaten. Scaffolds met georiënteerde poriën werden geplaatst met de porieoriëntatie loodrecht of parallel aan het kraakbeenoppervlakte. Na 4 en 12 weken werd de kwaliteit van de weefselingroei beoordeeld op basis van weefselcoupes. Na 4 weken was de eerste

aanzet tot kraakbeenherstel gelijk in alle vier de groepen. Na 12 weken werd er in alle groepen kraakbeenherstel aangetroffen. Scaffolds met georiënteerde poriën parallel verlopend aan het oppervlak van het kraakbeen en lege defecten lieten zelfs een verbeterd herstel zien in vergelijking met de situatie na 4 weken. Verder waren de random scaffolds nog steeds zichtbaar terwijl de georiënteerde scaffolds geresorbeerd waren. De resultaten laten zien dat deze scaffolds in staat zijn om kraakbeenherstel te stimuleren. Deze stimulatie blijkt echter niet afhankelijk van de oriëntatie van de kanalen in de scaffold. Mogelijk werden potentiële verschillen gemaskeerd door andere factoren, zoals de aanwezigheid van kleinere poriën en dunnere wanden in de georiënteerde scaffolds. Dit zal verder moeten worden onderzocht.

Dankwoord

Een proefschrift maken doe je niet alleen. Het is een “hels” karwei en elke hulp is daarbij een welkome aanvulling. Tijdens het maken van dit werk heb ik daarom ook de nodige hulp gehad van legio collega’s, vrienden en familie.

Pieter Buma, als promotor en hoofd van de onderzoeksafdeling heb jij ervoor gezorgd dat ik de mogelijkheid kreeg om dit onderzoek uit te mogen voeren. Naast inspiratie zorgde je ook voor de spreekwoordelijke schop onder mijn kont als iets op tijd af moest zijn. Naast werkbesprekingen hadden we ook voldoende niet werkgerelateerde gesprekken die vaak langer duurden dan de werkbesprekingen zelf. Hier heb ik altijd erg van genoten en dank hiervoor.

Nico Verdonschot, ondanks je drukke agenda schoof je met grote regelmaat aan bij de projectoverleggen. Met je achtergrond in de biomechanica begreep je soms weinig van ons biologisch onderzoek. Desondanks wist je je vinger altijd op de zere plek te leggen. Hierdoor zorgde je ervoor dat het onderzoek kwalitatief verbeterde en de artikelen strak en duidelijk werden opgeschreven. Mijn dank is groot.

Gerjon Hannink, als co-promotor en oud kamergenoot stond je altijd open voor de nodige hulp en discussies. Hierdoor is mijn promotie zeker een stuk soepeler verlopen. Verder zorgde je altijd voor een vrolijke noot, zowel met je muziek, humor, youtube filmpjes en verhalen. Bedankt voor al je hulp en de ontspanning.

Léon Driessen, de belangrijkste man achter de schermen. Jij zorgde ervoor dat de vele coupes gesneden en gekleurd werden. Als leider van de GDS zorgde je ervoor dat ik mijn nodige geitenmenisci kreeg waaruit ik al die miljoenen cellen uit heb kunnen isoleren. Dit werk deed je altijd met een vrolijke noot. Bijna nooit heb ik je kunnen betrappen op een valse noot.

Wojtek “could you please turn the heating down” Madej, you where my roommate during my last two years. After a rough start we continued as good colleagues and even better friends. Dziękuje za pomoc!

Zo uitgebreid kan ik helaas niet alle collega's van het ORL beschrijven in verband met plaatsgebrek. Het boekje zou dan minstens twee keer zo dik worden. Dit betekent niet dat ik al jullie hulp en gezelschap minder waardeer. Ook jullie waren van onschatbare waarde bij het totstandkoming van dit boekje. Anne, Astrid, Daan, Dennis, Erwin, Esther, Hendi, Ineke, Lennert, Liesbeth, Loes, Maria, Maud, Pawel, Pieter, René, Thom, Tony en Willem, bedankt voor alle gezelschap, de belangrijke én de minder belangrijke gesprekken.

Tijdens mijn promotie heb ik meerdere studenten mogen begeleiden. Hun experimenten en resultaten hebben direct en indirect geleid tot de hoofdstukken in dit boekje. Filippo Livraghi, Hendrik Gussen, Marcel Bosch, Joselin Schutten en Maurice Bruinier bedankt voor jullie bijdrage. Een student wil ik extra bedanken aangezien haar experimenten hebben geleid tot een hoofdstuk in dit boekje waarbij wij gedeeld eerste auteur van zijn. Tevens is zij aangenomen om mijn onderzoek voort te zetten. Veronica Gonzales, bedankt en succes met het onderzoek.

Het meeste onderzoek is uitgevoerd op een lab dat wij deelden met de afdeling KNO. Edith en Theo, bedankt voor de vele leuke gesprekken en de memorabele nieuwjaarsborrels.

Graag wil ik nog een paar personen van Polyganics extra bedanken voor hun hulp bij het krijgen en maken van de scaffolds. Jacintha en Robbert dank hiervoor.

Om dierexperimenten goed uit te kunnen voeren heb je bekwame hulp nodig. Alex, Conrad, Daphne, Jeroen, Maikel en Wilma bedankt voor de ondersteuning en de goede zorgen voor de dieren.

Naast de makkelijke, in een hokje te plaatsen, collega's wil ik ook een aantal collega's bedankt voor hun hulp bij mijn onderzoek, de sociale ondersteuning in de Aesculaaf of de gezelligheid bij congressen. Matrix Biochemie: Martin, Gerwen, Katrien, Etienne, Elly, Willeke en Toin. Reumatologie: Arjen, Dennis, Elly, Henk en Peter. Hematologie: Robert, Trix en Waander. Cognitive Neuroscience: Michel, Francisca, Sjefke en Lourens. Urologie: Bronte, Dorien, Henk en Paul. Tandheelkunde: Arnold, Frank, Ljupcho en Na. Dermatologie: Meike. Nucleaire geneeskunde: Annemarie. Radiologie: Thiele.

Vanuit de middelbare school bestaat er nog steeds een fijne vriendengroep. Een gezelschap waarbij je weer even lekker man kan zijn. Arjan, Hans, Jeroen, Jop, Joppe, Jos, Paul, Reinier en Tim bedankt voor het stukje ontspannen.

Vrienden vanuit de studie BioMedische Wetenschappen, jullie wil ik ook niet overslaan uit deze rij dankbetuigingen. Dankzij jullie heb ik genoten van de studie en van vele plezierige uitstapjes en diners door heel het land. Ben, Irene, Jacoline,

Jorike, Judith, Linda, Luc, Monique B, Monique van M, Santha, Saskia en Stan bedankt voor alle leuke jaren.

Ontspannen na drukke dagen in het lab kan ook door te zweten in de sporthal. Daarom wil ik graag mijn teamgenoten van Radbal: Anchel, Anneke, Antoine, Bart, Bianca, Ellis, Eric, Floor, Jochem, Johnny, Joke, Jonathan, Joris, Martijn, Phillip, Naima, Pim, Robert-Jan, Sietse en Sip bedanken voor de wekelijkse actieve ontspanning.

De persoon die ik ben geworden komt door jarenlange vorming waarbij familie een belangrijke rol heeft gespeeld. Alle ooms en tantes, neefjes en nichtjes, peetoom Leo, peettante Anja, schoonbroer Micha en schoonzus Chantal, bedankt voor jullie jarenlange gezelschap. Degene die nog meer invloed hebben gehad op mijn persoonlijke ontwikkeling zijn mijn zus Saskia, broer David en ouders Corry en Winfried. Jullie hebben me mijn hele leven begeleid en gesteund in al mijn keuzes en ik hoop dat jullie dit nog vele jaren zullen doen.

De ere plaats is behouden voor mijn vriendin An. Zonder jou zou deze periode van promoveren een stuk zwaarder zijn geweest. Je gezelschap, het feit dat je om al mijn grapjes lacht ongeacht hoe slecht ze zijn en je uitstekende kookkunsten waren dingen om naar uit te kijken als ik weer naar huis fietste.

Curriculum Vitae

Born in 1984, on the 31st of May in Velp, he lived till his early twienties with his parents, sister and brother in Duiven. He finished high school in 2002 and continued to study BioMedical Sciences at the Radboud University Nijmegen, The Netherlands. After five years he finished the study with a major in Pathobiologie and a minor in molecular life sciences. Soon after his gradaution he started as a PhD-student at the Orthopedic Research Laboratory, of the Radboud University Nijmegen Medical Centre under the supervision of Prof dr Pieter Buma. During the following five years he designed and performed research, attended and presented at international congresses and supervised a number of students. All research performed are bundeled in this thesis and defended on the 10th of June, 2013.

Publications

Platelet rich plasma can replace foetal bovine serum in human meniscus cell cultures
Tissue Engineering, Part C, in press
VK Gonzales, ELW de Mulder, T de Boer, G Hannink, TG van Tienen, W van Heerde, P Buma

Effect of polyurethane scaffold architecture on ingrowth speed and collagen orientation in a subcutaneous rat pocket model
Biomedical Materials; 2013 Apr;8(2):025004
ELW de Mulder, G Hannink, N Verdonschot, P Buma

Characterization of polyurethane scaffold surface functionalization with diamines and heparin
Journal of Biomedical Materials Research Part A; 2013 Apr; 101(4):919-22
ELW de Mulder, G Hannink, MJW Koens, DWPM Löwik, N Verdonschot, P Buma

Effect of load on the repair of osteochondral defects using a porous polymer scaffold
Journal of Biomedical Material Research Part B: Applied Biomaterials; 2012 Nov;100(8):2082-9
G Hannink, ELW de Mulder, TG van Tienen, P Buma

Enzymatic mineralization of gellan gum hydrogel for bone tissue-engineering applications and its enhancement by polydopamine.
Journal of Tssue Engineering and Regenerative Medicin; in press
TEL Douglas, M Wlodarczyk, E Pamula, HA Declercq, ELW de Mulder, , M Bucko, L Balcaen, F Vanhaecke, R Cornelissen, P Dubruel, JA Jansen, SCG Leeuwenburgh

Enzymatic Mineralization of Hydrogels for Bone Tissue Engineering by Incorporation of Alkaline Phosphatase.
Macromolecular Bioscience; 2012 Aug;12(8):1077-89
TEL Douglas, PB Messersmith, S Chasan, AG Mikos, ELW de Mulder, G Dickson, D Schaubroeck, L Balcaen, F Vanhaecke, P Dubruel, JA Jansen, SC Leeuwenburgh

Improving the Cell Distribution in Collagen Coated PCL Knittings
Tissue Engineering Part C: Methods; 2012 Oct;18(10):731-9
W Sun, D Tiemessen, M Sloff, RJ Lammers, ELW de Mulder, J Hilborn, B Bhuvnesh Gupta, WF Feitz, WF Daamen, TH van Kuppevelt, P Geutjes

Enzymatically Induced Mineralization of Platelet-rich Fibrin
Journal of Biomedical Materials Research Part A; 2012 May;100(5):1335-46
TEL Douglas, V Gassling, HA Declercq, N Purcz, E Pamula, HJ Haugen, S Chasan, ELW de Mulder, JA Jansen, SCG Leeuwenburgh

Proliferation of meniscal fibrochondrocytes cultured on a new polyurethane scaffold is stimulated by TGF-beta
Journal of Biomaterials Applications; 2013 Jan;27(5):617-26
ELW de Mulder, G Hannink, M Giele, N Verdonschot, P Buma

Anisotropic Porous Biodegradable Scaffolds for Musculoskeletal Tissue Engineering
Materials; 2009 Oct;2(4):1674-1696
ELW de Mulder, P Buma, G Hannink

Degradable Polymers in Meniscus Reconstruction
Degradable Polymers for Skeletal Implants; 2009; ISBN: 978-1-60692-426-6: 295-312
ELW de Mulder, G Hannink, TG van Tienen, P Buma

Rats that Differentially Respond to Cocaine Differ in their Dopaminergic Storage Capacity of the Nucleus Accumbens
Journal of Neurochemistry; 2008 Jun 1;105(6):2122-33
MMM Verheij, ELW de Mulder, E de Leonibus, KMJ van Loo, AR Cools